Supporting Information

Yeast-based High-Throughput Screen Identifies *Plasmodium falciparum* Equilibrative Nucleoside Transporter 1 Inhibitors That Kill Malaria Parasites

I. J. Frame[†,▽], Roman Deniskin[†,▽], Alison Rinderspacher[‡], Francine Katz[‡], Shi-Xian Deng[‡], Robyn D. Moir[§], Sophie H. Adjalley[⊥], Olivia Coburn-Flynn[⊥], David A. Fidock[‡,⊥], Ian M. Willis[§], Donald W. Landry[‡], Myles H. Akabas[†,‖,‖,*]

[†]Department of Physiology & Biophysics, [§]Department of Biochemistry, [‖]Department of Neuroscience and [‖]Department of Medicine, Albert Einstein College of Medicine, 1300 Morris Park Avenue, Bronx, NY, 10461, United States

[‡]Department of Medicine and [⊥]Department of Microbiology & Immunology, Columbia University Medical Center, 630 West 168th Street, New York, NY, 10032, United States

[▽]IJF and RD contributed equally.

*To whom correspondence should be addressed.

Myles H. Akabas, M.D., Ph.D.

Department of Physiology and Biophysics

Albert Einstein College of Medicine

1300 Morris Park Avenue

Bronx, NY 10461, United States

myles.akabas@einstein.yu.edu

Phone: 718-430-3360

Fax: 718-430-8819

Table of Contents – Supporting Information

Figure S1. Nucleotide sequence of the *S. cerevisiae* codon optimized PfENT1-HA-CO construct ..……. p. 3

Figure S2. Integration of PfENT1-HA-CO into *S. cerevisiae* genome ……..….. p. 4

Figure S3. HTS Robustness Characterization ……. p. 5

Figure S4. Characterization of growth and transport by PfENT1-CO-expressing purine auxotrophic *ade2*Δ yeast ….…….. p. 6

Figure S5. Correlation of growth IC_{50} values for the nine compounds examined in the primary 5-FUrd assay and the orthogonal adenosine growth inhibition assay ……. p. 7

Figure S6. Compound **3** does not affect radiolabeled substrate uptake into PfENT4-expressing *Xenopus* oocytes ……. p. 8

Figure S7. Comparison of the concentration dependent inhibition of growth of chloroquine sensitive, 3D7, and chloroquine resistant, Dd2, parasites by four compounds ……. p. 9

Figure S8. Generation of PfENT1 knockout parasites ……. p. 10

Figure S9. Validation of Efficacy Target with PfENT1-knockout Parasites ……. p. 11

Figure S10. General structure of the coumarins found in our library ……. p. 12

Table S1. Small molecule screening data……. p. 13

Table S2. High throughput screen hits…….. p. 15

Table S3. Structure-activity characterization of 4-methyl-7-[(3,4,5-trimethoxybenzyl)oxy]-2H-chromen-2-one derivatives……. p. 40

Chemical Synthesis and Characterization Of Compounds Used In This Study…….. p. 43

Methods…….. p. 88

Supporting Information References……. p. 101

ATGAGTACAGGAAAAGAGTCCTCCAAAGCTTACGCTGACATCGAATCAAGGGGCGA
TTACAAAGATGATGGCAAAAAGGGTAGTACTCTATCTTCTAAACAACATTTTATGTTGTCTTT
AACATTCATCTTGATAGGATTATCATCTTTAAACGTTTGGAATACAGCATTAGGTCTGAATAT
CAATTTCAAATACAATACTTTCCAAATAACGGGGTTAGTTTGTAGTTCTATTGTTGCGCTTTT
TGTGGAAATTCCTAAGATTATGCTTCCATTTTTGCTCGGTGGCTTGTCAATATTGTGCGCTG
GTTTTCAAATATCTCATTCATTTTTCACTGACACACAGTTTGATACCTACTGTTTGGTGGCAT
TCATTGTCATCGGTGTTGTGGCTGGCTTGGCCCAAACAATTGCCTTTAACATCGGTTCCAC
TATGGAAGATAATATGGGCGGTTACATGTCTGCAGGAATTGGAATATCAGGTGTATTCATTT
TTGTAATCAACTTGTTGCTCGACCAATTCGTTTCACCAGAGAAGCATTACGGTGTGAATAAG
GCAAAGTTGCTGTACCTATACATTATCTGTGAGCTATGCTTAATCCTTGCAATCGTTTTCTG
TGTTTGTAATTTGGACCTAACCAACAAAAACAACAAAAAGGACGAGGAAAATAAGGAAAACA
ATGCTACTCTAAGCTACATGGAATTGTTTAAAGACAGCTATAAGGCAATTTTGACAATGTTTT
TAGTCAATTGGCTCACACTTCAATTGTTTCCAGGGGTAGGCCATAAAAAGTGGCAGGAATC
TCACAATATTTCAGATTATAACGTAACCATTATCGTTGGGATGTTTCAGGTTTTCGATTTCCT
TTCTAGATACCCTCCTAATCTTACACACATCAAAATCTTCAAAAACTTTACTTTTTCATTAAAC
AAATTACTGGTCGCCAATTCTCTGAGATTGCTGTTCATACCTTGGTTTATCTTAAACGCTTG
CGTAGATCACCCATTTTTCAAAAACATCGTCCAACAATGCGTGTGTATGGCCATGCTCGCTT
TTACTAATGGTTGGTTTAATACCGTACCATTTTTAGTCTTTGTCAAGGAACTAAAGAAAGCTA
AAAAGAAAAAGGAAATTGAAATAATCTCCACATTCCTTGTTATTGCAATGTTTGTTGGTCTAT
TTTGTGGAATATGGACAACTTACATCTACAATTTGTTCAATATTGTTTTACCAAAACCAGATC
TACCTCCAATCGATGTGACTCAATATCCTTATGATGTCCCAGATTATGCCTAA

Figure S1. Nucleotide sequence of the *S. cerevisiae* codon optimized PfENT1-HA-CO construct. (underlined portion denotes HA tag sequence)

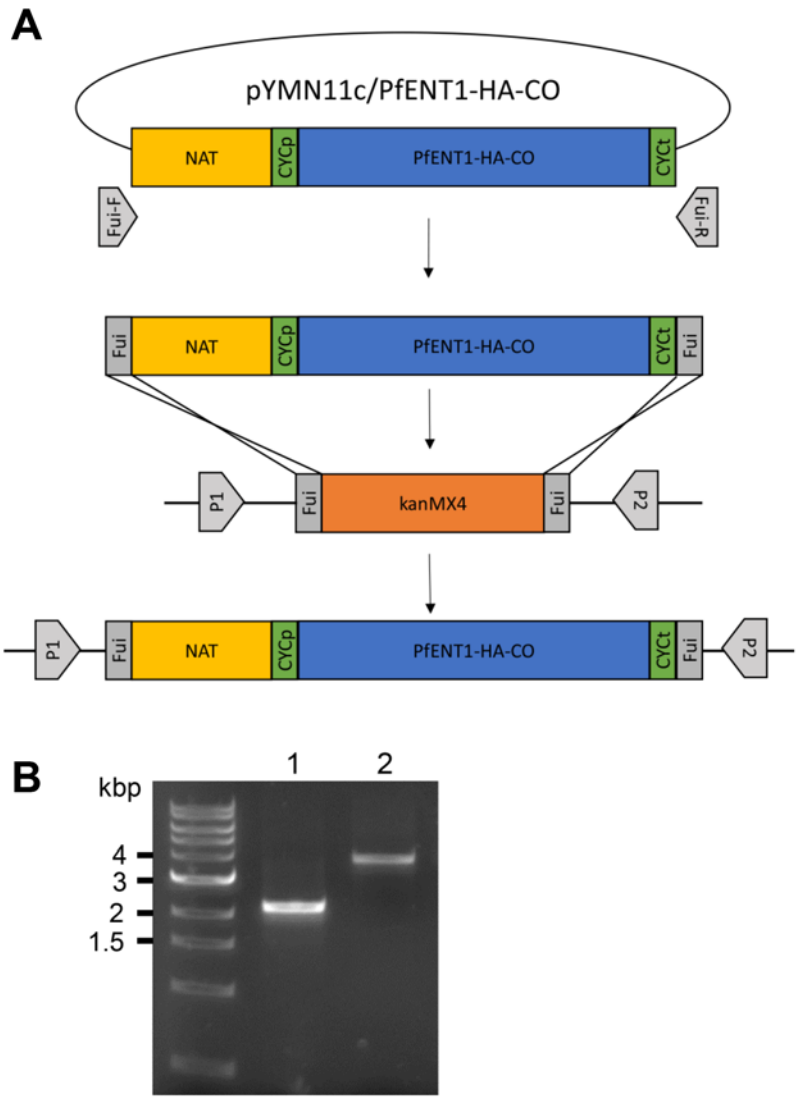

Figure S2. Integration of PfENT1-HA-CO into *S. cerevisiae* genome. (A) Schematic of integration strategy. The pYMN11c/PfENT1-HA-CO plasmid was used as a template for PCR using primers (Fui1-F, Fui1-R) that added DNA that was homologous to the FUI1 locus. (NAT = nourseothricin acetyl transferase [confers resistance to nourseothricin]; CYCp and CYCt are the promoter and terminator for the *S. cerevisiae* CYC1 gene that are used to drive expression of PfENT1). The PCR product was transformed into the *fui1*Δ::kanMX4 strain of *S. cerevisiae* and clones were selected on nourseothricin-agar plates; positive clones would have undergone homologous recombination at the FUI1 site, replacing the kanMX4 cassette with the NAT/PfENT1-HA-CO cassette. Genomic DNA was isolated and PCR was performed to confirm cassette replacement using primers P1 and P2. (B) Agarose gel showing PCR products from gDNA amplification of *fui1*Δ::kanMX4 (Lane 1) and *fui1*Δ::PfENT1-HA-CO (Lane 2) using primers P1 and P2. The expected product lengths are 2,183 bp and 3,843 bp, respectively. (kbp, kilobase pairs)

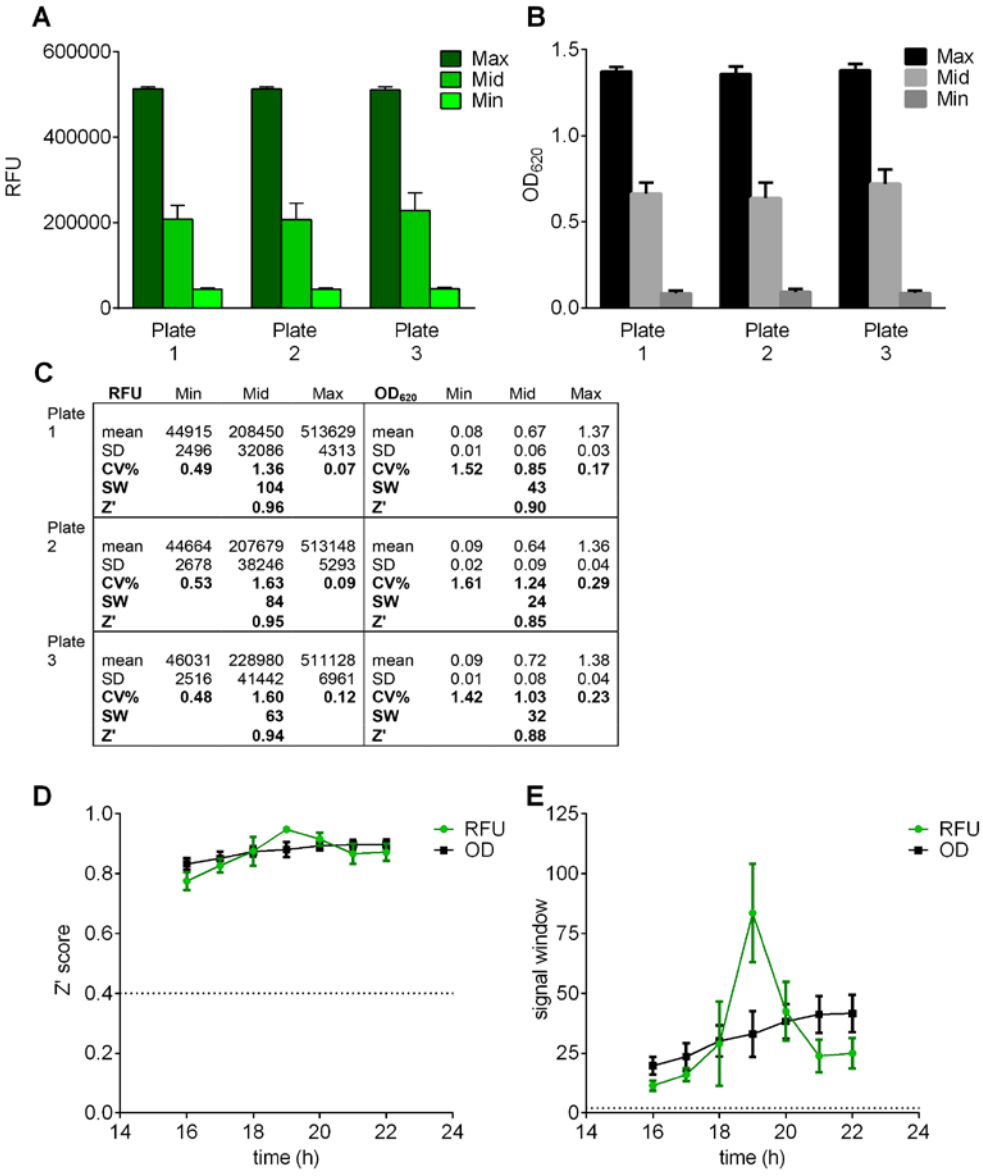

Figure S3. HTS Robustness Characterization.
High Throughput Screen Plate Uniformity: (A,B) Three separate 384 well plates had every third column containing conditions that would give rise to a low signal, medium signal, and a high signal. All conditions had 125 µM 5-FUrd in each well. The low signal had 0 inosine, the medium signal had 3 mM inosine, and the high signal had 12.2 mM inosine. Plates were grown for 22 h with GFP and OD_{620} readings obtained every hour. The average maximum, medium, and minimum signal after 19 h of growth are shown in panel (A) for Relative Fluorescence Units (RFU), panel (B) for OD. (C) Numerical data for plates shown in panels A and B. Robustness statistics were calculated and the Z'-factor (panel D) and signal window (panel E) increased over time for OD_{620} and peaked at 19 h for GFP. The dashed lines indicate the minimum values suggested by Iversen et al., (2004) in the chapter entitled HTS Assay Validation in Assay Guidance Manual.[1]

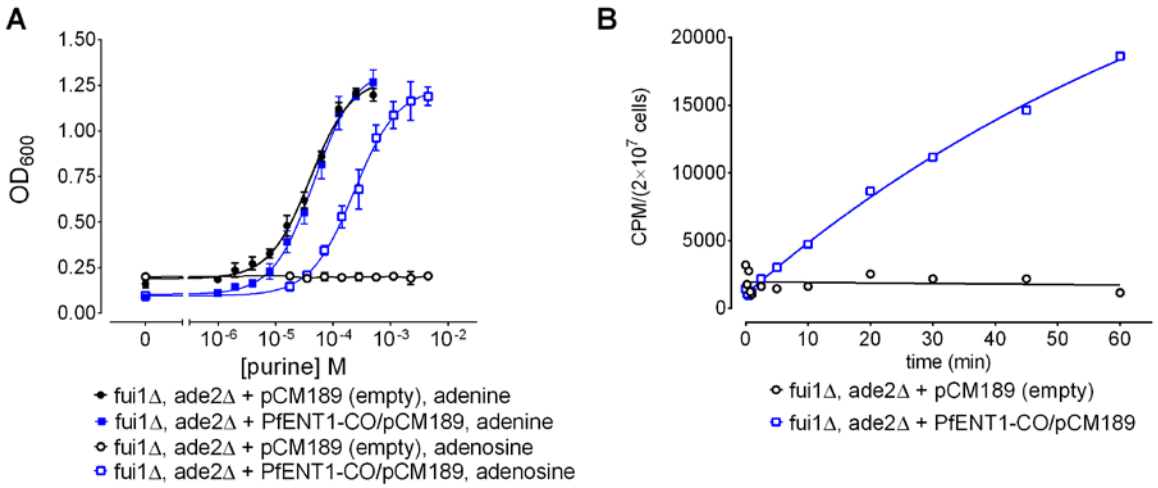

Figure S4. Characterization of growth and transport by PfENT1-CO-expressing purine auxotrophic *ade2*Δ yeast. (A) Purine concentration dependence for the growth of PfENT1-CO-expressing *ade2*Δ yeast and empty plasmid transformed *ade2*Δ yeast. Y-axis scale is OD_{600}. (B) [^{3}H]adenosine uptake as a function of incubation time into PfENT1-CO-expressing *ade2*Δ yeast and empty plasmid transformed *ade2*Δ yeast.

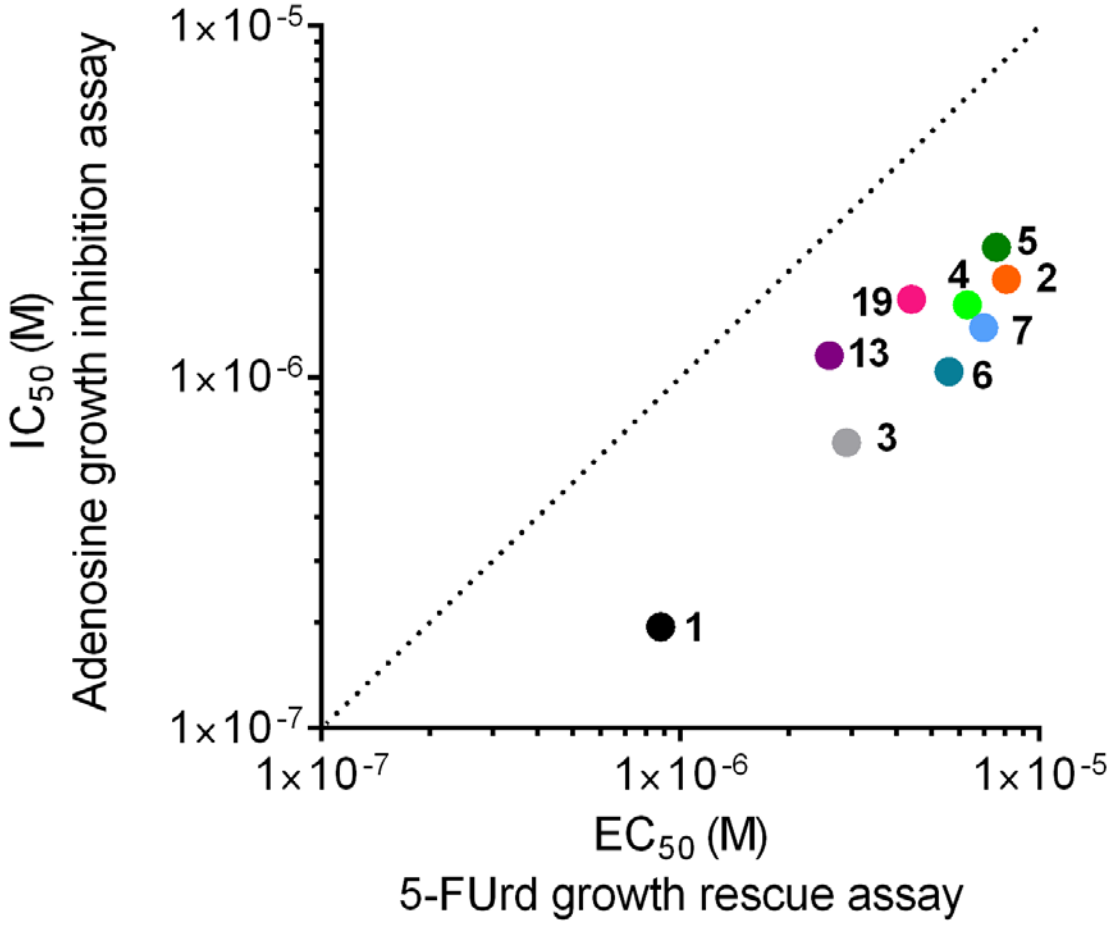

Figure S5. Correlation of growth IC_{50} values for the nine compounds examined in the primary 5-FUrd assay and the orthogonal adenosine growth inhibition assay. Points correspond to the compound IC_{50} determined using the primary assay (growth of PfENT1-HA-CO-expressing *fui1*Δ yeast in the presence of 125 μM 5-FUrd) relative to the compound IC_{50} for the secondary adenosine growth assay (inhibition of PfENT1-CO-expressing *ade2*Δ yeast growth in media containing 1 mM adenosine). Data are from Table 1. Compounds are identified by their Rank Number in SI Table S3. Dashed line delineates line of identity. Linear regression fit $R^2 = 0.71$ (GraphPad Prism 6.0).

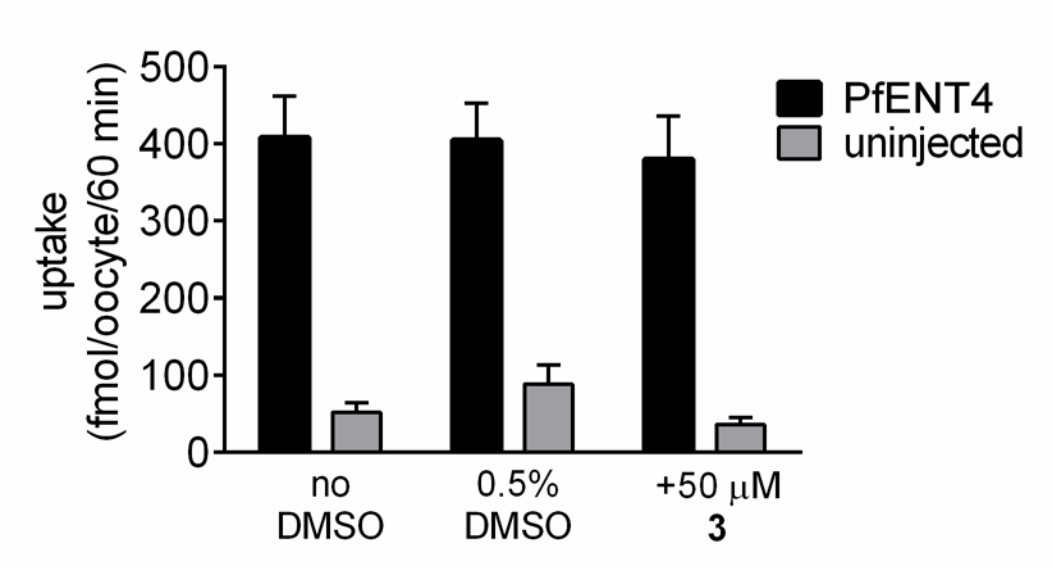

Figure S6. Compound 3 does not inhibit radiolabeled substrate uptake into PfENT4-expressing *Xenopus* oocytes. PfENT4-expressing oocytes were incubated with 1.5 μM [^{14}C]2-deoxyadenosine for 60 min in the presence of 50 μM compound **3**. Radiolabel uptake was quantified by liquid scintillation counting of individual oocytes. Experiment condition had 5 oocytes each, technical triplicates (15 oocytes per data point per experiment) and was repeated. The data are mean and SEM of 30 oocyte determinations.

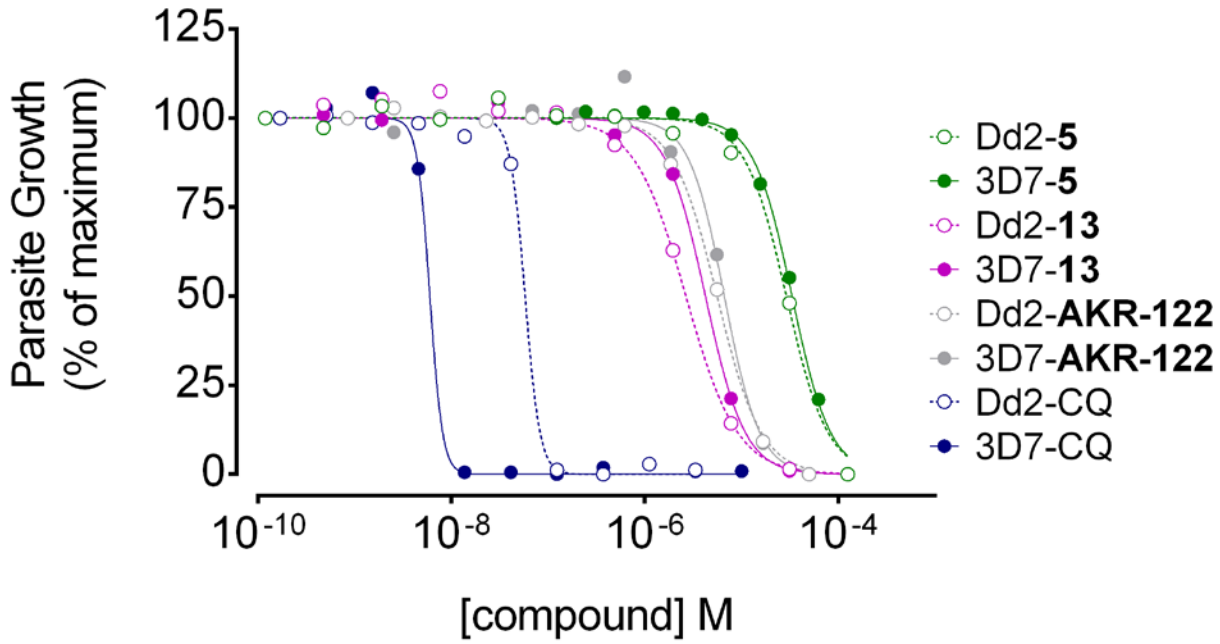

Figure S7. Comparison of the concentration dependent inhibition of growth of chloroquine sensitive, 3D7 (filled circles, solid lines), and chloroquine resistant, Dd2 (open circles, dashed lines), parasites by four compounds. Parasites were grown for 72 h in the presence of the indicated concentration of compound in 96 well plates. DNA content was quantified by SYBR Green I method. Note that the IC_{50} values for the three PfENT1 inhibitors, **5**, **13**, and **AKR–122** are not significantly different between the two parasite strains. In contrast, as expected, the IC_{50} values are 10-fold different for chloroquine (CQ). Culture media contained 367 μM hypoxanthine. Average IC_{50} values for 3 biological replicates are in Table 1 and Table S4.

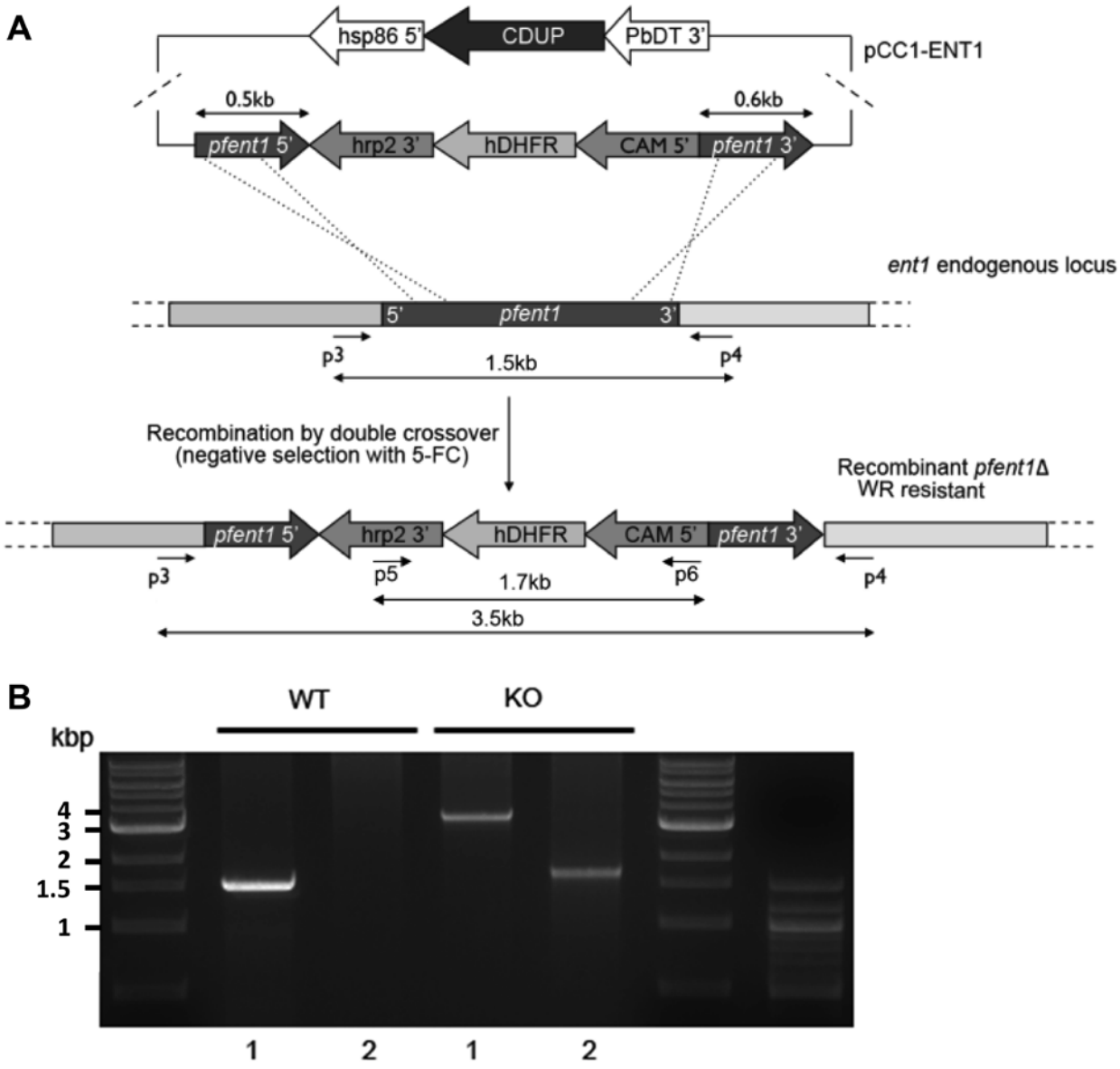

Figure S8. Generation of PfENT1 knockout parasites. (A) Cartoon illustrating *pfent1* knockout strategy.[2, 3] Hsp86, 5' untranslated region of the heat-shock protein 86 gene; Hrp2 3', 3' untranslated region of the Histidine-rich protein 2 gene; PbDT 3', 3' untranslated region of the *P. berghei* dhfr-thymidylate synthase gene; CAM 5', 5' untranslated region of the calmodulin gene; hDHFR, human dihydrofolate reductase coding sequence; CDUP, cytidine deaminase - uracil phosphotransferase fusion gene; 5-FC, 5-fluorocytosine; *pfent1* 5', 5' end of *pfent1* coding sequence; *pfent1* 3', 3' end of *pfent1* coding sequence (B) Agarose gel of PCR products to verify the knockout of *pfent1*. Product 1 results from PCR amplification using primers p3 and p4. PCR product 2 results from amplification using primers p5 and p6 (primer sequences in Methods, location shown in panel A).

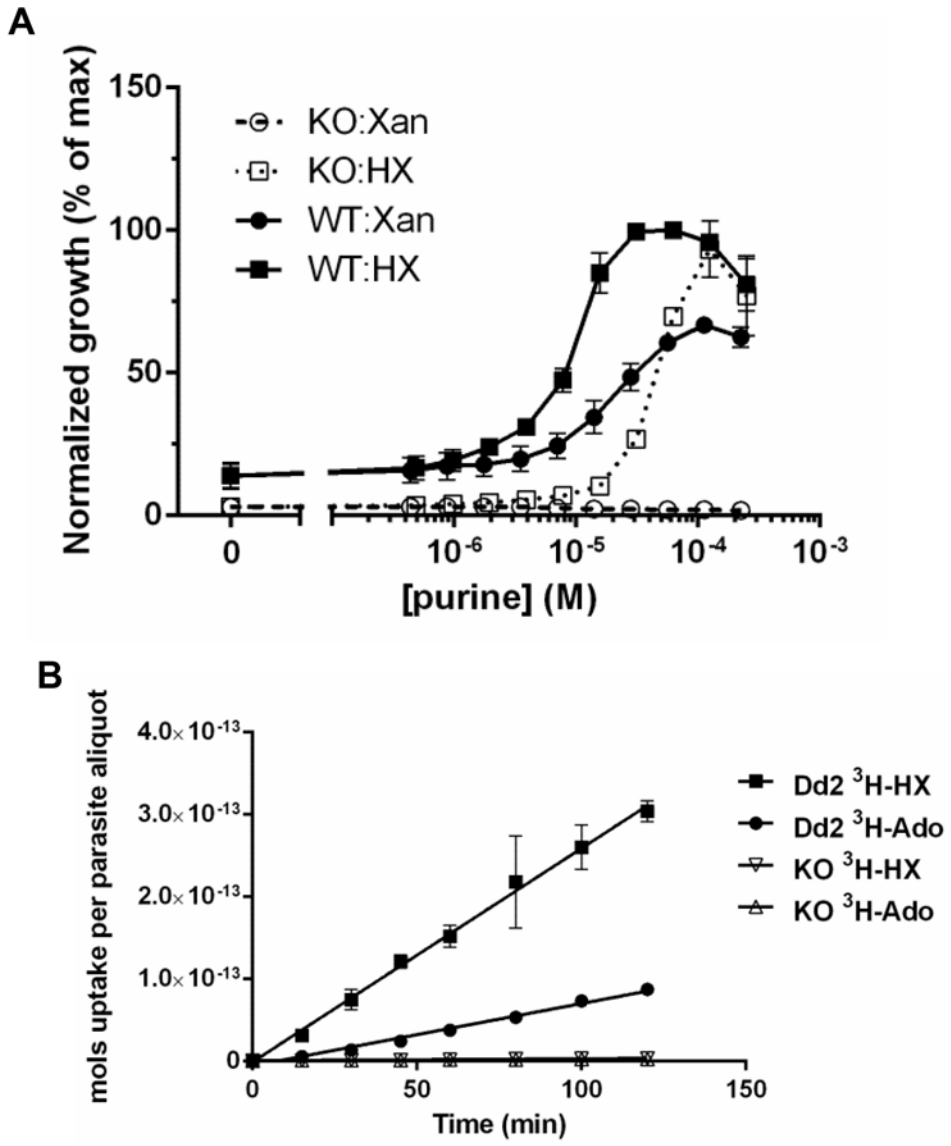

Figure S9. Validation of efficacy target with PfENT1-knockout parasites. (A) Illustrates the purine dependence of parasite growth after 96 h. Wild type Dd2 parasites (filled symbols) and PfENT1-knockout parasites (open symbols). Sole purine source: xanthine (circles) and hypoxanthine (squares). Note that the PfENT1-knockout parasites do not grow on xanthine and do grow with hypoxanthine but the curve is right shifted compared with the wild type. **(B)** Uptake of 50 nM [^{3}H]hypoxanthine (HX) and 150 nM [^{3}H]adenosine (Ado) into Dd2 and PfENT1-knockout parasites (KO). All data for a given day was normalized to maximum signal in the Dd2 parasites grown with hypoxanthine (n = 3 biological replicates). Mean ± SD shown. SD is smaller than symbol for many points.

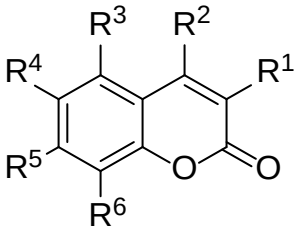

R^1 = H, CH_3, Et, Pr, Bn

R^2 = H, CH_3, CF_3, Et, Pr, *n*Bu, Ph, aryl

R^3 = H, CH_3, Et, Pr, *n*Bu, *i*Bu, OCH_3

R^4 = H, CH_3, Et, Pr, *n*Bu, *i*Bu, OR^{12}, Cl, NHR^{13}

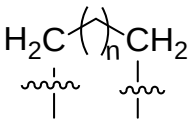

n = 1-2

R^5 = H, CH_3, OR^7

R^6 = H, CH_3, I, $CH_2N(R^8)_2$

R^7 = H, $C(O)CH_2R^9$, $C(O)R^{10}$, CH_2R^{11}

R^8 = alkyl

R^9 = alkyl, alkoxy

R^{10} = aryl

R^{11} = alkyl, aryl, heteroaryl, alkoxyalkyl chains, amide

R^{12} = $C(O)R^{15}$

R^{13} = $C(O)R^{14}$

R^{14} = aryl

R^{15} = alkyl, aryl

Figure S10. General structure of the coumarins found in our library. The various coumarin derivatives found in the 64,560 compounds that were screened are illustrated above. The structural diversity of these compounds probed the chemical space in the vicinity of the coumarin binding site. It provides a basis for future SAR studies.

Table S1. Small molecule screening data

Category	Parameter	Description
Assay	Type of assay	Cell-based
	Target	PfENT1
	Primary measurement	Yeast cell growth (OD_{620} and GFP fluorescence)
	Key reagents	Growth medium, 5-fluorouridine, test compounds, yeast cells, inosine for positive control
	Assay protocol	1) Add 40 µl media to wells containing 250 µM 5-FUrd 2) Add 0.8 µl of test compound (10 mM stock in 100% DMSO) to test wells 3) Add 40 µl cells (~80,000 cells) to each well; final 5-FUrd is 125 µM 4) Incubate for 19 h, 30 ^{o}C 5) Read OD_{620} and GFP fluorescence
Library	Library size	64,560
	Library composition	Diverse chemicals, antimalarial probes, FDA approved drugs, natural products
	Source	ChemBridge CNSet, Medicines for Malaria Venture Open Access Box, MicroSource Spectrum Collection
Screen	Format	384-well
	Concentration(s) tested	10 µM
	Plate controls	Minimum: no test compound +1% DMSO (v/v) Maximum: 12.2 mM inosine +1% DMSO (v/v)
	Reagent/ compound dispensing system	Perkin Elmer MiniTrak Liquid Handling System
	Detection instrument and software	Perkin Elmer Envision 2010
	Assay validation/QC	Every test plate contained positive and negative controls in the outer two columns; Z'-factors were determined to be > 0.8
	Correction factors	None
	Normalization	Well OD_{620} and RFU were normalized as a percentage of the maximum values in the control wells

Post-HTS analysis	Hit criteria	Compounds must have activity > 4 SD above the minimum control wells
	Hit rate	0.26%
	Additional assay(s)	Concentration-responses in primary growth-rescue assay, orthogonal growth inhibition assay, [^{3}H]adenosine uptake inhibition assay
	Confirmation of hit purity and structure	Fresh compound was purchased directly from ChemBridge; one compound and derivatives were synthesized by us and purity confirmed by NMR

Table S2. High throughput screen hits.

Rank #	Normalized % maximal activity RFU	Normalized % maximal activity OD	Avg Normalized % maximal activity	ChemBridge compound ID#	MW	Mol Name	Structure
1	98.73	95.70	97.22	9001893	353.4	N,N'–1,3-benzothiazole-2,6-diyldi(2-furamide)	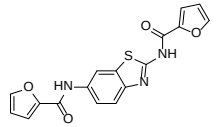
2	91.47	92.42	91.94	6718896	394.2	2-bromo-N-(4-[1,3]oxazolo[4,5-b]pyridin-2-ylphenyl)benzamide	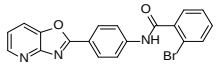
3	93.64	75.78	84.71	6946484	356.4	4-methyl-7-[(3,4,5-trimethoxybenzyl)oxy]-2H-chromen-2-one	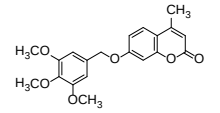
4	73.98	74.09	74.03	6081106	321.3	N-{4-[5-(2-furyl)–1,3,4-oxadiazol-2-yl]phenyl}-2-furamide	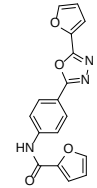

5	59.42	68.72	64.07	9039333	375.4	2-(1-methyl–1H-indol-3-yl)-2-oxo-N-[4-(pyrrolidin–1-ylcarbonyl)phenyl]acetamide	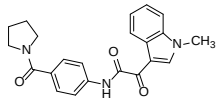
6	52.90	65.22	59.06	9011026	333.3	3-fluoro-N-(3-[1,3]oxazolo[4,5-b]pyridin-2-ylphenyl)benzamide	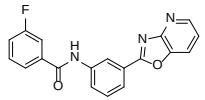
7	50.12	59.98	55.05	6736283	345.4	2-methoxy-N-(3-[1,3]oxazolo[4,5-b]pyridin-2-ylphenyl)benzamide	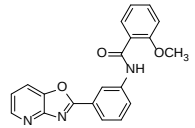
8	51.68	56.77	54.23	7993021	372.8	2-(2-chlorophenoxy)-N-[4-(1-piperidinylcarbonyl)phenyl]acetamide	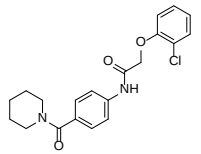
9	51.00	57.25	54.12	6838528	361	N-{3-[5-(2-furyl)–1,3,4-oxadiazol-2-yl]phenyl}-3-methoxybenzamide	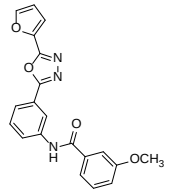
10	41.85	49.78	45.82	7240481	379.9	2-{[(3-chloro–1-benzothien-2-yl)carbonyl]amino}-N,N,4-trimethyl–1,3-thiazole-5-carboxamide	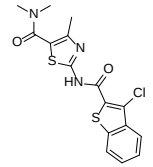
11	30.15	35.56	32.85	6770368	305.3	N-(3-[1,3]oxazolo[4,5-b]pyridin-2-ylphenyl)-2-furamide	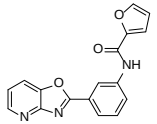

12	32.31	31.12	31.72	9008896	334.3	4-methyl-7-[(5-phenyl–1,3,4-oxadiazol-2-yl)methoxy]-2H-chromen-2-one	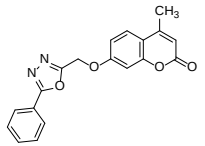
13	27.03	22.36	24.69	6517398	262.3	2-[2-(2-methylphenyl)vinyl]-4(3H)-quinazolinone	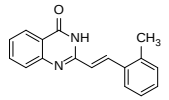
14	25.10	23.84	24.47	7925013	321.3	N-(4-{[(4-methyl-2-pyridinyl)amino]carbonyl}phenyl)-2-furamide	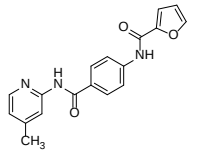
15	20.82	27.54	24.18	9010614	356.4	N-[2-methoxy-5-(2-quinoxalinyl)phenyl]isonicotinamide	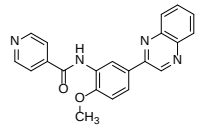
16	22.74	25.01	23.87	6783000	345.4	4-methoxy-N-(3-[1,3]oxazolo[4,5-b]pyridin-2-ylphenyl)benzamide	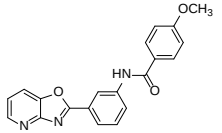
17	17.70	26.60	22.15	6877227	355.4	N,N-diethyl-2-[(8-methoxy-6-oxo-6H-benzo[c]chromen-3-yl)oxy]acetamide	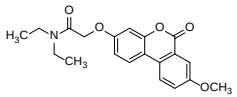
18	20.69	22.94	21.82	6559548	282.7	2-[2-(2-chlorophenyl)vinyl]-4(3H)-quinazolinone	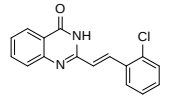
19	12.25	30.23	21.24	9011680	355.8	N-(4-chloro-3-[1,3]oxazolo[4,5-b]pyridin-2-ylphenyl)-2-thiophenecarboxamide	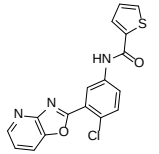

20	19.20	20.36	19.78	7657422	337.4	2-fluoro-N-(3-imidazo[2,1-b][1,3]thiazol-6-ylphenyl)benzamide	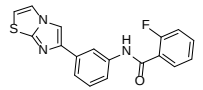
21	15.63	19.76	17.70	6879357	382.5	4-[4-(2-furoyl)–1-piperazinyl]-6-methyl-5,6,7,8-tetrahydro[1]benzothieno[2,3-d]pyrimidine	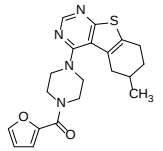
22	16.43	18.28	17.36	7946040	343.4	N,N,4-trimethyl-2-{[(3-methyl–1-benzofuran-2-yl)carbonyl]amino}–1,3-thiazole-5-carboxamide	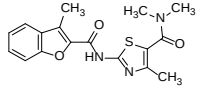
23	16.27	17.27	16.77	7683456	284.3	5-(4-fluorophenyl)-7-(2-furyl)-4,5,6,7-tetrahydro[1,2,4]triazolo[1,5-a]pyrimidine	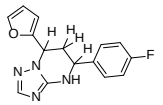
24	6.00	26.33	16.16	5968546	306.8	2-chloro-N-(7-oxo-4,5,6,7-tetrahydro–1,3-benzothiazol-2-yl)benzamide	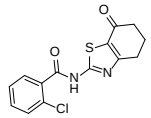
25	17.79	13.39	15.59	9006419	373.5	1-{4-[3-(4-ethoxy-3-methoxyphenyl)–1,2,4-oxadiazol-5-yl]butanoyl}piperidine	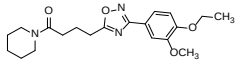
26	15.50	14.95	15.22	9010523	325.3	N-{4-[5-(2-furyl)–1,3,4-oxadiazol-2-yl]phenyl}tetrahydro-2-furancarboxamide	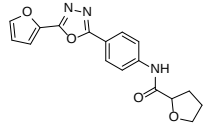
27	15.86	12.20	14.03	9064718	345.4	N-[5-(1,3-benzoxazol-2-yl)-2-methoxyphenyl]nicotinamide	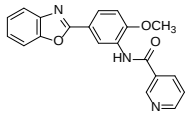

28	16.42	11.54	13.98	6553394	293.3	2-methyl-N-(4-methyl-2-oxo-2H-chromen-7-yl)benzamide	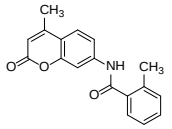
29	13.86	13.30	13.58	6038917	266.3	1-methoxy-4-(4-methoxyphenyl)phthalazine	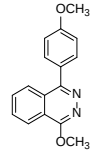
30	13.00	13.86	13.43	6537559	331.3	N-[4-(5-phenyl–1,3,4-oxadiazol-2-yl)phenyl]-2-furamide	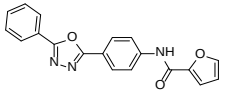
31	13.19	12.80	13.00	7928241	350	N-(3-{[(2-ethoxyphenyl)amino]carbonyl}phenyl)-2-furamide	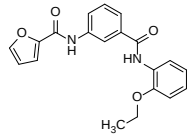
32	12.97	11.08	12.03	7993034	319.8	N-(5-chloro-2-methoxyphenyl)-5-(2-pyrazinyl)–1,3,4-thiadiazol-2-amine	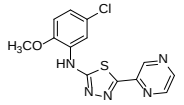
33	14.14	9.81	11.98	7959093	378.4	methyl 2-{[3-(2-furoylamino)-2-methylbenzoyl]amino}benzoate	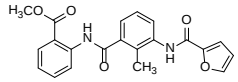
34	10.97	12.47	11.72	5705452	315.4	2-[2-(1,2-dimethyl–1H-indol-3-yl)vinyl]-4(3H)-quinazolinone	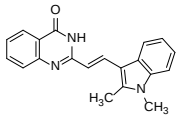
35	11.99	10.81	11.40	6564017	361.4	N-{4-[5-(2-furyl)–1,3,4-oxadiazol-2-yl]phenyl}-3-methoxybenzamide	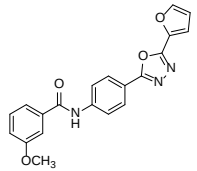

36	2.30	19.99	11.14	7798230	281.4	N-(2-ethyl-6-methylphenyl)-2-thiophenesulfonamide	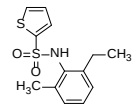
37	12.52	8.70	10.61	7994462	389.4	3,4-dimethoxy-N-(2-methyl-4-[1,3]oxazolo[4,5-b]pyridin-2-ylphenyl)benzamide	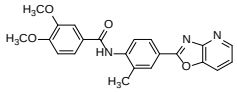
38	15.45	5.77	10.61	01504018	1221.407	HEDERACOSIDE C	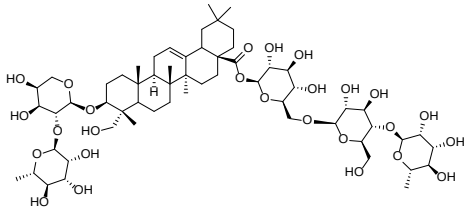
39	12.12	8.93	10.52	7962796	322.4	N-[4-(5-methyl–1,3-benzoxazol-2-yl)phenyl]tetrahydro-2-furancarboxamide	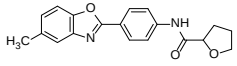
40	10.61	9.96	10.29	9028215	372.4	ethyl 5-[(2-fluorobenzoyl)amino]-2-(4-morpholinyl)benzoate	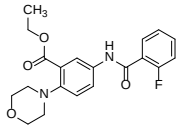
41	9.31	11.25	10.28	9010768	319.3	N-(2-methyl-4-[1,3]oxazolo[4,5-b]pyridin-2-ylphenyl)-2-furamide	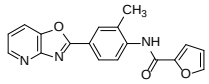
42	12.60	7.72	10.16	7893379	335.4	N-[4-(5-phenyl–1,3,4-oxadiazol-2-yl)phenyl]tetrahydro-2-furancarboxamide	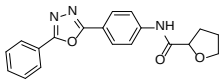

43	11.73	7.31	9.52	9006085	327.3	N-({[6-(4-morpholinyl)-4-pyrimidinyl]amino}carbonyl)benzamide	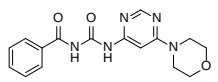
44	10.58	7.55	9.07	7961939	345.4	N-{4-[5-(2-furyl)–1,3,4-oxadiazol-2-yl]phenyl}-3-methylbenzamide	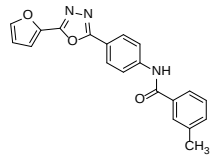
45	11.15	6.79	8.97	7985495	372.3	1-({[5-(2,4-dichlorophenyl)–1,3,4-oxadiazol-2-yl]thio}acetyl)piperidine	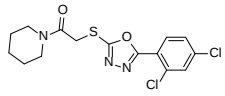
46	*34.50*	8.94	8.94	9048901	349.5	2-({[2-(1,3-benzodioxol-5-yl)–1,3-thiazol-4-yl]methyl}thio)-5-methyl–1,3,4-thiadiazole	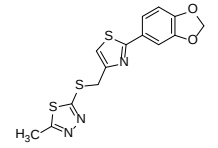
47	1.48	15.84	8.66	7747935	293.3	N-[5-(ethoxymethyl)–1,3,4-thiadiazol-2-yl]-4-methoxybenzamide	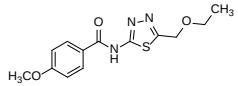
48	1.53	15.35	8.44	6817240	244.3	N-[1-(4-ethylphenyl)ethyl]–1H–1,2,4-triazole-3-carboxamide	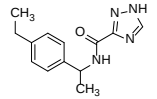
49	10.73	5.99	8.36	7496480	308.3	N-[4-(1,3-benzoxazol-2-yl)phenyl]tetrahydro-2-furancarboxamide	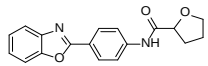
50	1.00	15.47	8.23	6404083	355.5	N-(4-ethoxyphenyl)-N-[2-(4-methyl–1-piperazinyl)-2-oxoethyl]methanesulfonamide (non-preferred name)	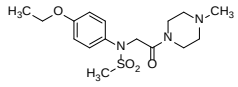

51	8.08	8.15	8.11	9039418	344.4	ethyl 5-(2-furoylamino)-2-morpholin-4-ylbenzoate	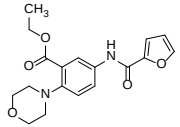
52	7.03	9.02	8.03	7452875	340.4	methyl 2-{[3-(isobutyrylamino)benzoyl]amino}benzoate	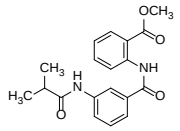
53	10.43	5.44	7.94	7850005	357.4	3-amino-4-(methoxymethyl)-N-(3-methoxyphenyl)-6-methylthieno[2,3-b]pyridine-2-carboxamide	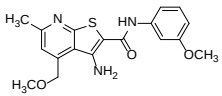
54	7.29	8.37	7.83	9010110	345.4	N-[2-methoxy-5-(2-quinoxalinyl)phenyl]-2-furamide	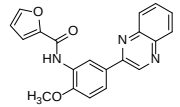
55	10.22	5.27	7.75	7959285	327.4	N-cyclopentyl-9-methyl-4-oxo-4H-pyrido[1,2-a]thieno[2,3-d]pyrimidine-2-carboxamide	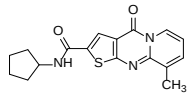
56	9.83	5.56	7.69	7367373	352.4	N-(2-fluorophenyl)-2-([1,2,4]triazolo[4,3-a]quinolin–1-ylthio)acetamide	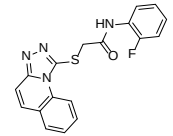
57	7.37	7.91	7.64	6522581	390.5	N,N-diethyl-4-[4-(4-morpholinyl)–1-phthalazinyl]benzamide	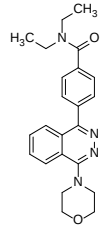

58	8.78	6.48	7.63	7937664	361.4	N-[5-(1,3-benzothiazol-2-yl)-2-methoxyphenyl]nicotinamide	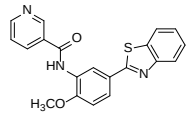
59	8.77	6.42	7.59	7760781	347.4	2-methyl-4-[4-(1-piperidinylcarbonyl)phenyl]–1(2H)-phthalazinone	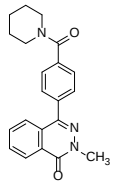
60	*12.74*	7.53	7.53	7239935	302.8	3-chloro-6-methyl-N-3-pyridinyl–1-benzothiophene-2-carboxamide	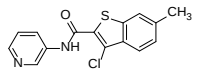
61	*33.16*	7.27	7.27	7440531	318.4	N-(5,5-dimethyl-7-oxo-4,5,6,7-tetrahydro–1,3-benzothiazol-2-yl)-2-fluorobenzamide	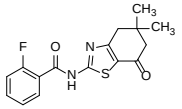
62	7.53	7.01	7.27	6766980	269.3	2-(1-naphthyl)-N–1,3,4-thiadiazol-2-ylacetamide	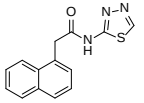
63	7.05	7.33	7.19	7905968	315.4	2-[(2,5-dimethoxyphenyl)amino]-4H-pyrido[3,2-e][1,3]thiazin-4-one	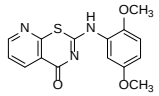
64	8.97	5.31	7.14	7996110	373.5	1-{4-[3-(3-ethoxy-4-methoxyphenyl)–1,2,4-oxadiazol-5-yl]butanoyl}piperidine	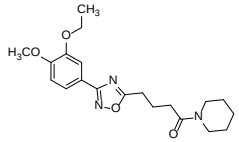

65	8.35	5.83	7.09	7965947	321.3	N-(3-{[(4-methyl-2-pyridinyl)amino]carbonyl}phenyl)-2-furamide	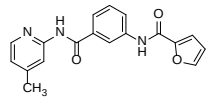
66	10.56	3.51	7.04	6412989	280.3	1-{5-[2-(1-methyl–1H-benzimidazol-2-yl)vinyl]-2-furyl}–1-propanone	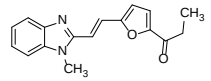
67	8.14	5.81	6.98	7912790	377.4	N-[2-methoxy-5-(2-oxo-2H-chromen-3-yl)phenyl]-2-thiophenecarboxamide	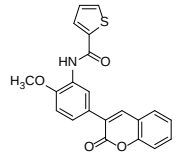
68	7.88	5.69	6.79	6040127	295.8	N-(5-tert-butyl–1,3,4-thiadiazol-2-yl)-3-chlorobenzamide	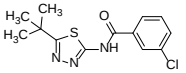
69	8.63	4.84	6.74	5977021	297.4	1-(2-methoxybenzyl)-4-(2-pyridinylmethyl)piperazine	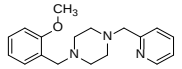
70	8.90	4.51	6.71	7948013	376.4	2-oxo-N-[4-(1-piperidinylcarbonyl)phenyl]-2H-chromene-3-carboxamide	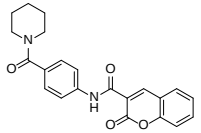
71	7.78	5.56	6.67	6013429	350.4	2-[4-oxo-4-(1-piperidinyl)butyl]–1H-benzo[de]isoquinoline–1,3(2H)-dione	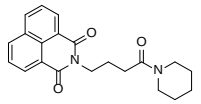
72	5.37	7.75	6.56	01500872	387.8	PALMATINE CHLORIDE	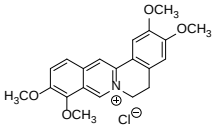

73	7.29	5.56	6.43	9038800	380.4	methyl 5-[(1-benzofuran-2-ylcarbonyl)amino]-2-morpholin-4-ylbenzoate	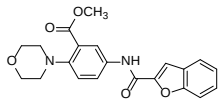
74	3.30	9.40	6.35	01500439	298.4	NORETHYNODREL	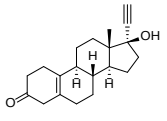
75	7.48	5.06	6.27	7794138	334.4	N-{3-[(3,5-dimethylbenzoyl)amino]phenyl}-2-furamide	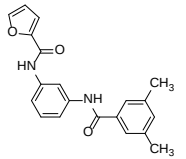
76	7.59	4.87	6.23	6738335	385	N-{3-[(3-bromobenzoyl)amino]phenyl}-2-furamide	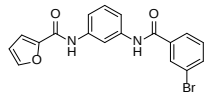
77	5.25	7.11	6.18	01500308	244.2681	FLURBIPROFEN	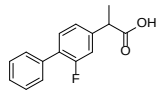
78	*27.39*	6.16	6.16	7367458	325.3	N-(4-methoxyphenyl)-2-[(2-oxo-2H-chromen-7-yl)oxy]acetamide	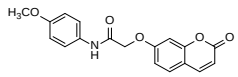
79	6.92	5.11	6.01	7903471	366.2	ethyl-4-{[(4-bromo–1-ethyl–1H-pyrazol-3-yl)carbonyl]amino}benzoate	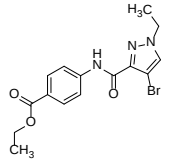

80	6.71	5.27	5.99	7967399	395.8	5-chloro-N-{3-[5-(2-furyl)–1,3,4-oxadiazol-2-yl]phenyl}-2-methoxybenzamide	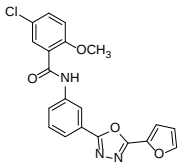
81	6.80	4.82	5.81	00300548	332.4	SPARTEINE SULFATE	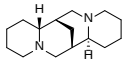
82	5.96	5.56	5.76	01500213	279.1	CYCLOPHOSPHAMIDE HYDRATE	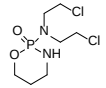
83	6.00	5.51	5.75	7288111	333.4	2-[(2-ethoxybenzoyl)amino]-N,N,4-trimethyl–1,3-thiazole-5-carboxamide	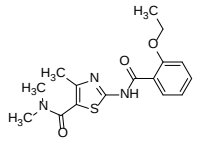
84	7.15	4.30	5.72	01500450	205.6	OXIDOPAMINE HYDROCHLORIDE	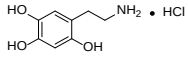
85	8.03	3.25	5.64	6021809	384.2	5-bromo-N-[2-(3-pyridinyl)–1,3-benzoxazol-5-yl]-2-furamide	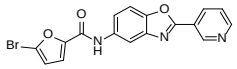
86	*27.24*	5.63	5.63	7414973	322.4	4-methyl-N-[4-(1-piperidinylcarbonyl)phenyl]benzamide	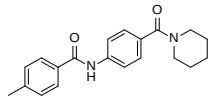
87	5.51	5.74	5.62	7975466	313.7	N-(5-chloro-2-methoxyphenyl)-6-quinoxalinecarboxamide	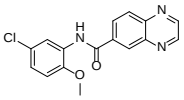

88	6.91	3.93	5.42	7035480	353.4	N-(4-methoxyphenyl)-2-[(4-methyl-2-oxo-2H-chromen-6-yl)oxy]propanamide	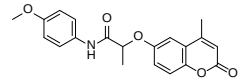
89	6.36	4.35	5.35	9008857	359.4	3-methoxy-N-(2-methyl-4-[1,3]oxazolo[4,5-b]pyridin-2-ylphenyl)benzamide	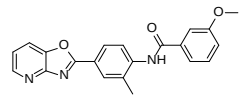
90	5.84	4.59	5.22	7849244	311.4	2-(methylthio)-N-(4-oxo–1,4-dihydro-2-quinazolinyl)benzamide	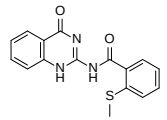
91	6.81	3.57	5.19	7991640	351.8	ethyl 4-({[5-chloro-2-(methylthio)-4-pyrimidinyl]carbonyl}amino)benzoate	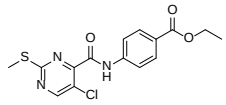
92	5.50	4.82	5.16	9009463	361.4	N-[2-methoxy-5-(2-quinoxalinyl)phenyl]-2-thiophenecarboxamide	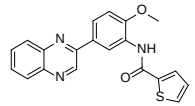
93	4.48	5.83	5.16	01503267	354.4	NOMIFENSINE MALEATE	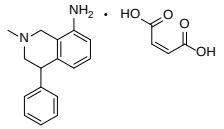

94	5.16	4.86	5.01	6081762	247.3	3,5-dimethyl-N-(5-methyl–1,3,4-thiadiazol-2-yl)benzamide	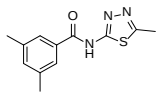
95	3.94	6.05	5.00	01504079	994.1	TOMATINE	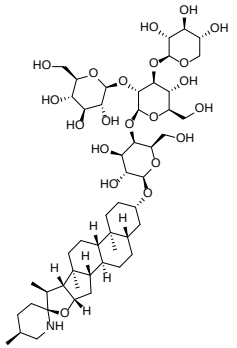
96	6.98	2.87	4.92	6695225	333	2-fluoro-N-(3-[1,3]oxazolo[4,5-b]pyridin-2-ylphenyl)benzamide	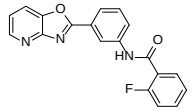
97	5.78	3.95	4.86	9064465	237.6	3-(4-chlorophenyl)-N-methyl–1,2,4-oxadiazole-5-carboxamide	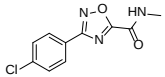
98	4.51	5.16	4.84	01504173	345.7	FLUOXETINE	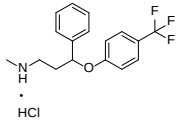
99	6.75	2.90	4.83	7888484	368.4	methyl 2-({4-[(tetrahydro-2-furanylcarbonyl)amino]benzoyl}amino)benzoate	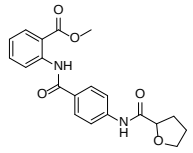

100	3.05	6.60	4.83	7988613	347.3	5-cyclopropyl-N-3-pyridinyl-7-(trifluoromethyl)pyrazolo[1,5-a]pyrimidine-2-carboxamide	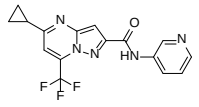
101	5.16	4.40	4.78	5360051	338.2	3-bromo-N-(2,6-dimethoxy-4-pyrimidinyl)benzamide	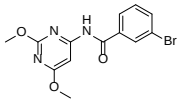
102	5.64	3.88	4.76	01503092	178.1	GLUCONOLACTONE	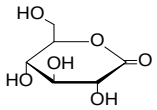
103	4.82	4.66	4.74	9011206	337.8	N-[5-(1H-benzimidazol-2-yl)-2-chlorophenyl]-2-furamide	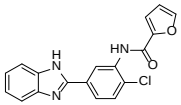
104	6.84	2.60	4.72	7588223	272.3	3-(cyclopentylamino)–1-(3-methylphenyl)-2,5-pyrrolidinedione	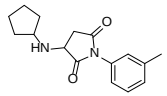
105	4.97	4.43	4.70	6725477	329.4	2-methyl-N-(4-[1,3]oxazolo[4,5-b]pyridin-2-ylphenyl)benzamide	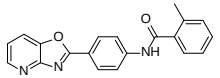
106	5.30	4.07	4.69	7650421	297.3	N-(4-methoxyphenyl)–1-oxo-3,4-dihydro–1H-isochromene-3-carboxamide	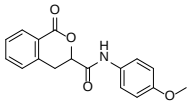

107	3.46	5.87	4.67	6233363	398.9	N~1~-(4-chlorophenyl)-N~2~-(2,4-dimethoxyphenyl)-N~2~-(methylsulfonyl)glycinamide	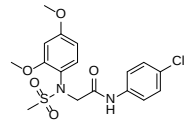
108	5.79	3.54	4.66	6955524	363.5	3-amino-N-(5-ethyl–1,3,4-thiadiazol-2-yl)-4-(methoxymethyl)-6-methylthieno[2,3-b]pyridine-2-carboxamide	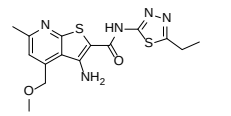
109	141.21	4.65	4.65	01300029	195.2	MEGLUMINE	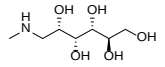
110	5.21	4.00	4.61	9025773	337.4	N-{4-[5-(2-furyl)–1,3,4-oxadiazol-2-yl]phenyl}cyclohexanecarboxamide	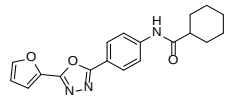
111	4.18	4.99	4.58	7013997	355.4	[2-(4-tert-butyl-2-methylphenoxy)ethyl](2-methoxyethyl)amine oxalate	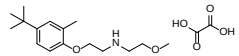
112	3.50	5.59	4.55	7956221	394.4	methyl 2-({2-methyl-3-[(2-thienylcarbonyl)amino]benzoyl}amino)benzoate	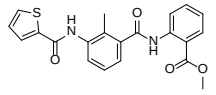
113	2.07	6.70	4.39	5576336	295.4	N-[5-(ethylthio)–1,3,4-thiadiazol-2-yl]-3-methoxybenzamide	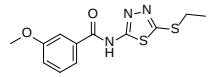

114	2.76	5.98	4.37	9010207	307.4	N-{3-[5-(2-methylphenyl)–1,3,4-oxadiazol-2-yl]phenyl}propanamide	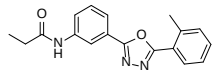
115	2.09	6.63	4.36	6430817	275.4	N-(3,4-dimethylphenyl)-2-[(1-methyl–1H-imidazol-2-yl)thio]acetamide	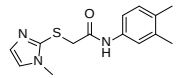
116	4.01	4.66	4.34	6719009	362.4	N-{3-[(2-thienylcarbonyl)amino]phenyl}–1-benzofuran-2-carboxamide	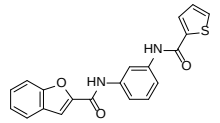
117	*22.76*	4.28	4.28	9053934	353.8	N-(4-chloro-2,5-dimethoxyphenyl)-2-[(4-methyl-2-pyrimidinyl)thio]acetamide	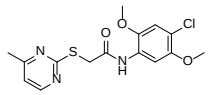
118	5.49	3.07	4.28	5140897	175.2	1-phenyl–1H–1,2,4-triazole-3,5-diamine	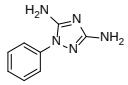
119	4.78	3.72	4.25	7746407	385.4	methyl 4-({[3-amino-4-(methoxymethyl)-6-methylthieno[2,3-b]pyridin-2-yl]carbonyl}amino)benzoate	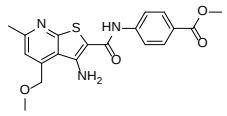
120	4.24	4.25	4.25	01505715	241.2	PANTOTHENIC ACID(d) Na salt	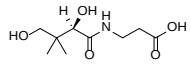
121	2.24	6.03	4.13	01500380	344.4	MEDRYSONE	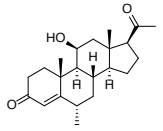

122	*13.67*	4.13	4.13	9016281	373.4	2-methoxy-3-methyl-N-(2-methyl-5-[1,3]oxazolo[4,5-b]pyridin-2-ylphenyl)benzamide	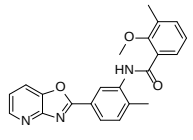
123	3.60	4.61	4.10	7240114	373.2	3-iodo-N-(5-isopropyl–1,3,4-thiadiazol-2-yl)benzamide	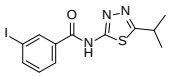
124	5.01	2.90	3.95	7815100	389.9	4-(5-chloro-2-methylphenyl)-N-(2,5-dimethoxyphenyl)–1-piperazinecarboxamide	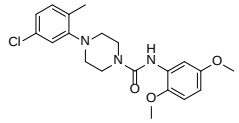
125	3.56	4.22	3.89	7947685	*379*	5-bromo-2-chloro-N-[5-(ethylthio)–1,3,4-thiadiazol-2-yl]benzamide	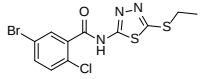
126	3.04	4.70	3.87	5932561	295.4	N-(4-methoxyphenyl)–1-phenylcyclopentanecarboxamide	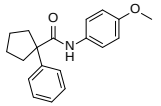
127	3.03	4.68	3.85	01504567	433.5	MYCOPHENOLATE MOFETIL	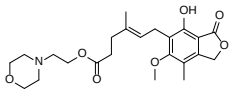

128	4.77	2.72	3.74	7999638	339.4	2-[2-(3,4-dimethoxyphenyl)vinyl]-5-(1-piperidinyl)–1,3-oxazole-4-carbonitrile	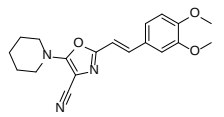
129	3.67	3.79	3.73	00300564	154.2	MENTHONE	
130	2.81	4.57	3.69	6159633	273.4	1-(cyclohexylcarbonyl)-4-(2-pyridinyl)piperazine	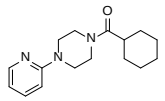
131	4.12	3.19	3.65	6943365	324.4	5-(diethylsulfonio)–1-(4-fluorobenzyl)-2,6-dioxo–1,2,3,6-tetrahydro-4-pyrimidinolate	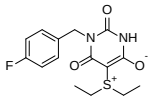
132	3.75	3.45	3.60	7887983	375.8	2-chloro-N-[4-(5-phenyl–1,3,4-oxadiazol-2-yl)phenyl]benzamide	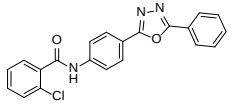
133	3.96	3.18	3.57	7682260	335.4	5-(4-methoxyphenyl)-7-(2-methylphenyl)-4,5,6,7-tetrahydro[1,2,4]triazolo[1,5-a]pyrimidin-2-amine	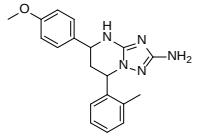
134	*7.80*	3.56	3.56	9025775	310.3	7-(1,3-benzodioxol-5-ylmethoxy)-4-methyl-2H-chromen-2-one	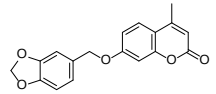

135	2.66	4.28	3.47	01500401	398.3	METHSCOPOLAMINE BROMIDE	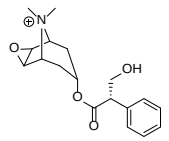
136	1.86	4.99	3.43	9038064	361.5	4-[(1,6-dimethyl-3,4-dihydropyrrolo[1,2-a]pyrazin-2(1H)-yl)carbonyl]-N,N-dimethylbenzenesulfonamide	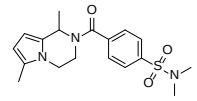
137	3.26	3.48	3.37	6778405	391.2	5-bromo-N-{3-[(2-thienylcarbonyl)amino]phenyl}-2-furamide	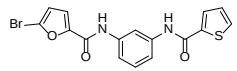
138	*16.56*	3.31	3.31	7953705	397.4	3,4,5-trimethoxy-N-[4-(2-thienylcarbonyl)phenyl]benzamide	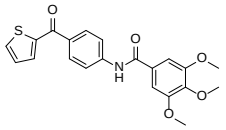
139	3.24	3.30	3.27	7946783	287	N-(4,6-dimethyl-2-pyrimidinyl)-4,5,6,7-tetrahydro–1-benzothiophene-2-carboxamide	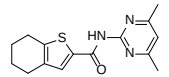
140	1.97	4.45	3.21	6080049	218.3	7-ethoxy-4,8-dimethyl-2H-chromen-2-one	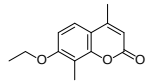

141	*18.94*	3.21	3.21	9017829	360.4	2-{[(4-methyl-6-phenyl-2-pyrimidinyl)thio]methyl}-4(3H)-quinazolinone	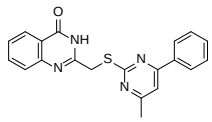
142	3.10	3.08	3.09	9035014	349.4	2-(3,4-dimethoxyphenyl)-5-{[(2-methyl–1,3-thiazol-4-yl)methyl]thio}–1,3,4-oxadiazole	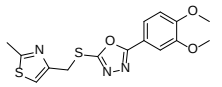
143	3.26	2.89	3.07	5920020	391.5	N-(4-acetylphenyl)-2-[(5-methyl-5H-[1,2,4]triazino[5,6-b]indol-3-yl)thio]acetamide	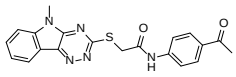
144	2.40	3.68	3.04	5967862	309.4	5,6-dimethyl-2-[(4,6,7-trimethyl-2-quinazolinyl)amino]-4(1H)-pyrimidinone	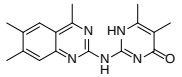
145	3.74	2.30	3.02	6698327	373.4	N-(3-[1,3]oxazolo[4,5-b]pyridin-2-ylphenyl)-2,3-dihydro–1,4-benzodioxine-6-carboxamide	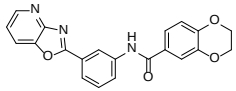
146	2.58	3.36	2.97	5932619	349.3	4-methyl-N-[4-(3-pyridinyl)–1,3-thiazol-2-yl]-2-pyridinamine hydrobromide	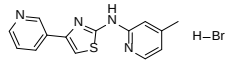
147	2.02	3.51	2.77	6303674	339	N-(4-acetylphenyl)-2-[(5-methyl–1H-benzimidazol-2-yl)thio]acetamide	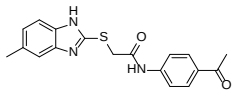

148	2.50	2.98	2.74	5150578	368.5	N-{3-[(cyclohexylamino)methyl]-4,5,6,7-tetrahydro–1-benzothien-2-yl}benzamide	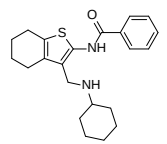
149	2.24	3.17	2.71	6097291	335.4	N-[3-(3,4-dimethylbenzoyl)phenyl]-2-thiophenecarboxamide	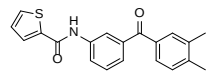
150	1.65	3.59	2.62	7982108	383.2	N-(2-bromophenyl)-3-methyl-2-oxo-2,3-dihydro–1,3-benzoxazole-6-sulfonamide	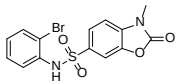
151	1.33	3.87	2.60	01500324	270.0	HALAZONE	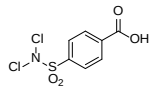
152	1.87	3.25	2.56	5847086	276.7	5-chloro-2-methoxy-N-(4-methyl-2-pyridinyl)benzamide	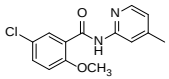
153	1.95	2.79	2.37	9037834	338.4	N-cyclohexyl-N,1-dimethyl-4-oxo–1,4-dihydropyrido[1,2-a]pyrrolo[2,3-d]pyrimidine-2-carboxamide	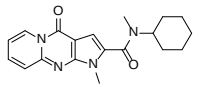
154	1.36	3.24	2.30	6985863	386.4	N-(2,4-dimethoxyphenyl)–1-(4-fluorobenzoyl)-4-piperidinecarboxamide	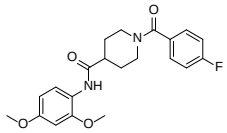

155	1.82	2.58	2.20	7925769	359	4-[(4-methyl–1-piperazinyl)sulfonyl]-N-phenylbenzamide	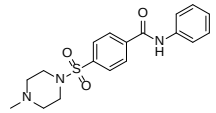
156	1.68	2.66	2.17	7254774	332.4	N-[3-methoxy-4-(pentanoylamino)phenyl]-2-thiophenecarboxamide	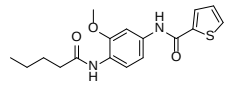
157	1.44	2.80	2.12	9001373	312.4	N-(2,4-dimethylphenyl)-2-(3H-imidazo[4,5-b]pyridin-2-ylthio)acetamide	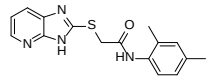
158	1.77	2.47	2.12	6039445	355.4	2-methoxy-N-{5-[(4-methylphenoxy)methyl]–1,3,4-thiadiazol-2-yl}benzamide	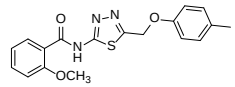
159	1.51	2.73	2.12	6207364	259.3	N-(3-methoxyphenyl)-N-(methylsulfonyl)glycine	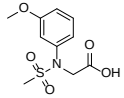
160	2.00	2.19	2.09	6317347	363.5	2-{[6-(acetylamino)–1,3-benzothiazol-2-yl]thio}-N-cyclohexylacetamide	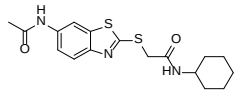
161	1.96	2.20	2.08	5921934	316.4	ethyl [(5-ethyl-5H-[1,2,4]triazino[5,6-b]indol-3-yl)thio]acetate	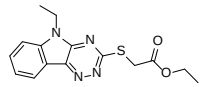

162	1.37	2.71	2.04	7878578	384.5	N-[4-(acetylamino)phenyl]-3-amino-4-(methoxymethyl)-6-methylthieno[2,3-b]pyridine-2-carboxamide	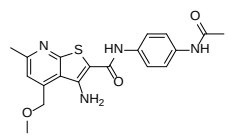
163	1.44	2.64	2.04	5942394	337.4	N-(2,5-dimethoxyphenyl)-2-(2-naphthyloxy)acetamide	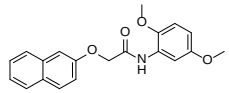
164	1.73	2.28	2.01	6835420	310.3	6-fluoro-4-(4-nitrophenyl)-3a,4,5,9b-tetrahydro-3H-cyclopenta[c]quinoline	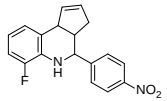
165	1.02	2.99	2.01	7949438	259.4	2-phenyl-N-(2-thienylmethyl)butanamide	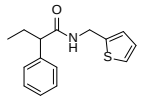
166	1.42	2.55	1.98	7999574	397.4	3,11-bis(2-furylmethyl)-3,11-dihydro-4H-pyrimido[5',4':4,5]pyrrolo[2,3-b]quinoxalin-4-one	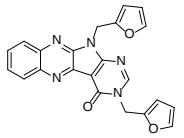
167	1.63	2.28	1.96	5143670	347.8	N-(6-chloro-2-phenylimidazo[1,2-a]pyridin-3-yl)benzamide	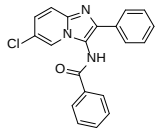
168	1.76	2.11	1.93	6303049	357.5	N-[4-(acetylamino)phenyl]-2-(1,3-benzothiazol-2-ylthio)acetamide	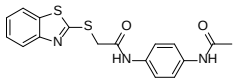

169	1.25	2.45	1.85	5859874	245.3	N-(4-fluorophenyl)-N'-(5-methyl-2-pyridinyl)urea	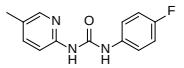
170	1.28	2.20	1.74	5834944	386.4	10-(1-pyrrolidinylcarbonyl)-7-(trifluoromethyl)-5,6-dihydrobenzo[h]pyrazolo[5,1-b]quinazoline	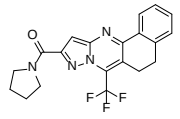
171	1.00	2.20	1.60	7649211	369.4	N-(2,5-dimethoxyphenyl)-2-(6,7-dimethyl-3-oxo–1,2,3,4-tetrahydro-2-quinoxalinyl)acetamide	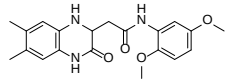

Note. The names of the compounds from the MicroSource Spectrum Collection are CAPITALIZED and the corresponding Compound number refers to the number in that collection. All other compounds are from the ChemBridge library.

Table S3. Structure-activity characterization of 4-methyl-7-[(3,4,5-trimethoxybenzyl)oxy]-2H-chromen-2-one derivatives.

Structure	Compound Name ChemBridge # or Identification #	EC_{50} 5-FUrd growth rescue of *fui1*Δ::PfENT1HA-CO (μM)	IC_{50} *ade2*Δ + PfENT1-CO adenosine growth inhibition (μM)	IC_{50} *ade2*Δ + PfENT1-CO [^{3}H]-adenosine uptake inhibition (nM)	IC_{50} [^{3}H]-adenosine uptake into parasites (nM)	IC_{50} 3D7 (CQS) Parasite viability – low purine (μM)	IC_{50} 3D7 (CQS) Parasite viability – high purine (μM)	IC_{50} Dd2 (CQR) Parasite viability – high purine (μM)
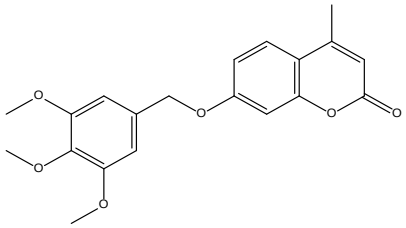	4-methyl-7-[(3,4,5-trimethoxybenzyl)oxy]-2H-chromen-2-one 6946484	2.3 ± 0.9	0.6 ± 0.1	2.4 ± 1.5	6.4 ± 3.0	19.2 ± 4.3	41.0 ± 4.3	36.2 ± 6.0
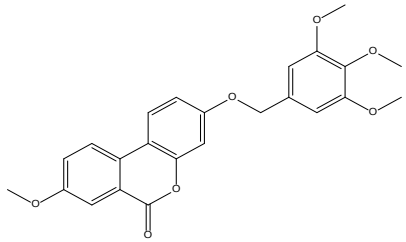	8-methoxy-3-[(3,4,5-trimethoxybenzyl)oxy]-6H-benzo[c]chromen-6-one 6943060	NE	NE	NE	NE	NE	NE	NE
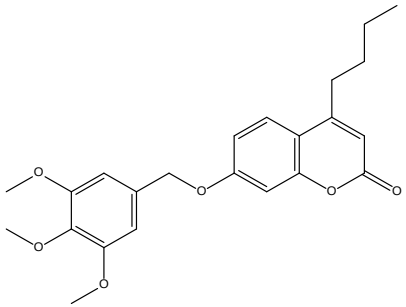	4-butyl-7-[(3,4,5-trimethoxybenzyl)oxy]-2H-chromen-2-one 6945908	209 ± 154 *	1.3 ± 0.8	38.3 ± 39.7	46.1 ± 4.2	45.4 ± 2.3	49.4 ± 2.2	

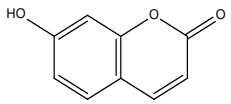	Umbelliferone 7-hydroxycoumarin	NE	NE			NE	NE	
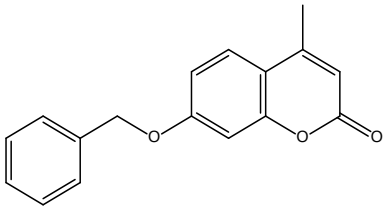	4-methyl-7-benzyl-oxy-2H-chromen-2-one AKR–121	47.9 ± 19 *	2.4 ± 0.6			49.4 ± 4.9	49.0 ± 4.5	29.7 ± 3.5
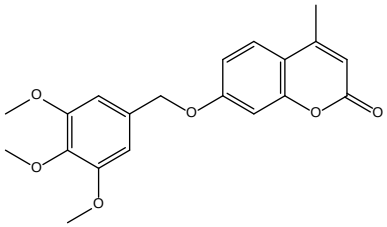	4-methyl-7-[(3,4,5-trimethoxybenzyl)oxy]-2H-chromen-2-one AKR–122 (6946484)	6.8 ± 1.1 n = 3	0.6 ± 0.2			7.5 ± 1.0	6.9 ± 1.5	5.7 ± 0.5
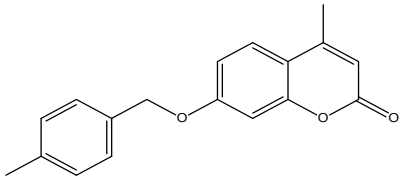	4-methyl-7-[(4-methylbenzyl)oxy]-2H-chromen-2-one AKR–124	>1000 *	3.7 ± 2.1 *			30.1 ± 3.2 *	29.3 ± 3.1 *	
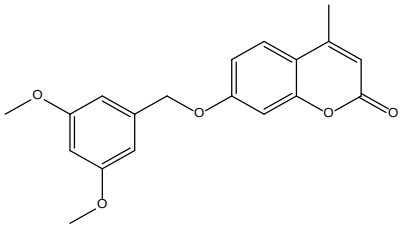	4-methyl-7-[(3,5-dimethoxybenzyl)oxy]-2H-chromen-2-one AKR–125	>1000 *	0.9 ± 0.2 *			30.1 ± 1.9 *	41.8 ± 5.5 *	
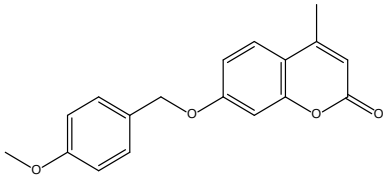	4-methyl-7-[(4-methoxybenzyl)oxy]-2H-chromen-2-one AKR–142	123 ± 57.9	1.6 ± 0.4 *			42.1 ± 6.8	36.1 ± 6.7	

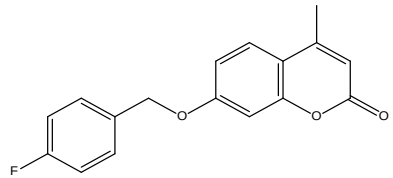	4-methyl-7-[(4-fluorobenzyl)oxy]-2H-chromen-2-one AKR–144	>1000 *	3.3 ± 2.5 *			39.7 ± 4.7 *	43.2 ± 0.1 *	
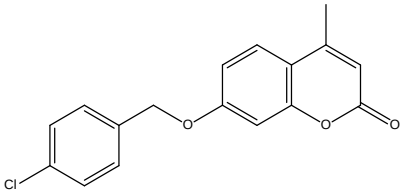	4-methyl-7-[(4-chlorobenzyl)oxy]-2H-chromen-2-one AKR–146	NE	19.3 ± 25.2 *			39.7 ± 7.4 *	37.5 ± 6.9 *	39.7 ± 7.4 *

All values are mean XC_{50} ± SD, n ≥ 3 biological replicates

XC_{50} indicates both EC_{50} and/or IC_{50}

NE = compound has no effect

Empty cells, not tested

CQS, chloroquine sensitive strain

CQR, chloroquine resistance strain

*Compound solubility limited our ability to perform complete concentration-response curves for these compounds. Available data was fit by fixing the minimum or maximum to zero or 100%. For these compounds, IC_{50} and EC_{50} values thus represent approximations of the actual values.

Chemical Synthesis and Characterization Of Compounds Used In This Study

All of the compounds were prepared according to the procedure reported by Lévai and Jekö [4].

Melting points were determined on a Mel-Temp II Laboratory Devices apparatus and are reported uncorrected. ^{1}H NMR and ^{13}C NMR spectra were recorded on an Agilent 400-MR 400-MHz NMR spectrometer. Chemical shifts are reported in parts per million using the residual proton or carbon signal ($(CD_3)_2CO$: δ_H 2.05, δ_c 29.84) as an internal reference. The apparent multiplicity (s = singlet, d = doublet, t = triplet, q = quartet, m = multiplet) and coupling constants (in Hz) are reported in that order in the parentheses after the chemical shift. Liquid chromatography and mass spectrometry were performed on a Shimadzu LCMS-2010 liquid chromatograph-mass spectrometer. High-resolution mass spectrometry was done by Dr. Yasuhiro Itagaki at Columbia University. Elemental analyses were performed by Atlantic Microlab, Inc. (Norcross, GA).

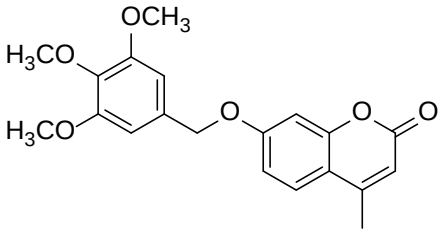

mp: 101.5–103.0 °C; 1H NMR (400 MHz, (CD3)2CO): δ 7.69 (d, *J* = 8.8 Hz, 1H), 7.02 (dd, *J* = 8.8 Hz, *J* = 2.4 Hz, 1H), 6.97 (d, *J* = 2.4 Hz, 1H), 6.84 (s, 2H), 6.13 (q, *J* = 1.2 Hz, 1H) 5.18 (s, 2H), 3.84 (s, 6H), 3.73 (s, 3H), 2.44 (d, *J* = 1.2 Hz, 3H); 13C NMR (101 MHz, (CD3)2CO): δ 162.8, 160.8, 156.2, 154.6, 153.7, 139.1, 132.9, 127.1, 114.5, 113.4, 112.5, 106.2, 102.5, 71.3, 60.5, 56.5, 18.5; LC-MS (M^+-H): 355.

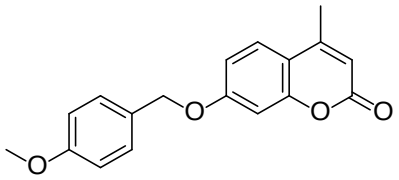

mp: 113.0-115.0 °C; 1H NMR (400 MHz, (CD3)2CO): δ 7.67 (d, *J* = 8.8 Hz, 1H), 7.44 (d, *J* = 8.8 Hz, 2H), 7.01-6.95 (m, *4*H), 6.12 (q, *J* = 1.2 Hz, 1H) 5.18 (s, 2H), 3.81 (s, 3H), 2.43 (d, *J* = 1.2 Hz, 3H); 13C NMR (101 MHz, (CD3)2CO): δ 162.9, 160.9, 160.7, 153.7, 130.4, 129.4, 127.0, 114.8, 114.4, 113.5, 112.4, 102.5, 70.9, 55.6, 18.5; LC-MS (M^+-H): 295; analysis (calcd., found for C18H16O4): C (72.96, 72.68), H (5.44, 5.57).

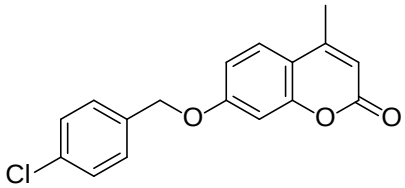

*1H NMR (400 MHz, (CD3)2CO): δ 7.69 (d, *J* = 8.8 Hz, 1H), 7.55 (d, *J* = 8.4 Hz 2H), 7.45 (dt, *J* = 8.4 Hz, *J* = 2.4 Hz, 2H),7.02 (dd, *J* = 8.8 Hz, *J* = 2.4 Hz, 1H), 6.97 (d, *J* = 2.4 Hz, 1H), 6.13 (dd, *J* = 2.4 Hz, *J* = 1.2 Hz, 1H) 5.28 (s, 2H), 2.44 (d, *J* = 1.6 Hz, 3H); 13C NMR (101 MHz, (CD3)2CO): δ 162.5, 160.8, 153.7, 136.6, 134.3, 130.3, 129.5, 127.1, 114.7, 113.4, 112.6, 102.6, 70.2, 18.5.

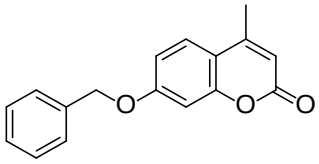

mp: 118.0-118.5 °C (lit.ref 129-130 °C){Jain, 1986 #65}; 1H NMR (400 MHz, (CD3)2CO): δ 7.69 (d, *J* = 9.2 Hz, 1H), 7.52 (d, *J* = 7.2 Hz, 2H), 7.42 (tt, *J* = 7.2 Hz, *J* = 1.2 Hz, 2H),7.35 (tt, *J* = 7.2 Hz, *J* = 1.2 Hz, 1H), 7.02 (dd, *J* = 8.8 Hz, *J* = 2.4 Hz, 1H), 6.97 (d, *J* = 2.4 Hz, 1H), 6.13 (q, *J* = 1.2 Hz, 1H) 5.27 (s, 2H), 2.44 (d, *J* = 1.6 Hz, 3H); 13C NMR (101 MHz, (CD3)2CO): δ 162.7, 160.8, 156.2, 153.7, 137.6, 129.4, 128.9, 128.6, 127.1, 114.5, 113.4, 112.5, 102.5, 71.0, 18.5; LC-MS (M^+-H): 265; analysis (calcd., found for C17H14O3): C (76.68, 76.51), H (5.30, 5.30).

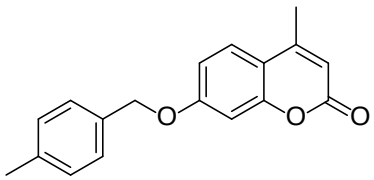

*1H NMR (400 MHz, (CD3)2CO): δ 7.68 (d, *J* = 8.8 Hz, 1H), 7.39 (d, *J* = 8.0 Hz 2H), 7.23 (d, *J* = 7.6 Hz), 7.00 (dd, *J* = 8.8 Hz, *J* = 2.4 Hz, 1H), 6.95 (d, *J* = 2.4 Hz, 1H), 6.12 (dd, *J* = 2.4 Hz, *J* = 1.2 Hz, 1H), 5.21 (s, 2H), 2.43 (d, *J* = 1.2 Hz, 3H), 2.34 (s, 3H); 13C NMR (101 MHz, (CD3)2CO): δ 162.8, 160.8, 156.3, 153.7, 134.5, 130.0, 128.7, 127.1, 114.5, 113.5, 112.5, 102.5, 71.0, 21.2, 18.5.

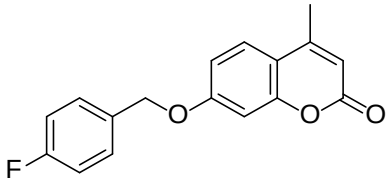

*1H NMR (400 MHz, (CD3)2CO): δ 7.69 (d, *J* = 8.8 Hz, 1H), 7.58 (dd, *J* = 9.2 Hz, *J* = 6.0 Hz, 2H), 7.18 (t, *J* = 9.2 Hz, 2H), 7.02 (dd, *J* = 8.8 Hz, *J* = 2.4 Hz), 6.97 (d, *J* = 2.4 Hz, 1H) 6.13 (s, 1H), 5.25 (s, 2H), 2.44 (d, *J* = 1.2 Hz, 3H); 13C NMR (101 MHz, (CD3)2CO): δ 163.4 ($^1J_{C\text{-}F}$ = 244.9 Hz), 162.6, 160.8, 156.2, 153.7,

133.7 ($^4J_{C\text{-}F}$ = 3.8 Hz), 130.8 ($^3J_{C\text{-}F}$ = 8.5 Hz), 127.1, 116.1 ($^2J_{C\text{-}F}$ = 21.3 Hz), 114.6, 113.4, 112.6, 102.5, 70.3, 18.5.

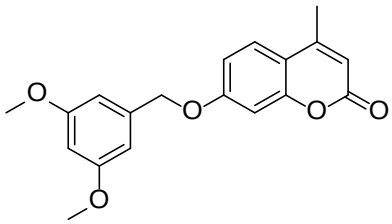

mp: 175.0-175.5 °C; 1H NMR (400 MHz, (CD3)2CO): δ 7.69 (d, *J* = 9.2 Hz, 1H), 7.02 (dd, *J* = 8.8 Hz, *J* = 2.4 Hz), 6.95 (d, *J* = 2.4 Hz, 1H), 6.67 (s, 2H), 6.46 (s, 1H), 6.13 (s, 1H), 5.21 (s, 2H), 3.79 (s, 6H), 2.44 (s, 3H); 13C NMR (101 MHz, (CD3)2CO): δ 162.7, 162.2, 156.2, 153.7, 139.9, 127.1, 114.6, 113.5, 112.5, 106.3, 102.6, 100.4, 70.9, 55.7, 18.5; FAB + HRMS (*m*/*z*): [M]+ calcd. for C19H19O5: 327.1227, Found: 327.1237.

*****known compounds as reported previously (*4*)

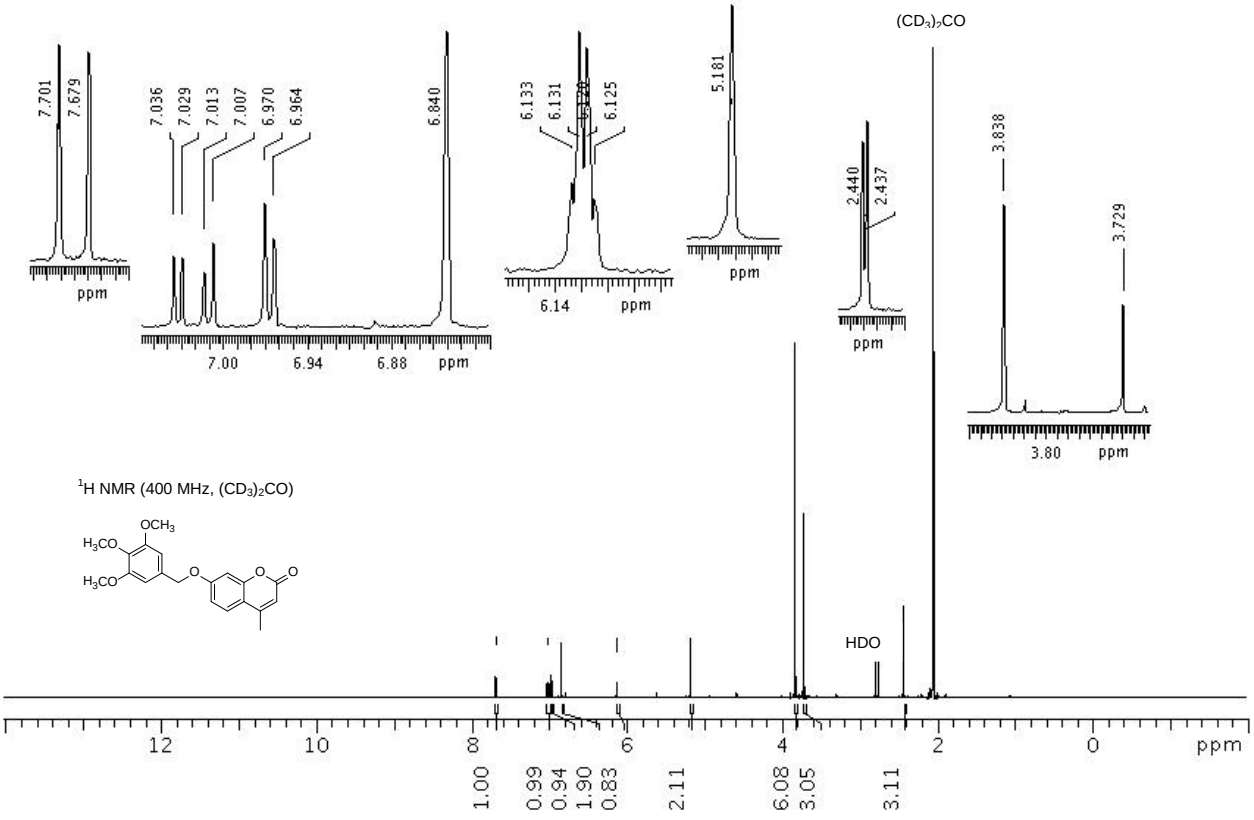

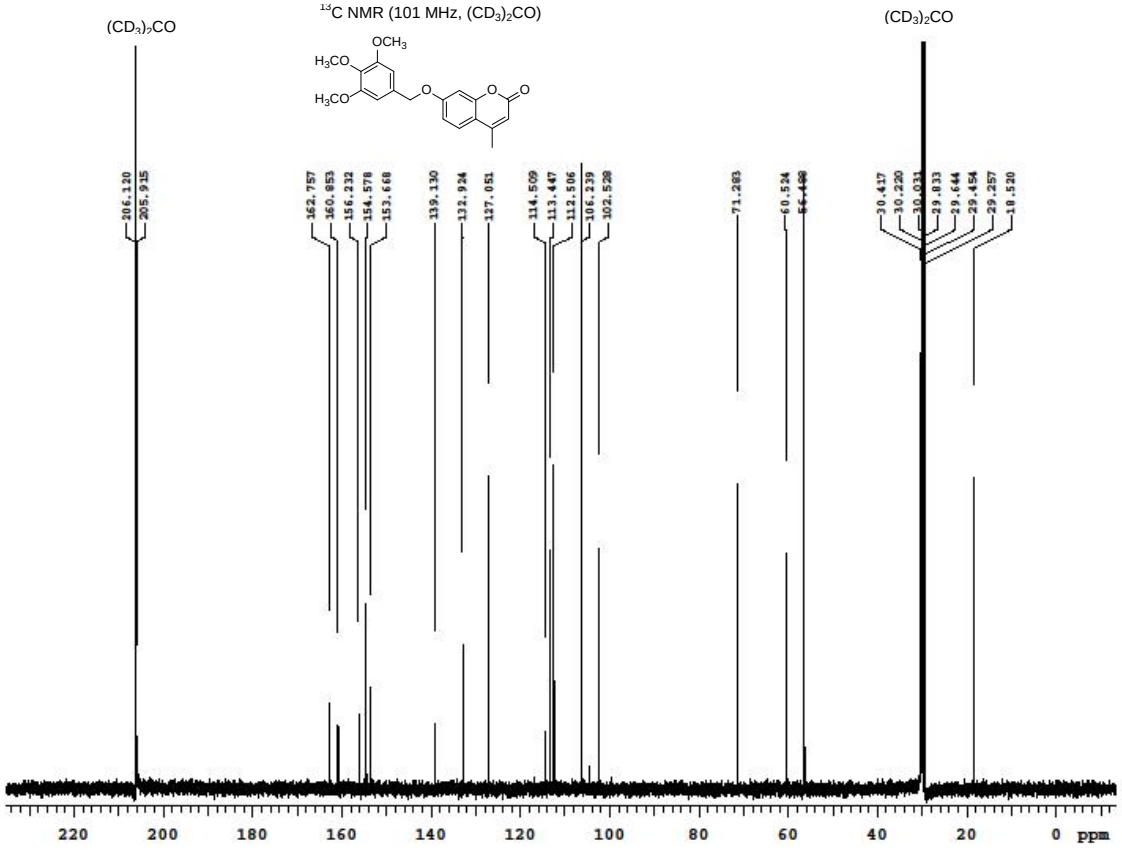
^{13}C NMR (101 MHz, $(CD_3)_2CO$)
$(CD_3)_2CO$
$(CD_3)_2CO$
OCH3
H3CO
H3CO
O
O
O
206.120
205.915
162.757
160.853
156.232
154.578
153.668
139.130
132.924
127.051
114.509
113.447
112.506
106.239
102.528
71.283
60.524
30.417
30.220
30.031
29.833
29.644
29.454
29.257
18.520
220
200
180
160
140
120
100
80
60
40
20
0 ppm

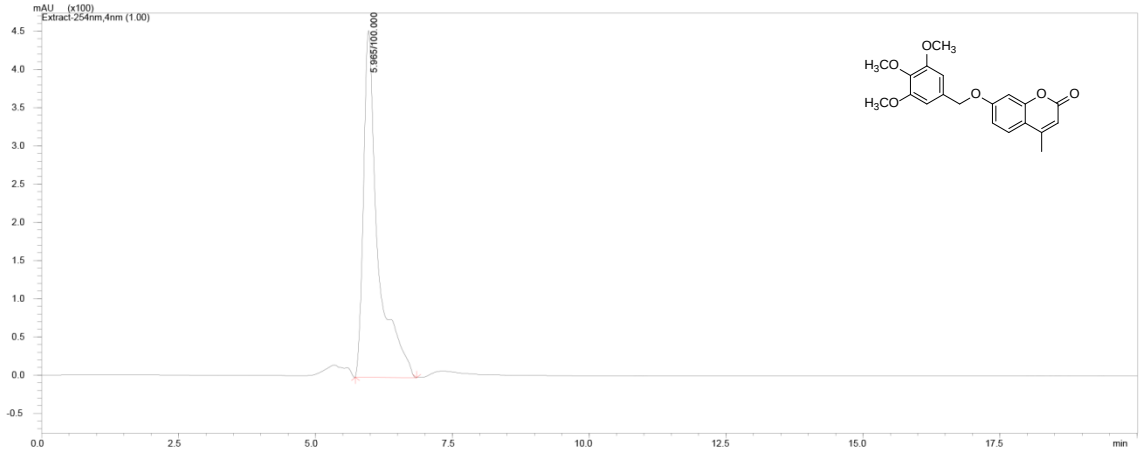

MS Spectrum Graph

Ret.Time:6.895(Scan#:395)
BG Mode:?
Mass Peaks:730 Base Peak:145.90(5604186) Polarity:Pos Segment1 - Event1

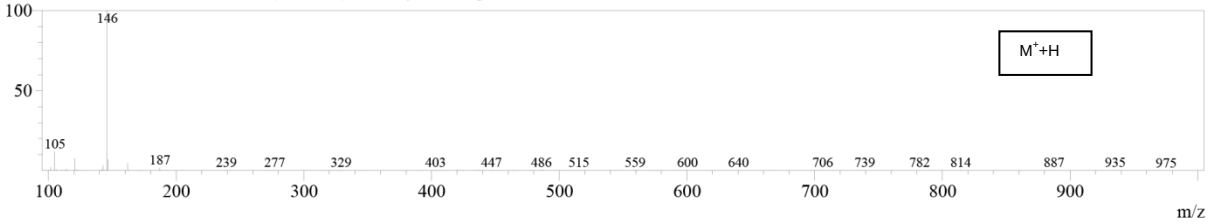

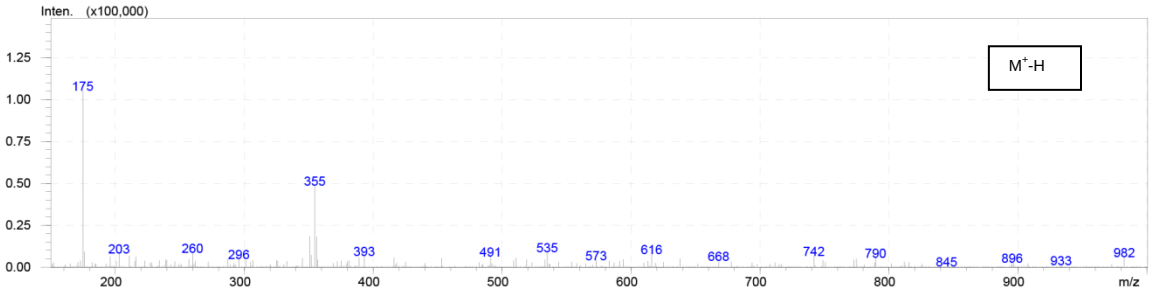

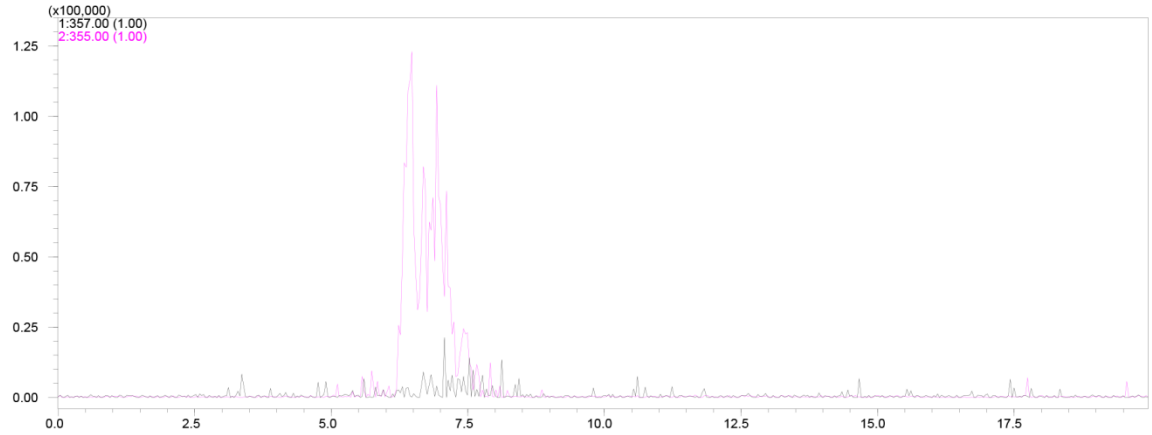

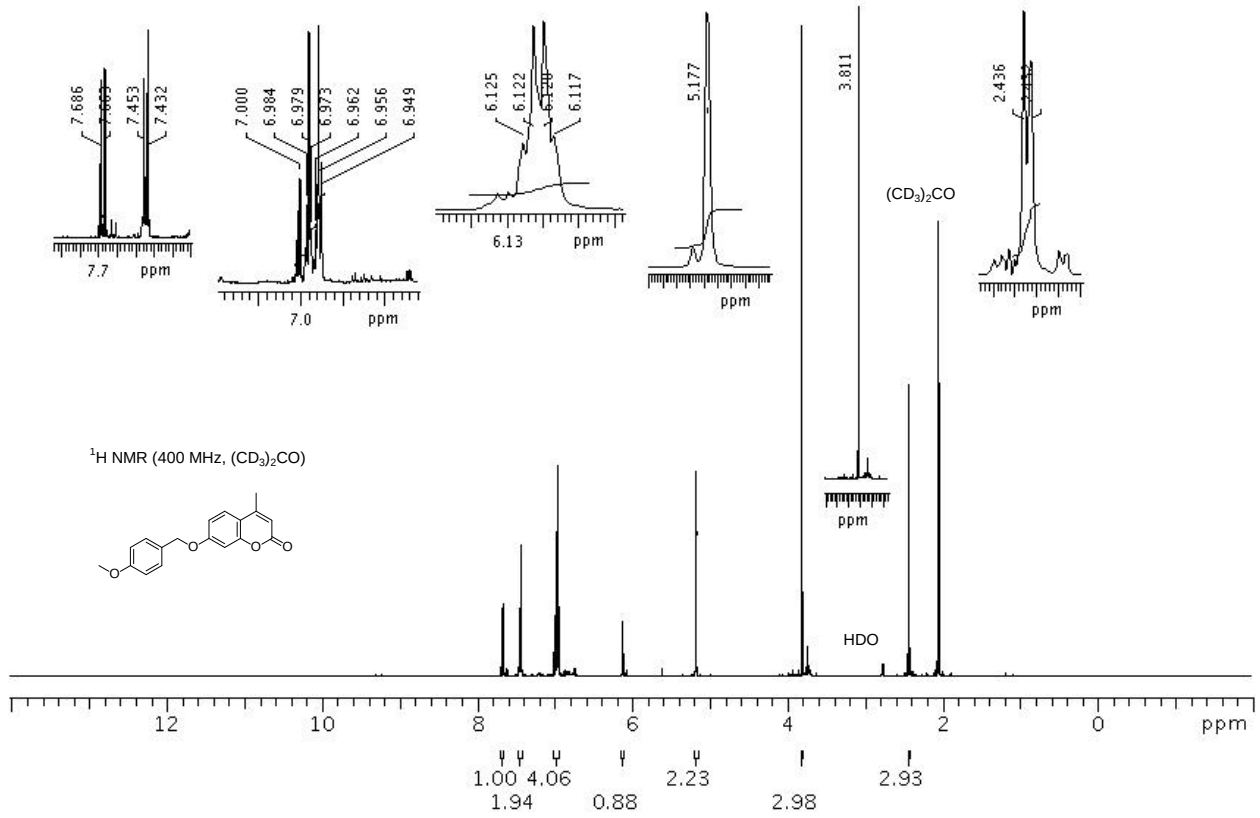
7.686
7.663
7.453
7.432
7.7 ppm
7.000
6.984
6.979
6.973
6.962
6.956
6.949
7.0 ppm
6.125
6.122
6.120
6.117
6.13 ppm
5.177
ppm
3.811
ppm
2.436
ppm
(CD3)2CO
HDO
1H NMR (400 MHz, (CD3)2CO)
12
10
8
6
4
2
0
ppm
1.00 4.06 2.23 2.93
1.94 0.88 2.98

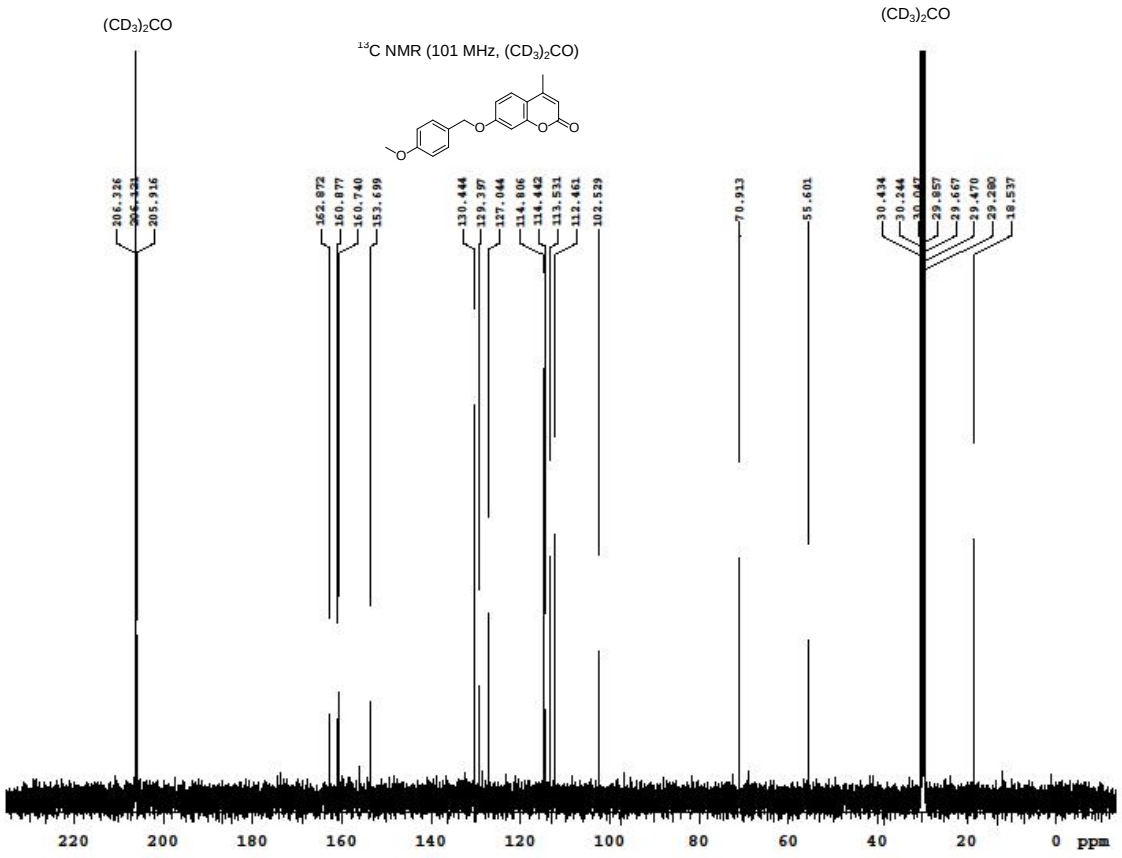
(CD3)2CO
13C NMR (101 MHz, (CD3)2CO)
(CD3)2CO
206.326
206.131
205.916
162.872
160.877
160.740
153.699
130.444
129.397
127.044
114.806
114.442
113.531
112.461
102.529
70.913
55.601
30.434
30.244
30.047
29.857
29.667
29.470
29.280
18.537
220
200
180
160
140
120
100
80
60
40
20
0 ppm

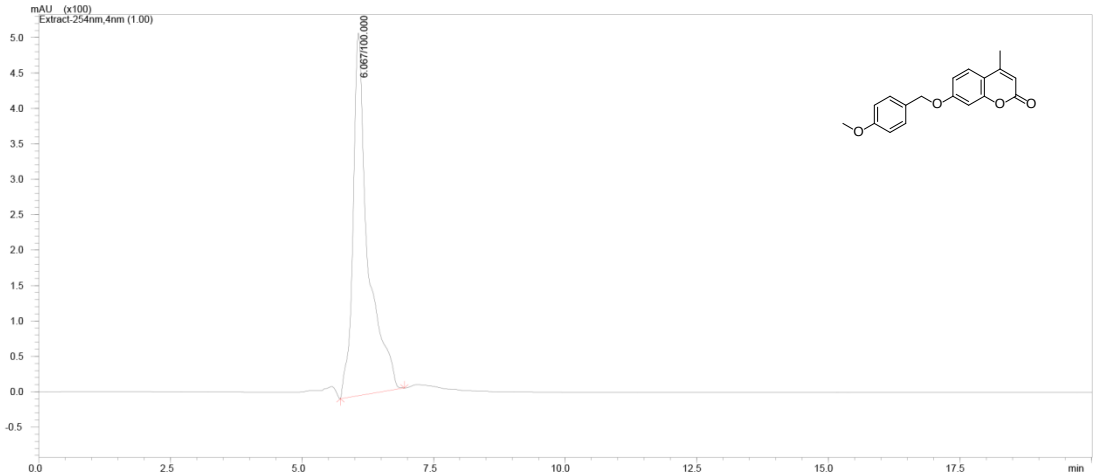

MS Spectrum Graph

Ret.Time:6.440(Scan#:369)
BG Mode:?
Mass Peaks:352 Base Peak:145.90(4957807) Polarity:Pos Segment1 - Event1

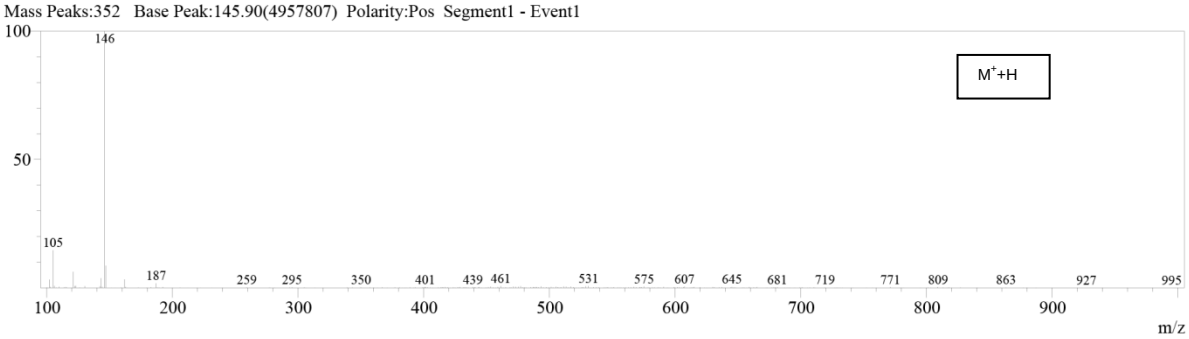

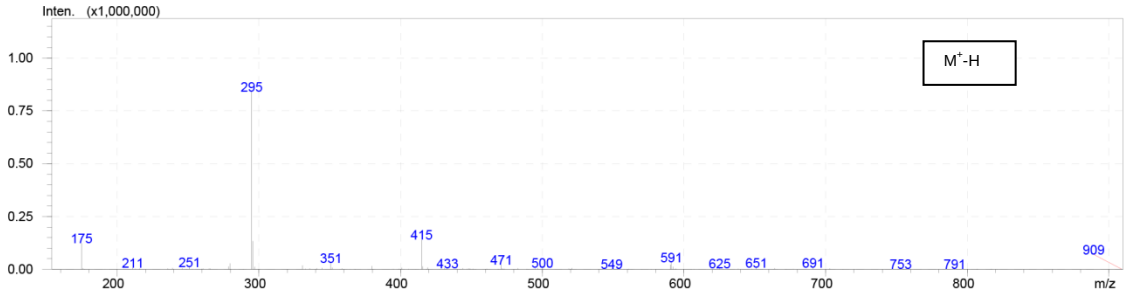

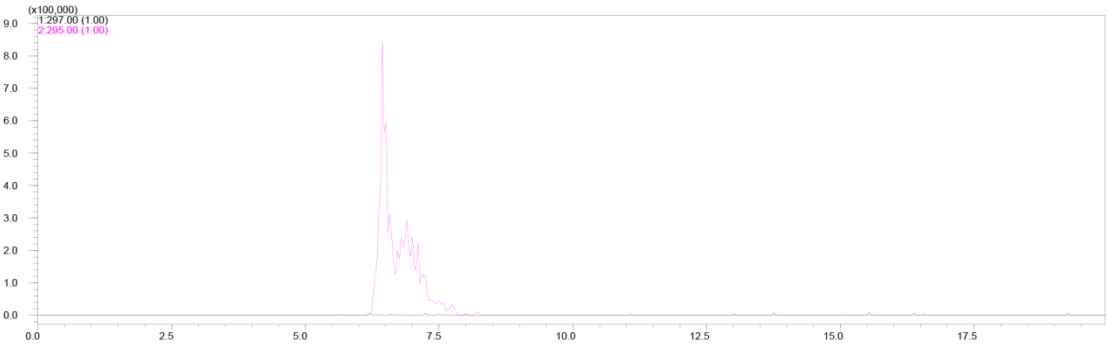

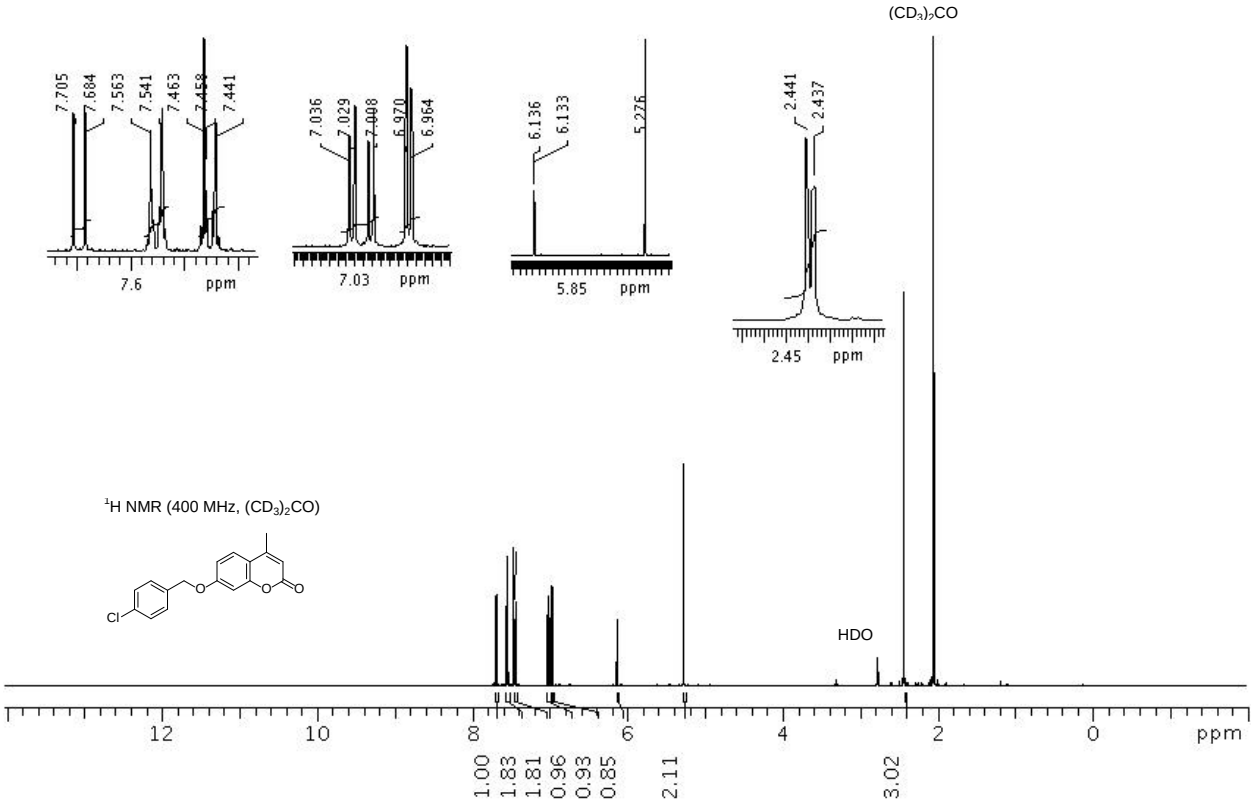
(CD3)2CO
7.705
7.684
7.563
7.541
7.463
7.458
7.441
7.6
ppm
7.036
7.029
7.008
6.970
6.964
7.03
ppm
6.136
6.133
5.276
5.85
ppm
2.441
2.437
2.45
ppm
1H NMR (400 MHz, (CD3)2CO)
Cl
O
O
O
HDO
12
10
8
6
4
2
0
ppm
1.00
1.83
1.81
0.96
0.93
0.85
2.11
3.02

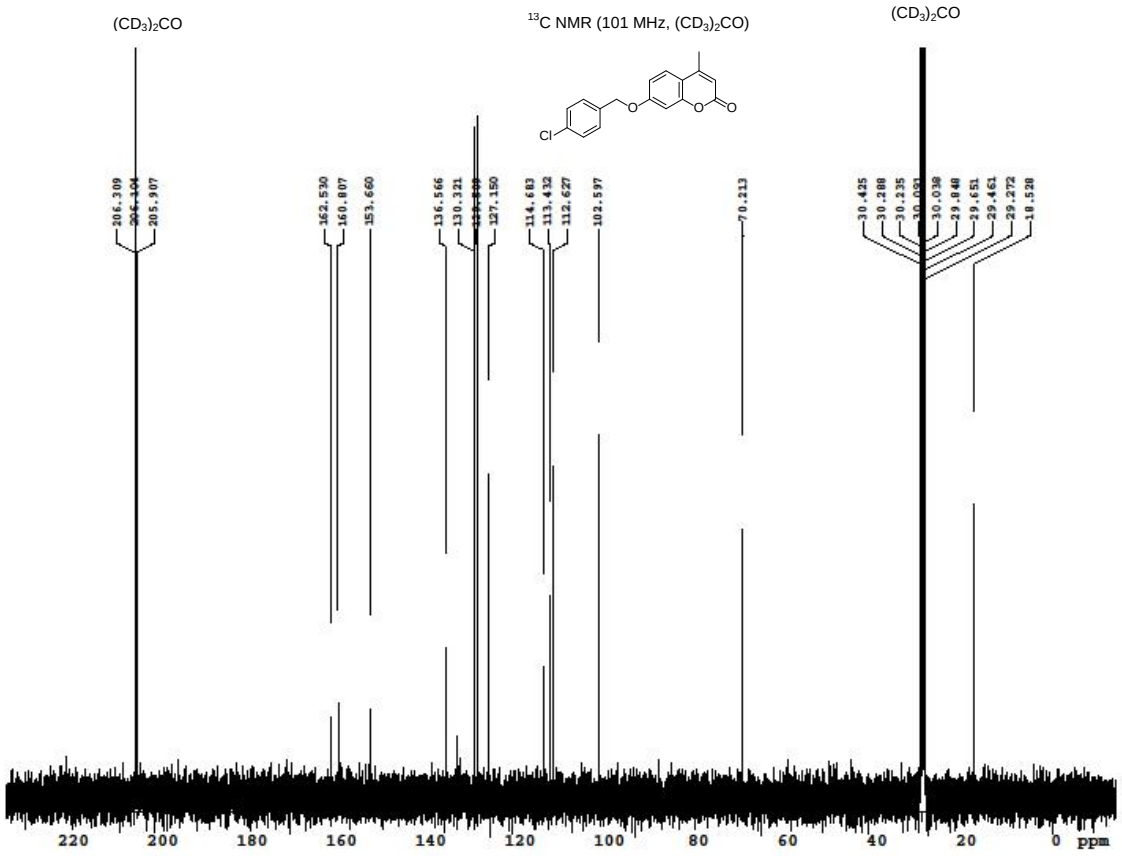
(CD3)2CO
13C NMR (101 MHz, (CD3)2CO)
(CD3)2CO
Cl
O
O
O
206.309
205.907
162.530
160.807
153.660
136.566
130.321
127.150
114.683
113.432
112.627
102.597
70.213
30.425
30.288
30.235
30.038
29.848
29.651
29.461
29.272
18.528
220
200
180
160
140
120
100
80
60
40
20
0 ppm

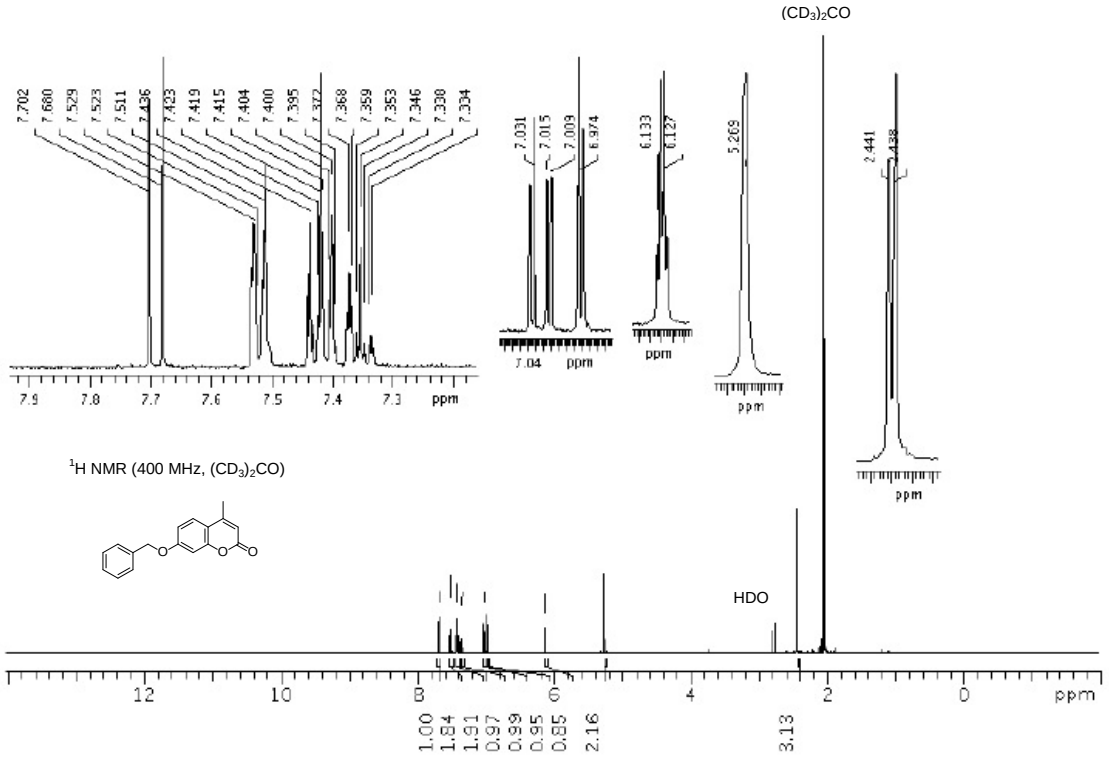
(CD3)2CO
7.702
7.680
7.529
7.523
7.511
7.436
7.423
7.419
7.415
7.404
7.400
7.395
7.372
7.368
7.359
7.353
7.346
7.338
7.334
7.031
7.015
7.009
6.974
6.133
6.127
5.269
2.441
2.438
ppm
1H NMR (400 MHz, (CD3)2CO)
HDO
12
10
8
6
4
2
0
ppm
1.00
1.84
1.91
0.97
0.99
0.95
0.85
2.16
3.13

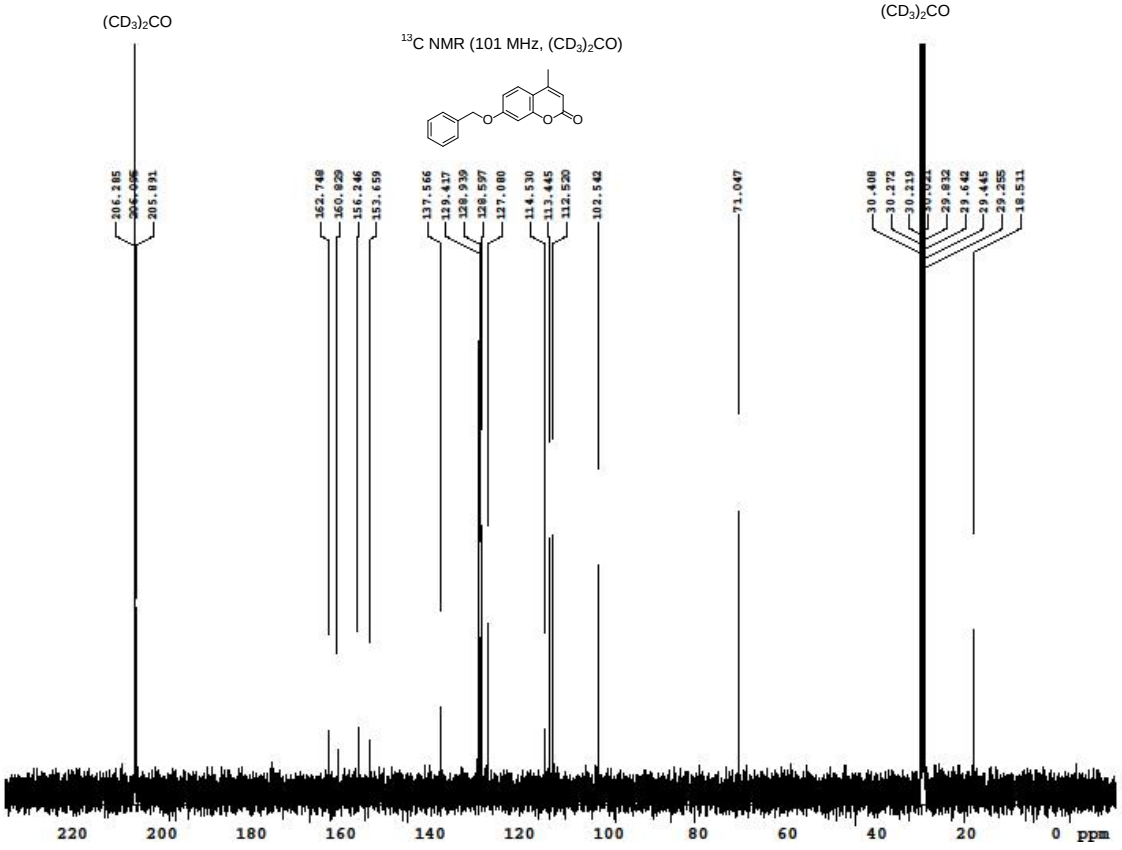
(CD3)2CO
13C NMR (101 MHz, (CD3)2CO)
(CD3)2CO
206.285
206.085
205.891
162.748
160.829
156.246
153.659
137.566
129.417
128.939
128.597
127.080
114.530
113.445
112.520
102.542
71.047
30.408
30.272
30.219
29.832
29.642
29.445
29.255
18.511
220
200
180
160
140
120
100
80
60
40
20
0
ppm

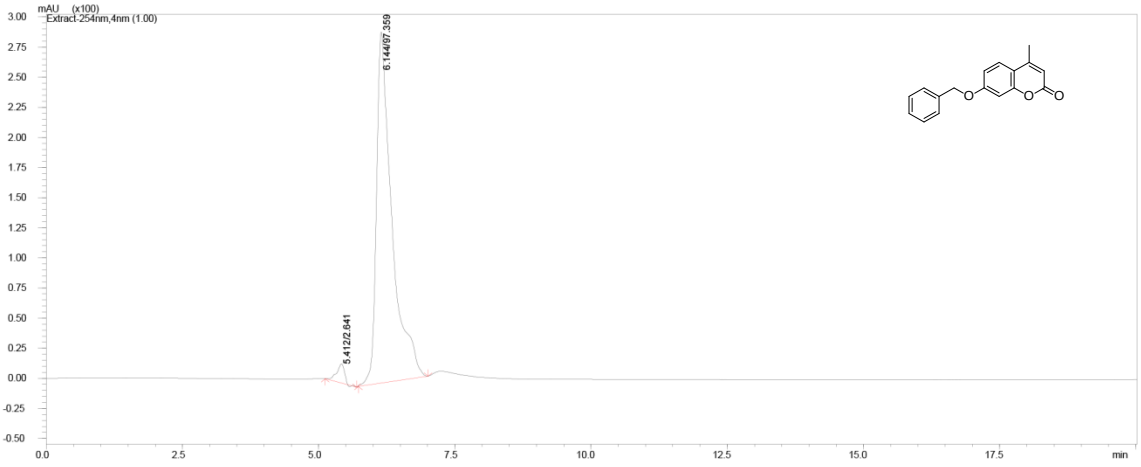

MS Spectrum Graph

Ret.Time:6.755(Scan#:387)
BG Mode:?
Mass Peaks:522 Base Peak:145.90(4103294) Polarity:Pos Segment1 - Event1

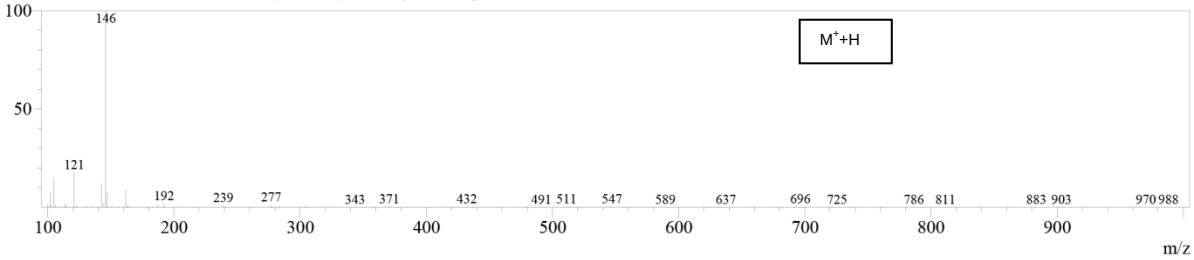

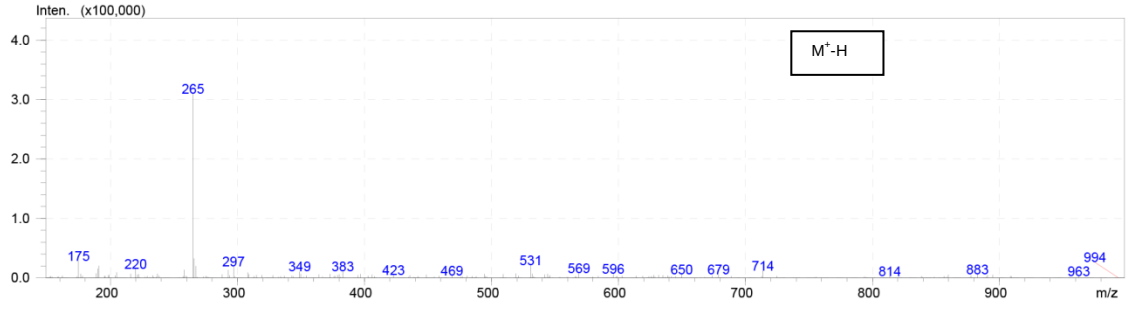

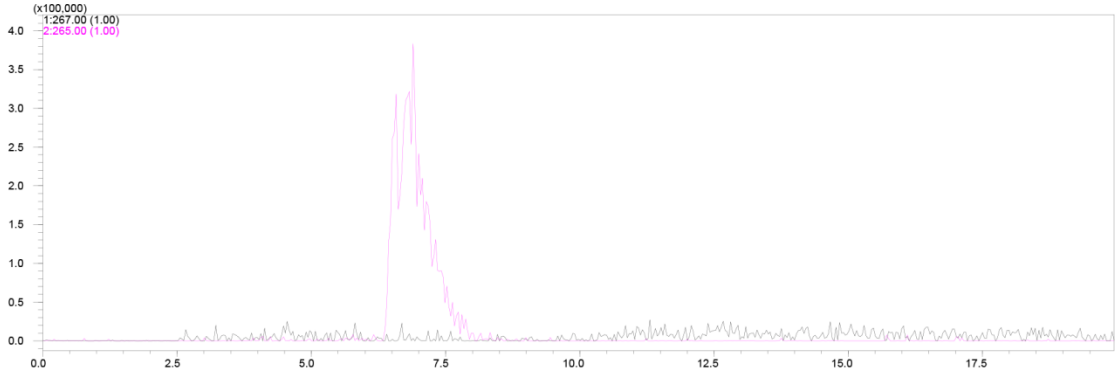

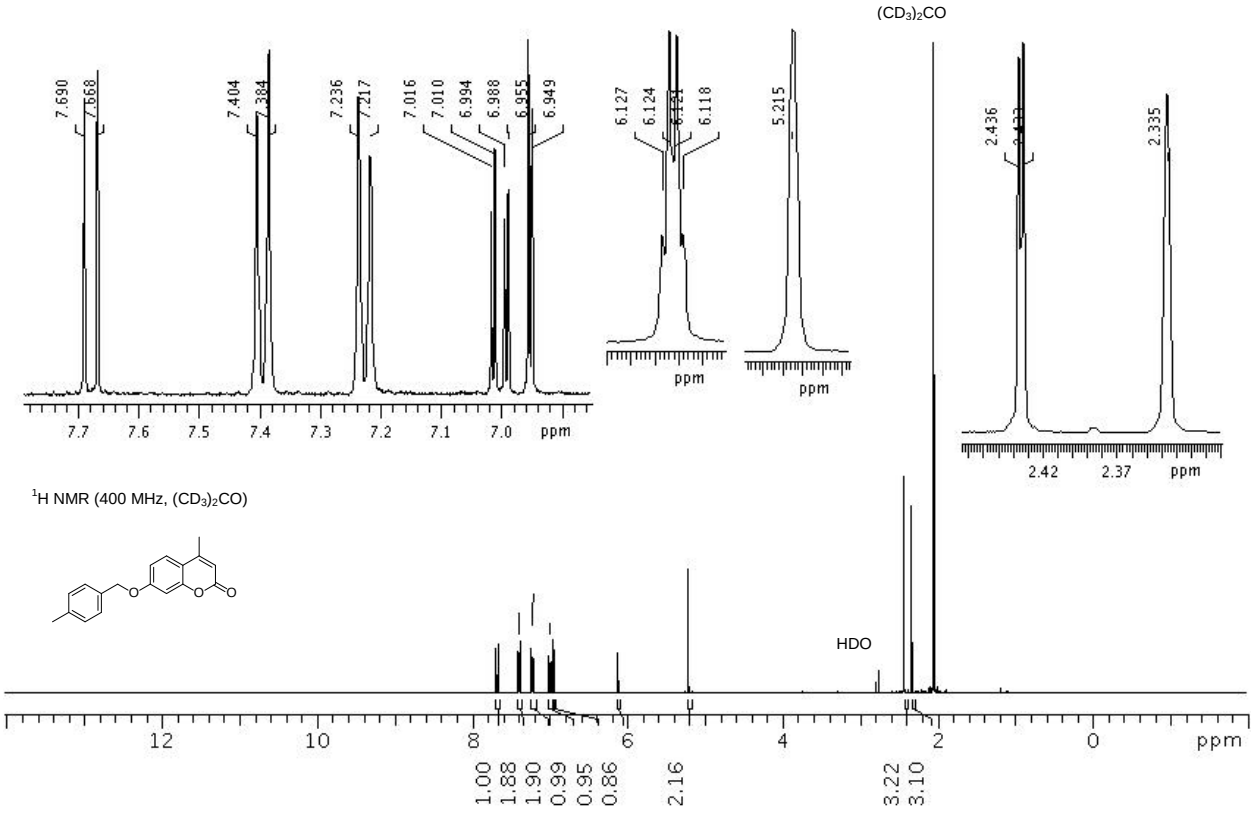
(CD3)2CO
7.690
7.668
7.404
7.384
7.236
7.217
7.016
7.010
6.994
6.988
6.955
6.949
6.127
6.124
6.118
5.215
2.436
2.335
ppm
2.42
2.37
1H NMR (400 MHz, (CD3)2CO)
HDO
12
10
8
6
4
2
0
ppm
1.00
1.88
1.90
0.99
0.95
0.86
2.16
3.22
3.10

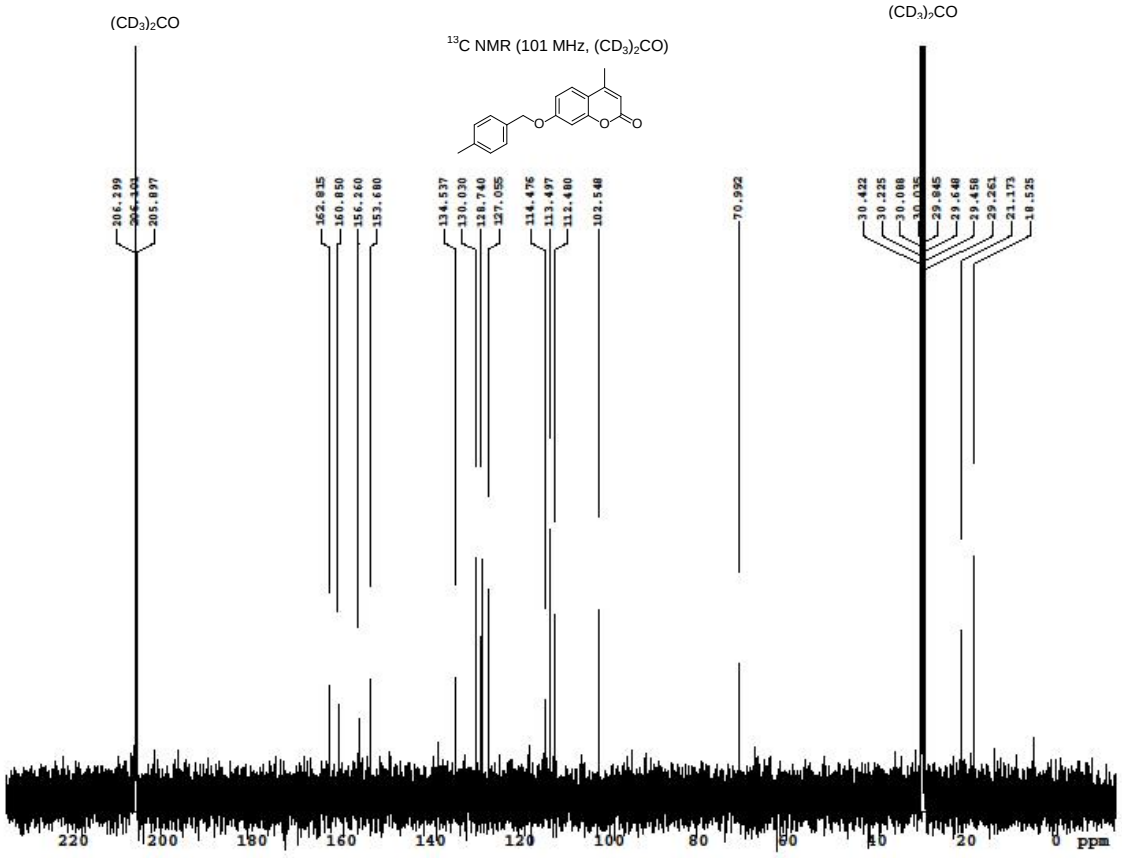
(CD3)2CO
13C NMR (101 MHz, (CD3)2CO)
(CD3)2CO
206.299
206.101
205.897
162.835
160.850
156.260
153.680
134.537
130.030
128.740
127.055
114.476
113.497
112.480
102.548
70.992
30.422
30.225
30.088
30.035
29.845
29.648
29.458
29.261
21.173
18.525
220
200
180
160
140
120
100
80
60
40
20
0 ppm

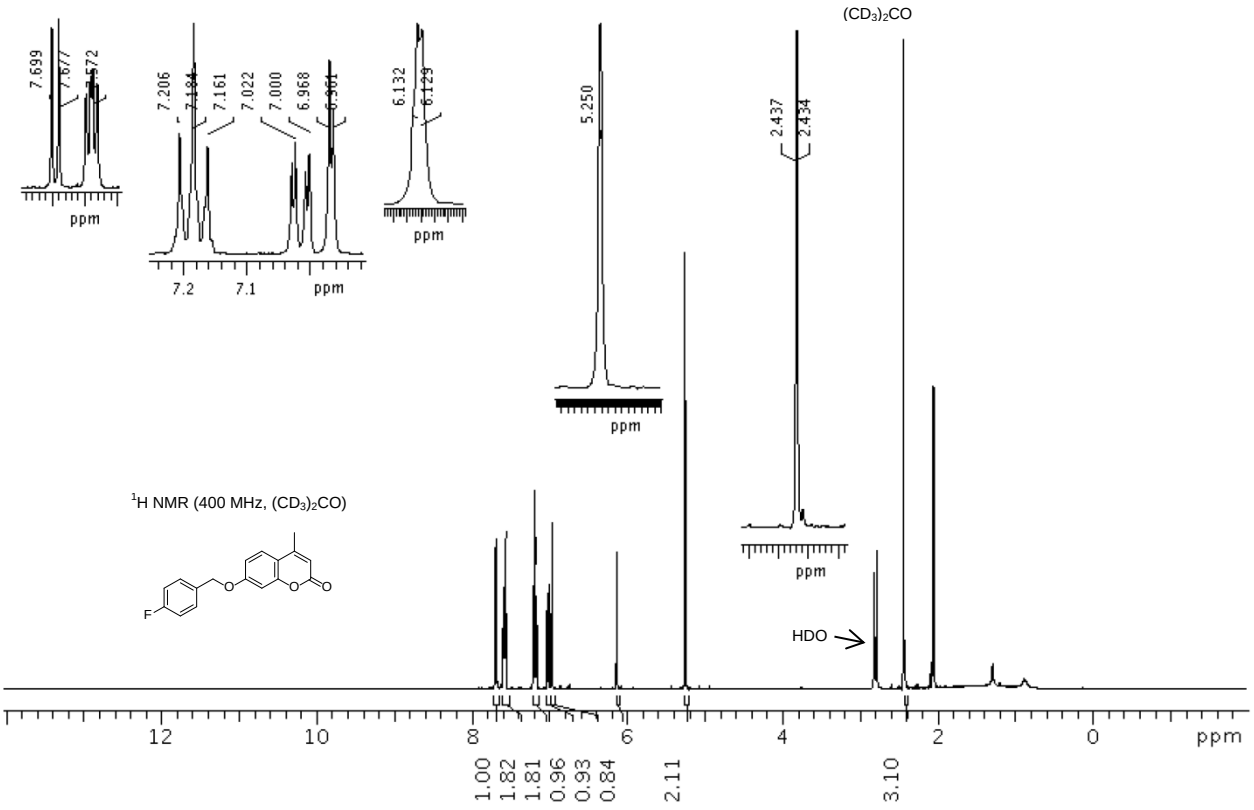
(CD3)2CO
7.699
7.677
7.572
7.206
7.184
7.161
7.022
7.000
6.968
6.961
6.132
6.129
5.250
2.437
2.434
ppm
7.2
7.1
HDO
1H NMR (400 MHz, (CD3)2CO)
F
O
O
O
12
10
8
6
4
2
0
1.00
1.82
1.81
0.96
0.93
0.84
2.11
3.10

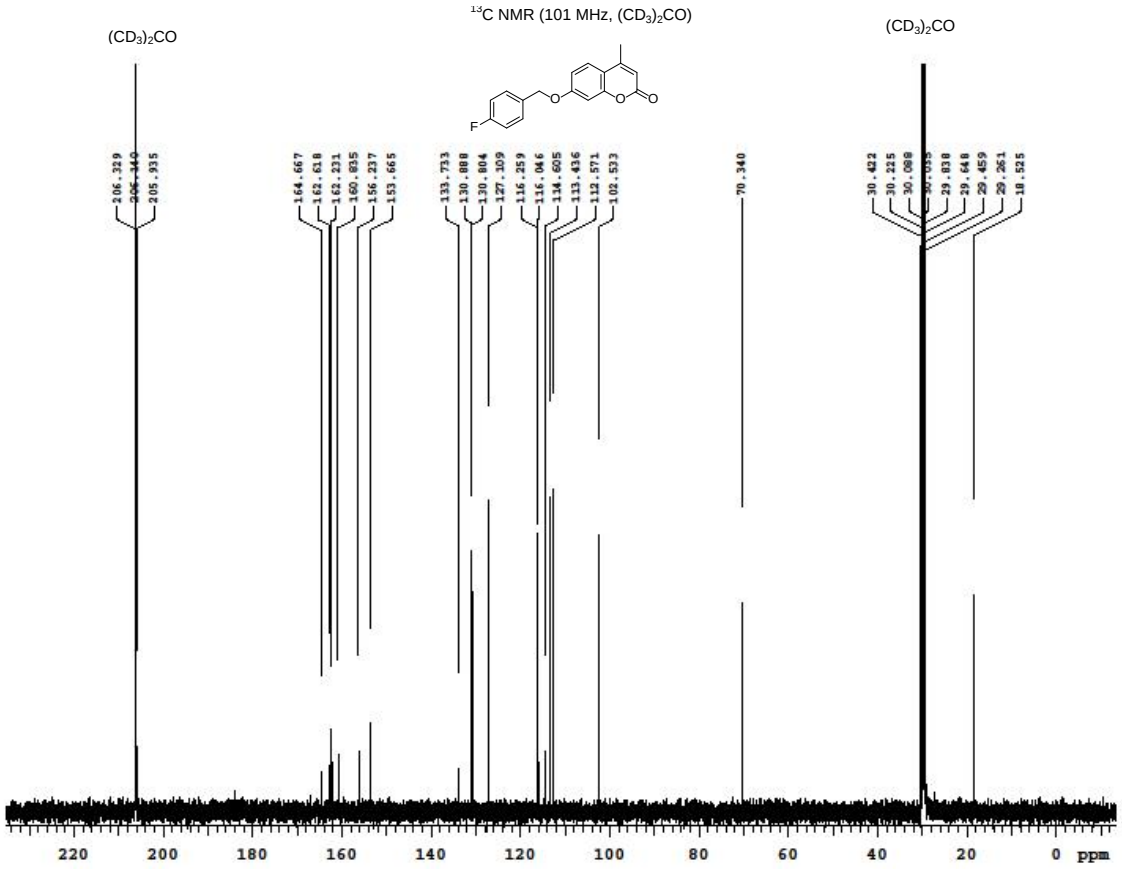
^{13}C NMR (101 MHz, $(CD_3)_2CO$)
$(CD_3)_2CO$
$(CD_3)_2CO$
F
O
O
O
206.329
205.935
164.667
162.618
162.231
160.835
156.237
153.665
133.733
130.888
130.804
127.109
116.259
116.046
114.605
113.436
112.571
102.533
70.340
30.422
30.225
30.088
29.838
29.648
29.459
29.261
18.525
220
200
180
160
140
120
100
80
60
40
20
0 ppm

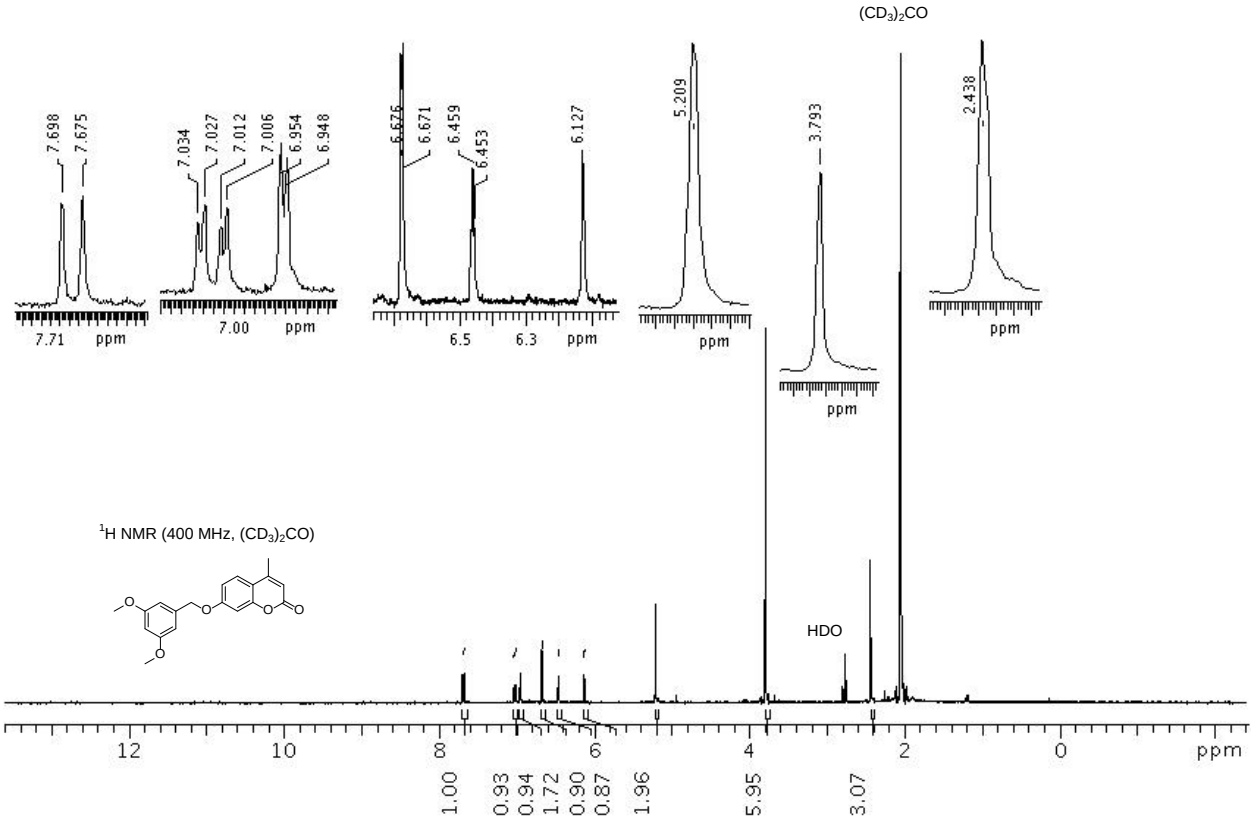
(CD3)2CO
7.698
7.675
7.034
7.027
7.012
7.006
6.954
6.948
6.676
6.671
6.459
6.453
6.127
5.209
3.793
2.438
7.71 ppm
7.00 ppm
6.5 6.3 ppm
ppm
1H NMR (400 MHz, (CD3)2CO)
HDO
12 10 8 6 4 2 0 ppm
1.00 0.93 0.94 1.72 0.90 0.87 1.96 5.95 3.07

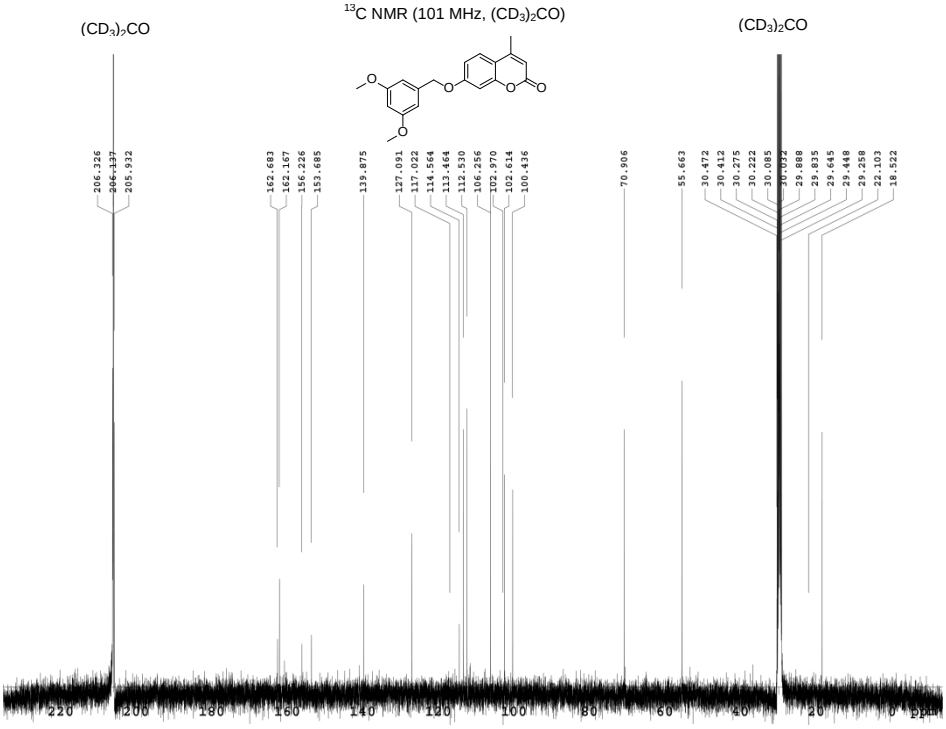
(CD3)2CO
13C NMR (101 MHz, (CD3)2CO)
(CD3)2CO
206.326
206.137
205.932
162.683
162.167
156.226
153.685
139.875
127.091
117.022
114.564
113.464
112.530
106.256
102.970
102.614
100.436
70.906
55.663
30.472
30.412
30.275
30.222
30.085
30.032
29.888
29.835
29.645
29.448
29.258
22.103
18.522
220 200 180 160 140 120 100 80 60 40 20 0 ppm

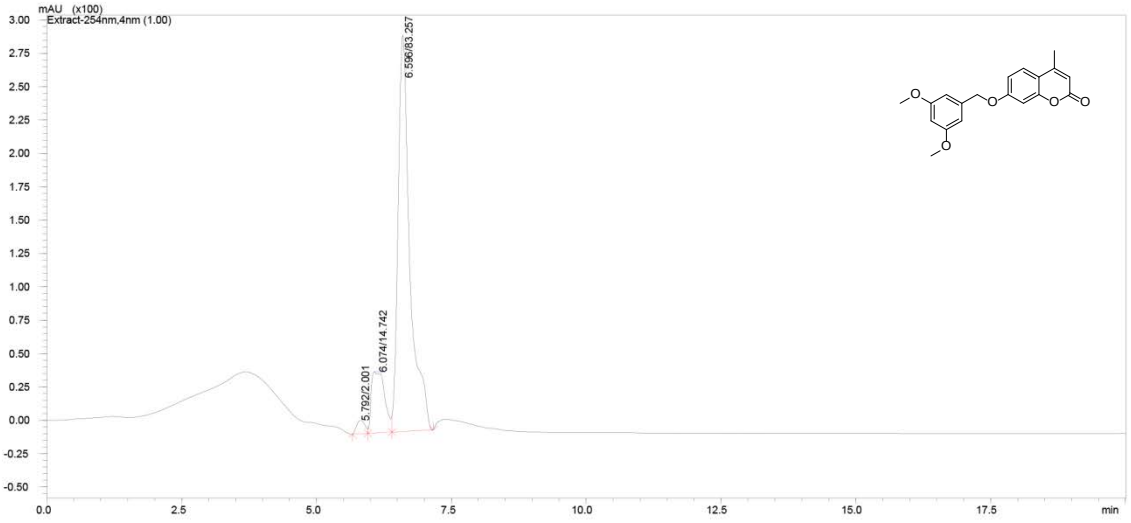

MS Spectrum Graph

Ret.Time:7.455(Scan#:427)
BG Mode:?
Mass Peaks:896 Base Peak:119.95(1947426) Polarity:Pos Segment1 - Event1

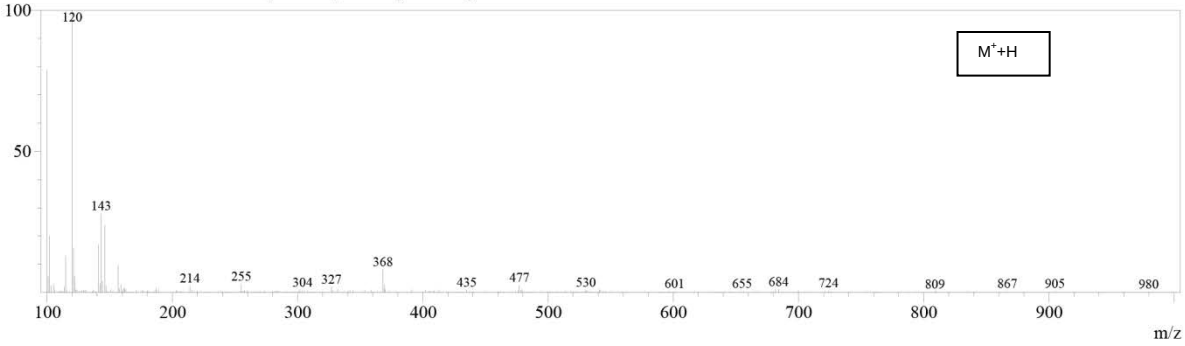

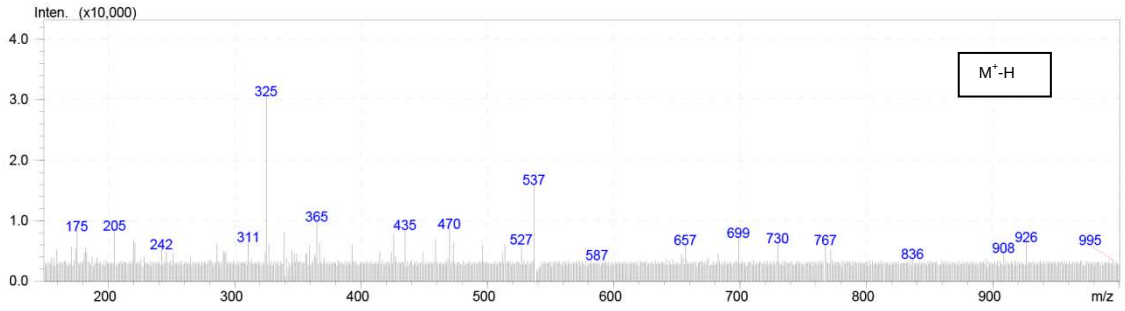

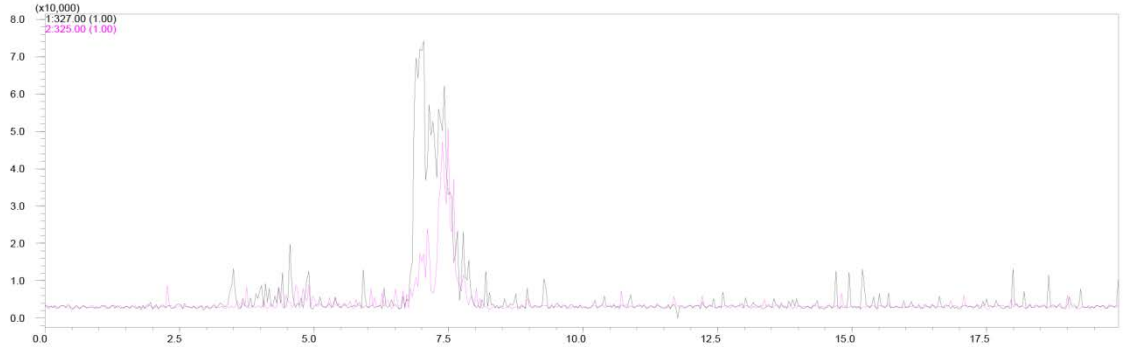

High Resolution Mass Spectrometry Confirmation of Purity and Identity of ChemBridge Compounds 1–7, 13 and 19

==== Shimadzu LabSolutions Data Report ====

<Spectrum>

Line#:1 R.Time:8.617(Scan#:4271)
MassPeaks:439
RawMode:Single 8.617(4271) BasePeak:141(4119439)
BG Mode:None Segment 1 - Event 1

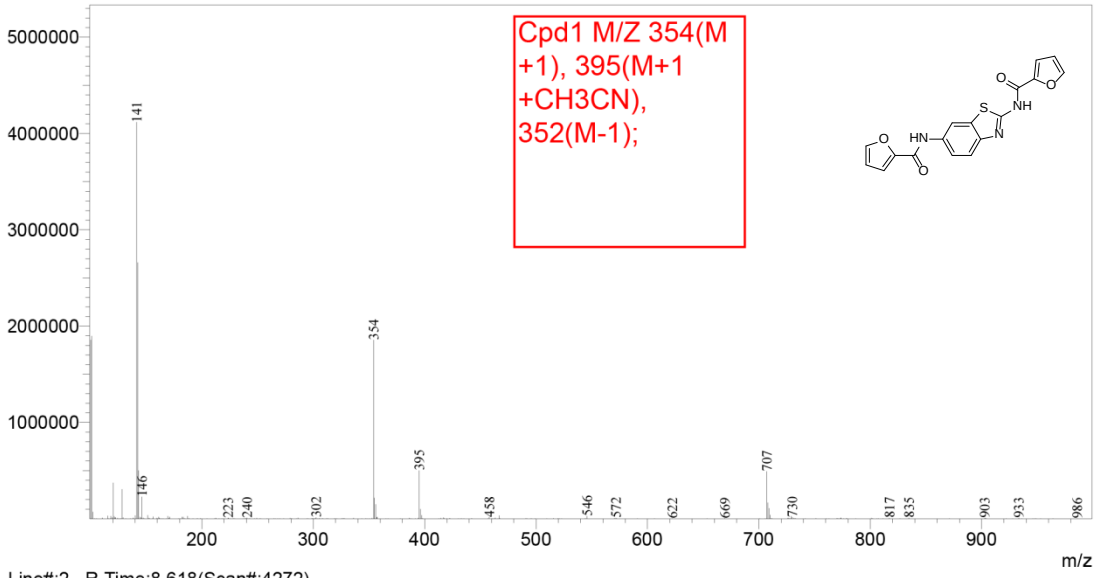

Line#:2 R.Time:8.618(Scan#:4272)
MassPeaks:435
RawMode:Single 8.618(4272) BasePeak:352(285102)
BG Mode:None Segment 1 - Event 2

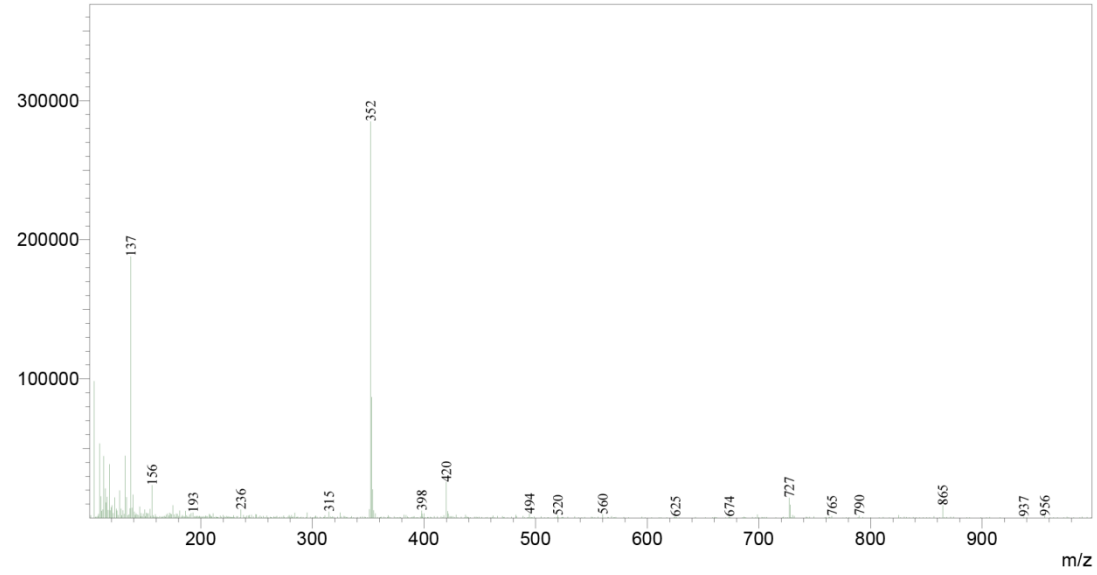

==== Shimadzu LabSolutions Multi-Chromatogram ====

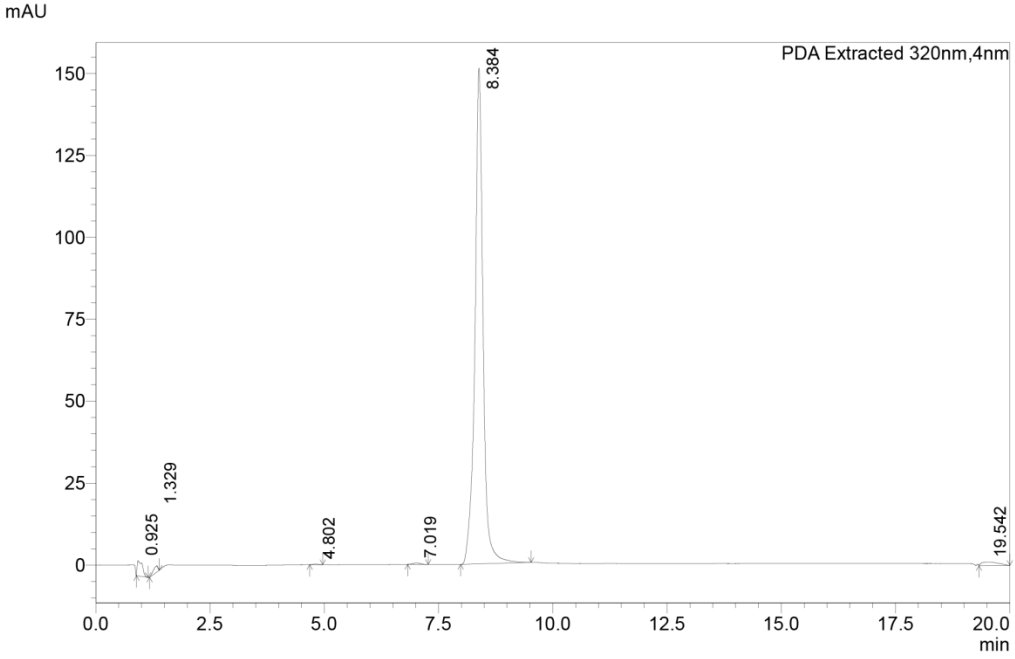

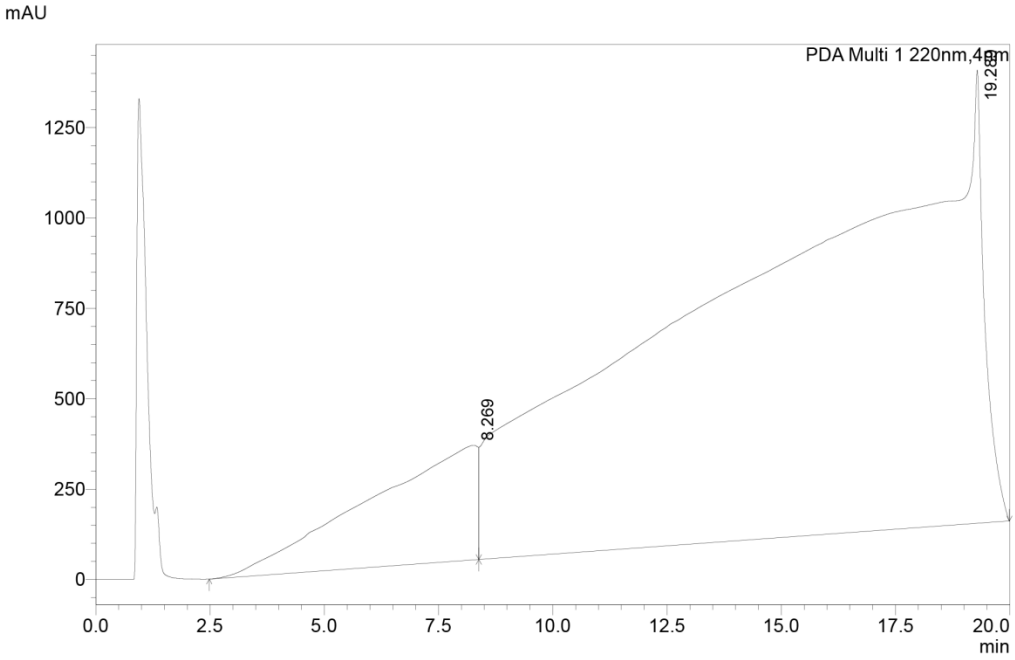

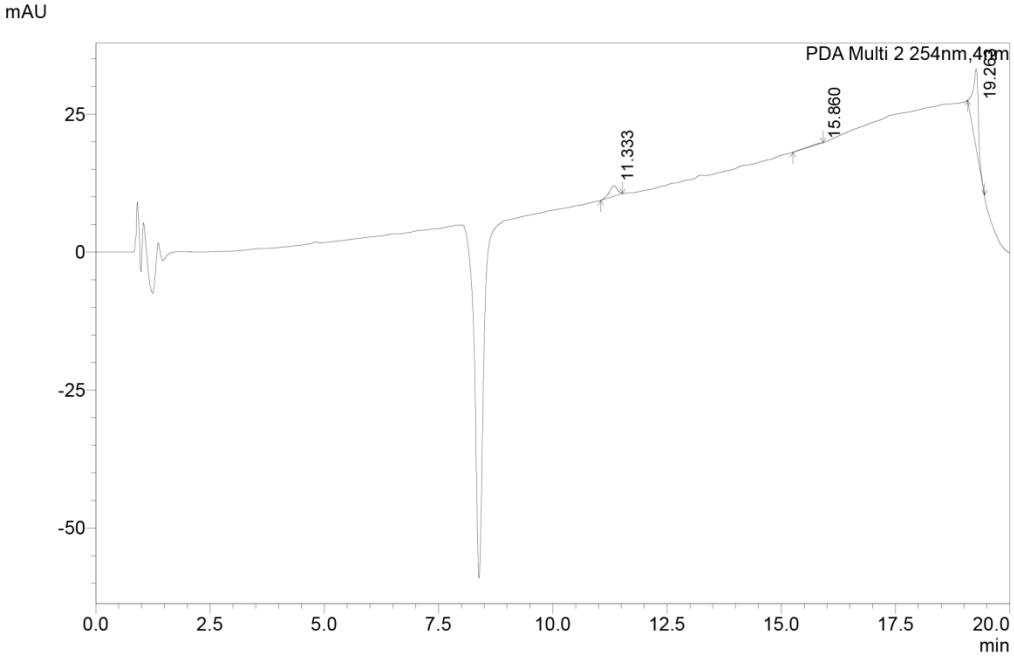
mAU
PDA Multi 2 254nm,4nm
11.333
15.860
19.258
25
0
-25
-50
0.0
2.5
5.0
7.5
10.0
12.5
15.0
17.5
20.0
min

==== Shimadzu LabSolutions Data Report ====

<Spectrum>

Line#:1 R.Time:9.917(Scan#:5051)
MassPeaks:441
RawMode:Single 9.917(5051) BasePeak:141(4317109)
BG Mode:None Segment 1 - Event 1

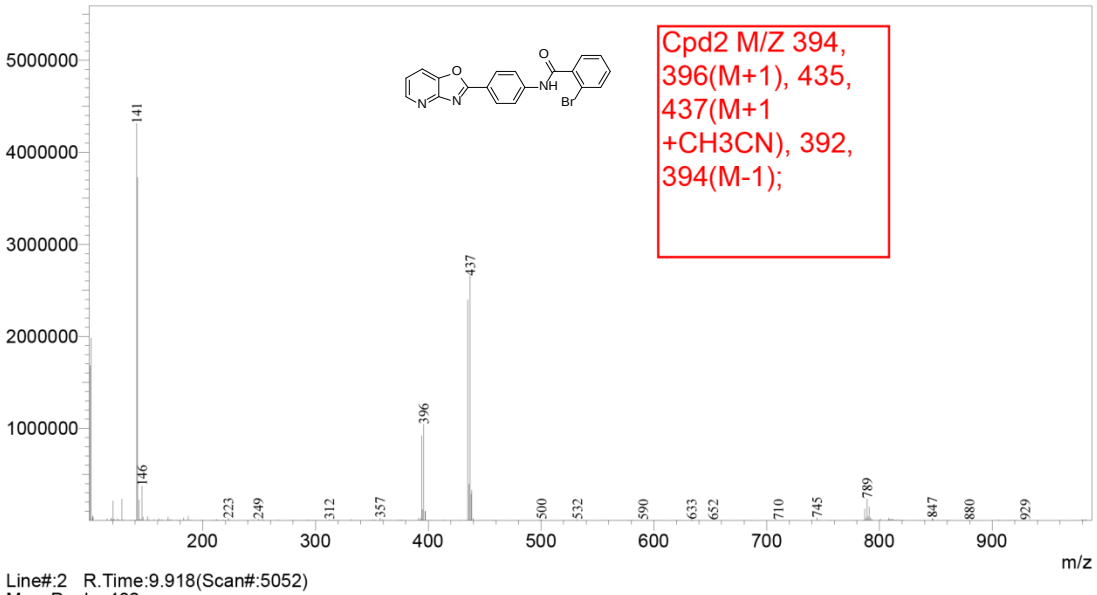

Line#:2 R.Time:9.918(Scan#:5052)
MassPeaks:482
RawMode:Single 9.918(5052) BasePeak:394(234494)
BG Mode:None Segment 1 - Event 2

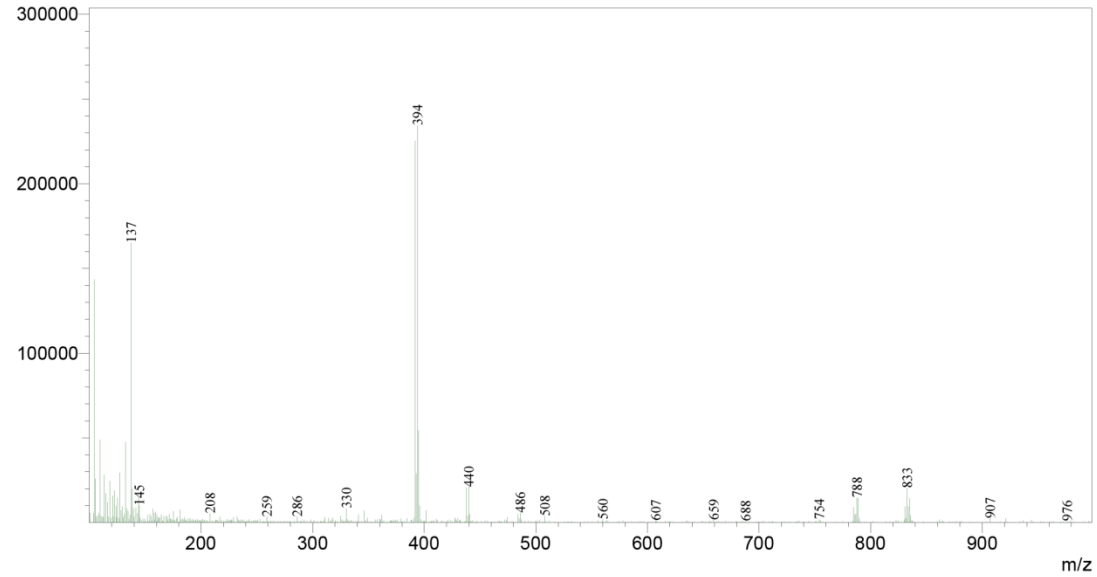

==== Shimadzu LabSolutions Multi-Chromatogram ====

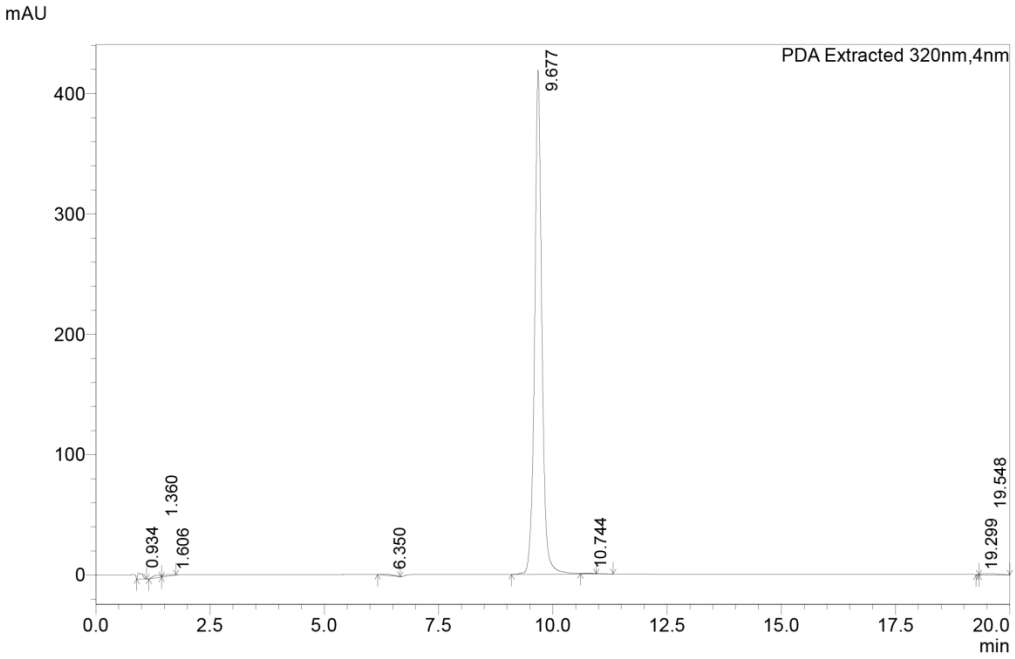

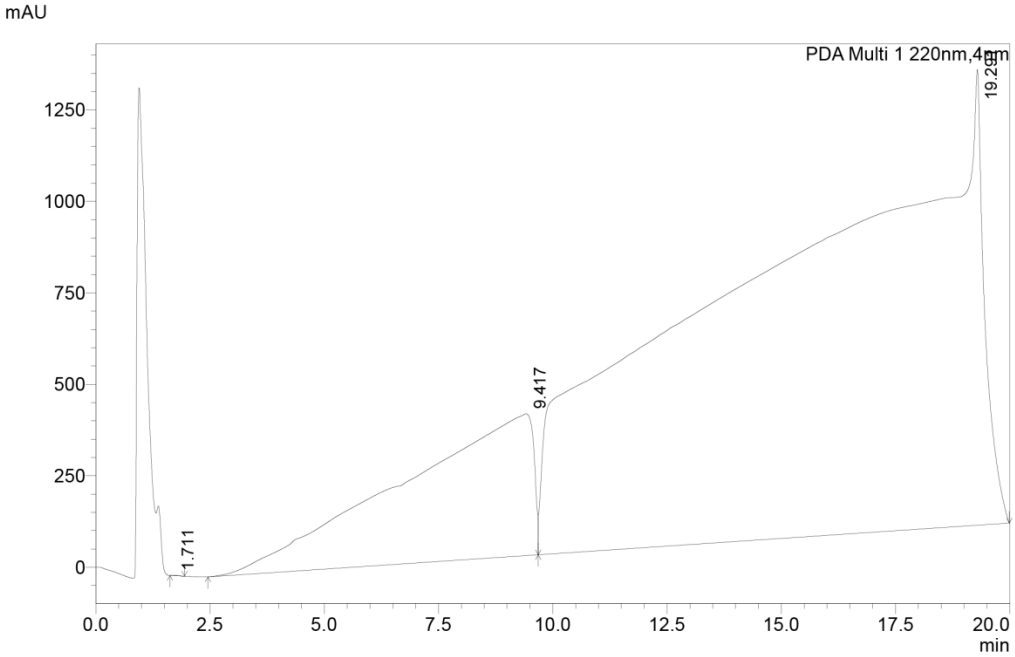

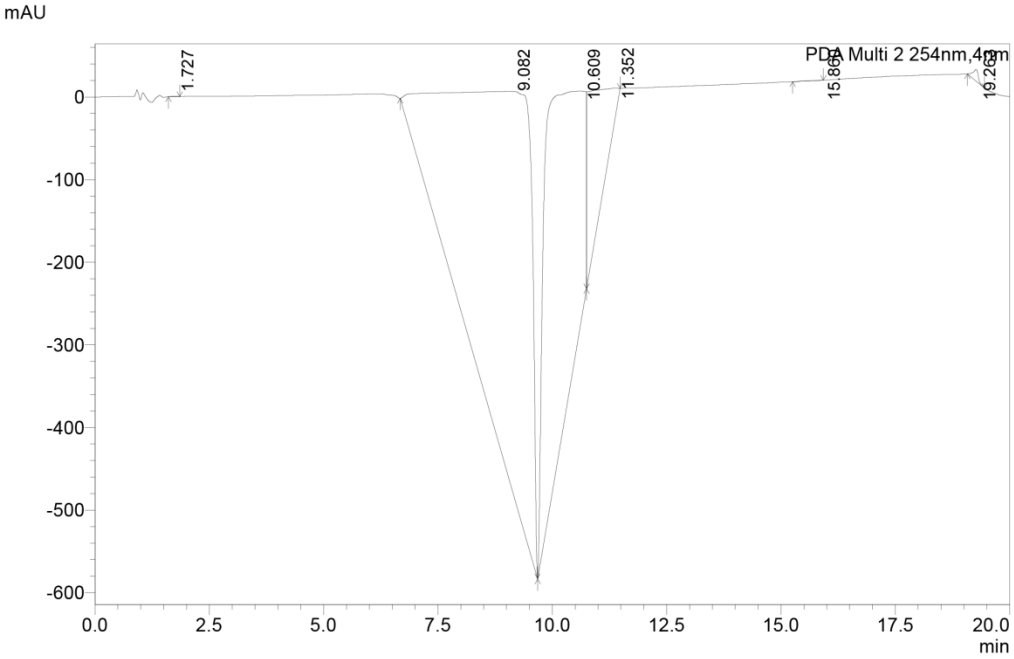
mAU
PDA Multi 2 254nm,4nm
1.727
9.082
10.609
11.352
15.869
19.263
0
-100
-200
-300
-400
-500
-600
0.0
2.5
5.0
7.5
10.0
12.5
15.0
17.5
20.0
min

==== Shimadzu LabSolutions Data Report ====

<Spectrum>

Line#:1 R.Time:10.577(Scan#:5447)
MassPeaks:476
RawMode:Single 10.577(5447) BasePeak:141(5376101)
BG Mode:None Segment 1 - Event 1

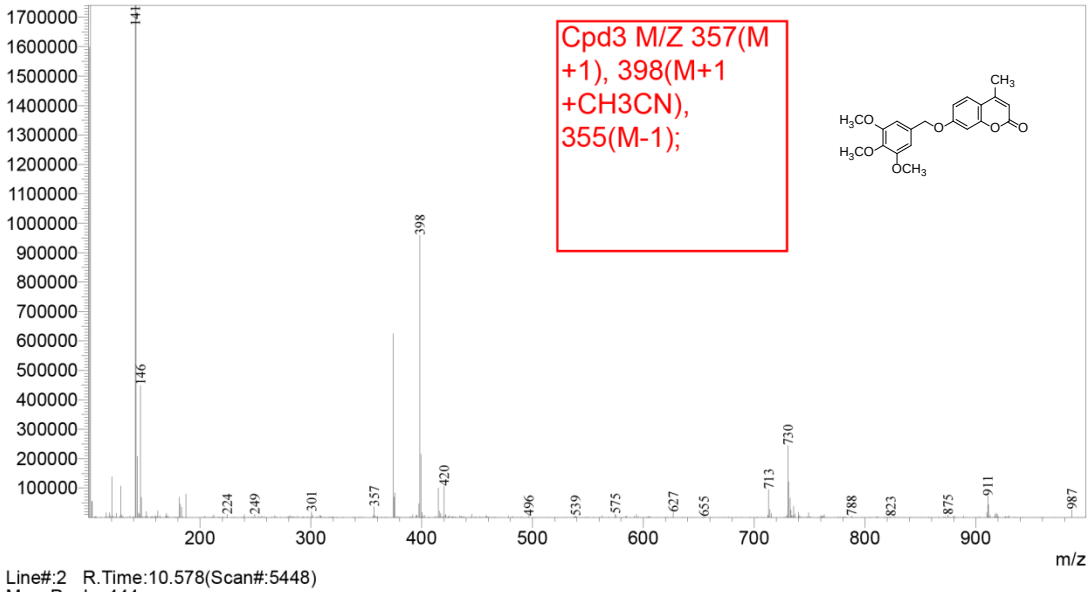

Line#:2 R.Time:10.578(Scan#:5448)
MassPeaks:444
RawMode:Single 10.578(5448) BasePeak:137(173558)
BG Mode:None Segment 1 - Event 2

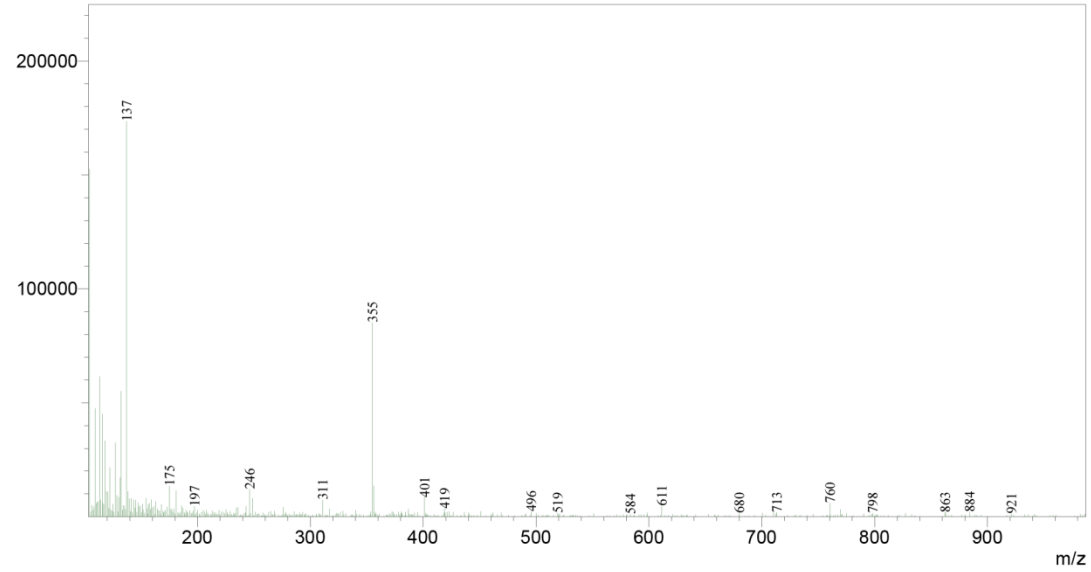

==== Shimadzu LabSolutions Multi-Chromatogram ====

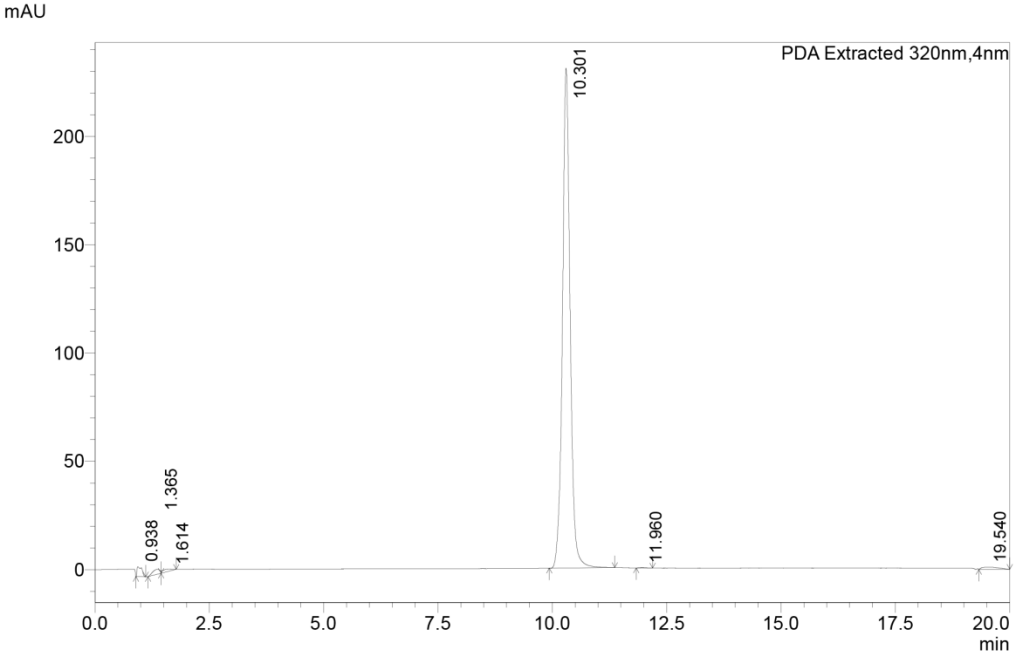

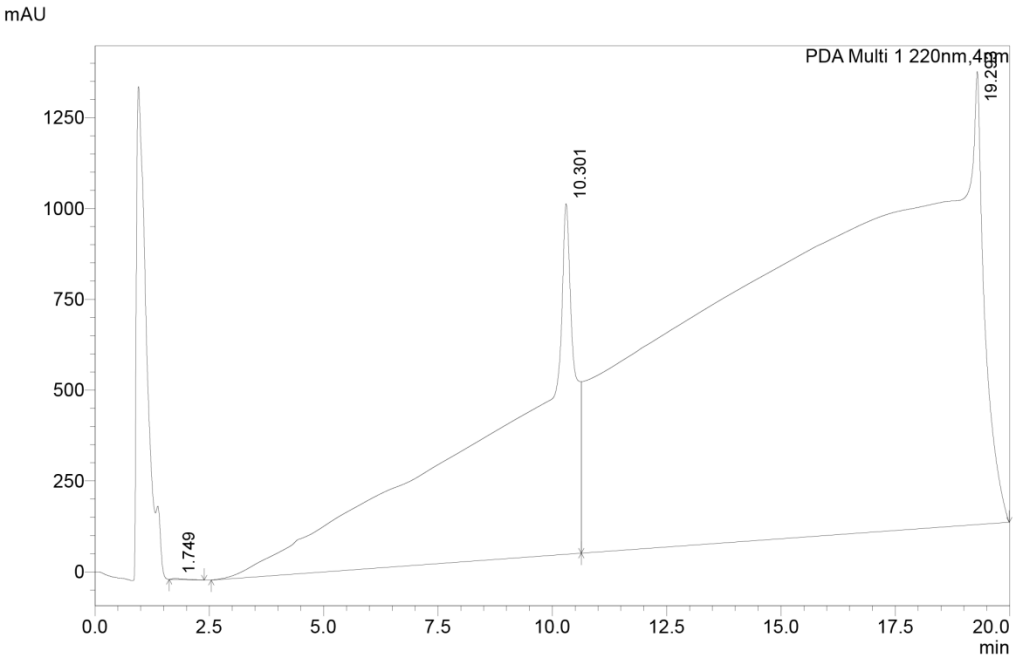

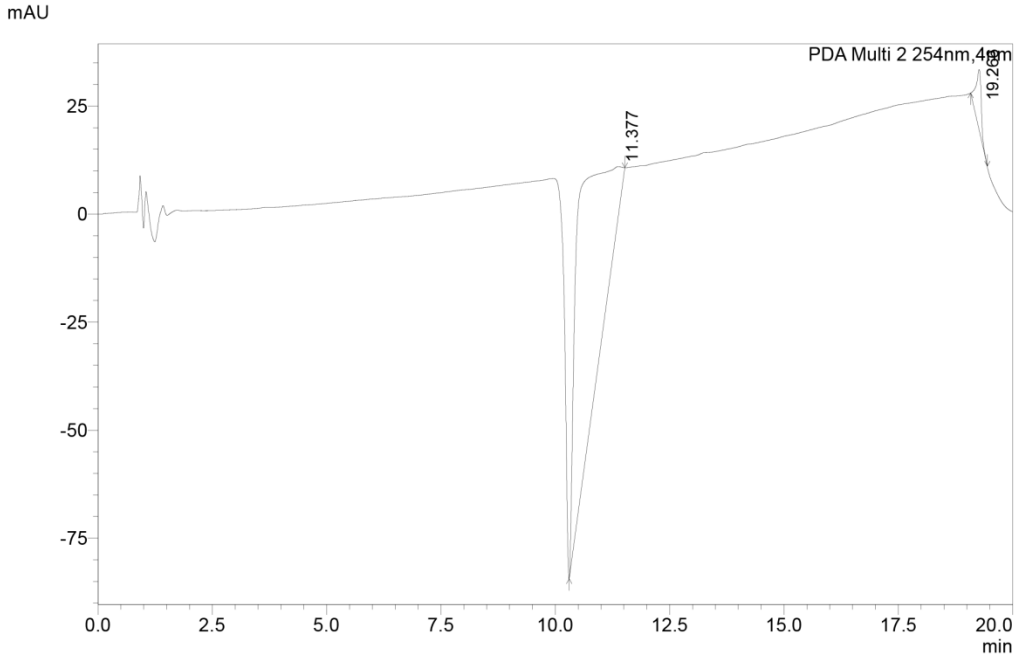
mAU
PDA Multi 2 254nm,4nm
11.377
19.263
25
0
-25
-50
-75
0.0
2.5
5.0
7.5
10.0
12.5
15.0
17.5
20.0
min

==== Shimadzu LabSolutions Data Report ====

<Spectrum>

Line#:1 R.Time:9.197(Scan#:4619)
MassPeaks:449
RawMode:Single 9.197(4619) BasePeak:363(6180054)
BG Mode:None Segment 1 - Event 1

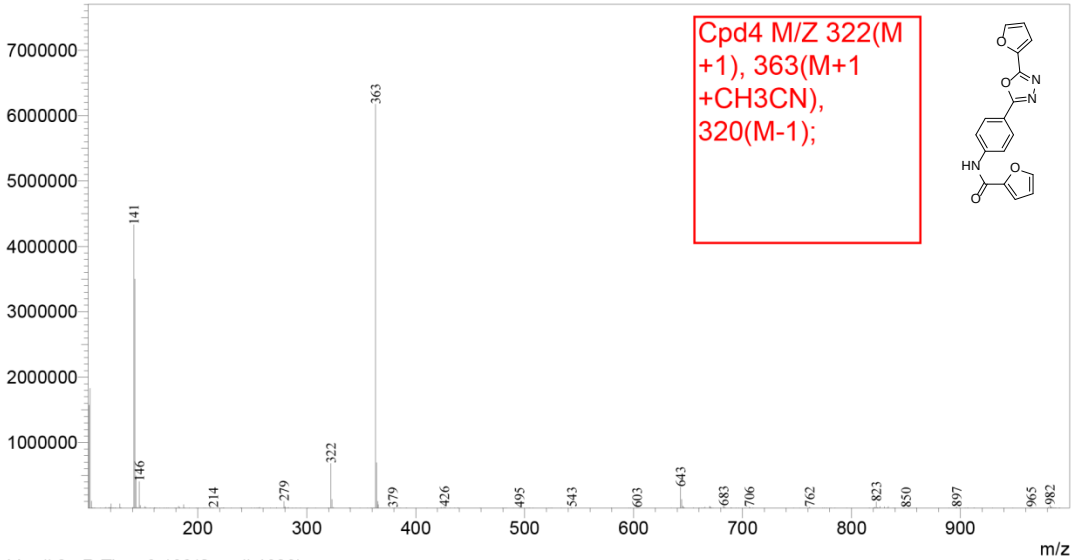

Line#:2 R.Time:9.198(Scan#:4620)
MassPeaks:466
RawMode:Single 9.198(4620) BasePeak:137(180904)
BG Mode:None Segment 1 - Event 2

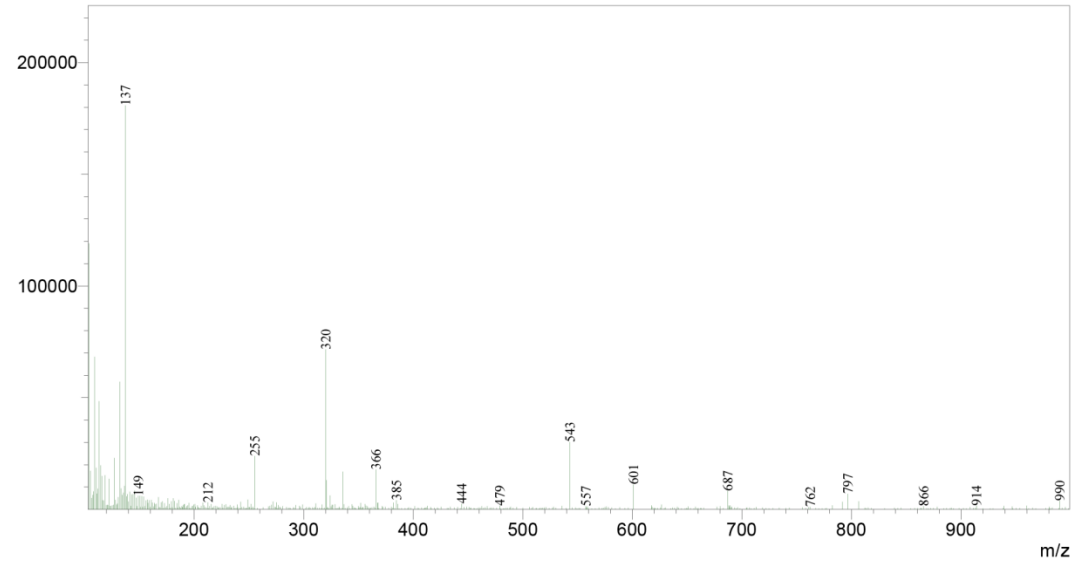

==== Shimadzu LabSolutions Multi-Chromatogram ====

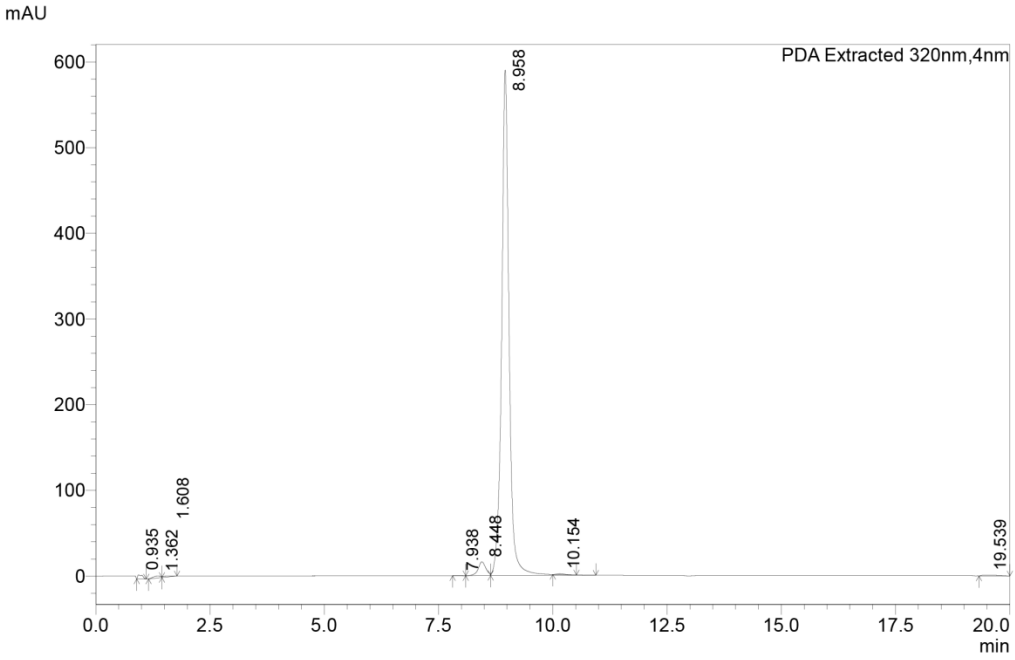

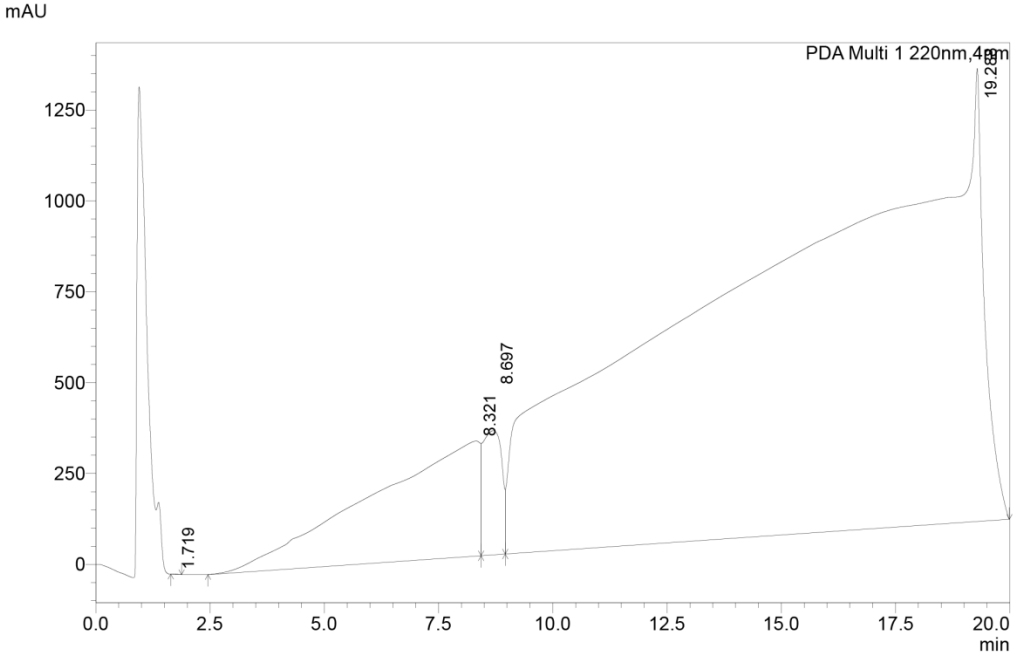

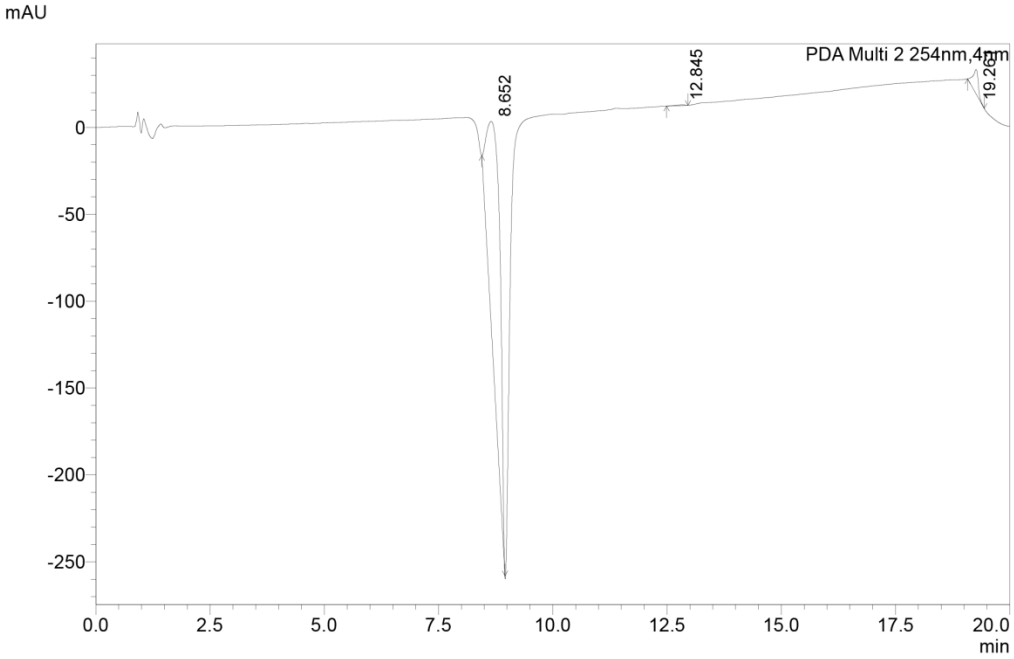
mAU
PDA Multi 2 254nm,4nm
8.652
12.845
19.263
0
-50
-100
-150
-200
-250
0.0
2.5
5.0
7.5
10.0
12.5
15.0
17.5
20.0
min

==== Shimadzu LabSolutions Data Report ====

<Spectrum>

Line#:1 R.Time:10.227(Scan#:5237)
MassPeaks:333
RawMode:Single 10.227(5237) BasePeak:141(3750161)
BG Mode:None Segment 1 - Event 1

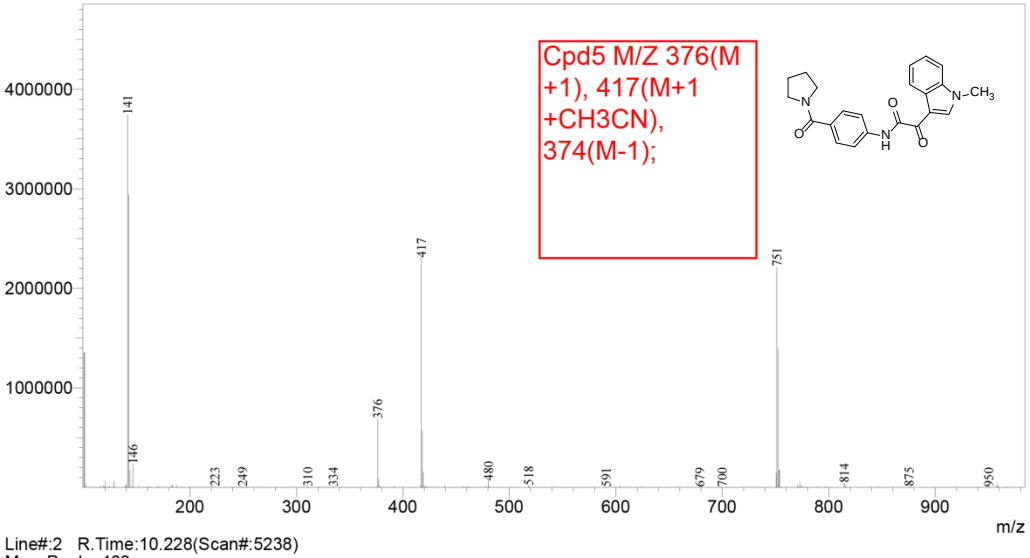

Line#:2 R.Time:10.228(Scan#:5238)
MassPeaks:403
RawMode:Single 10.228(5238) BasePeak:137(169648)
BG Mode:None Segment 1 - Event 2

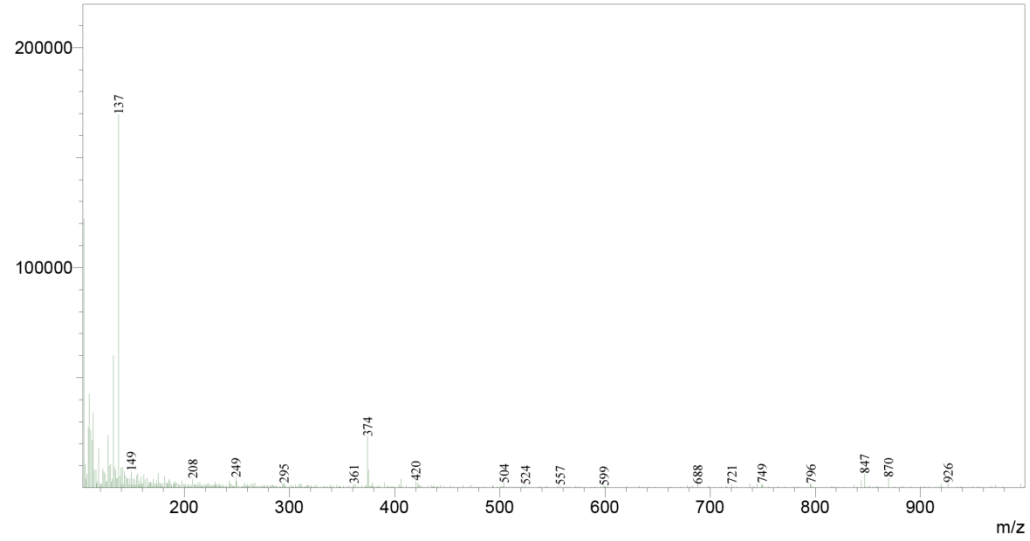

==== Shimadzu LabSolutions Multi-Chromatogram ====

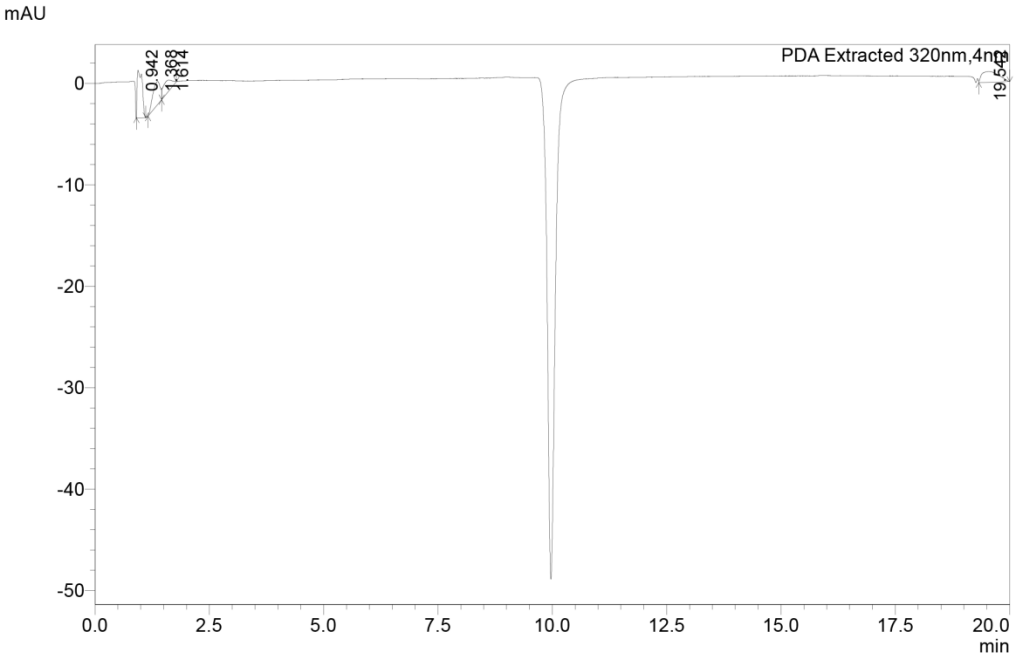

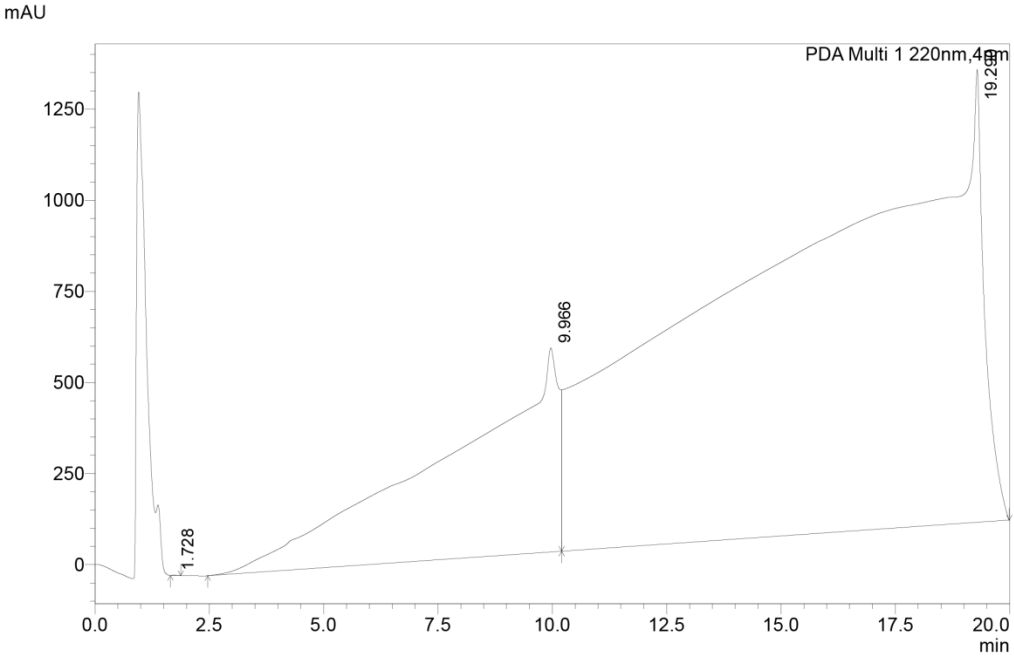

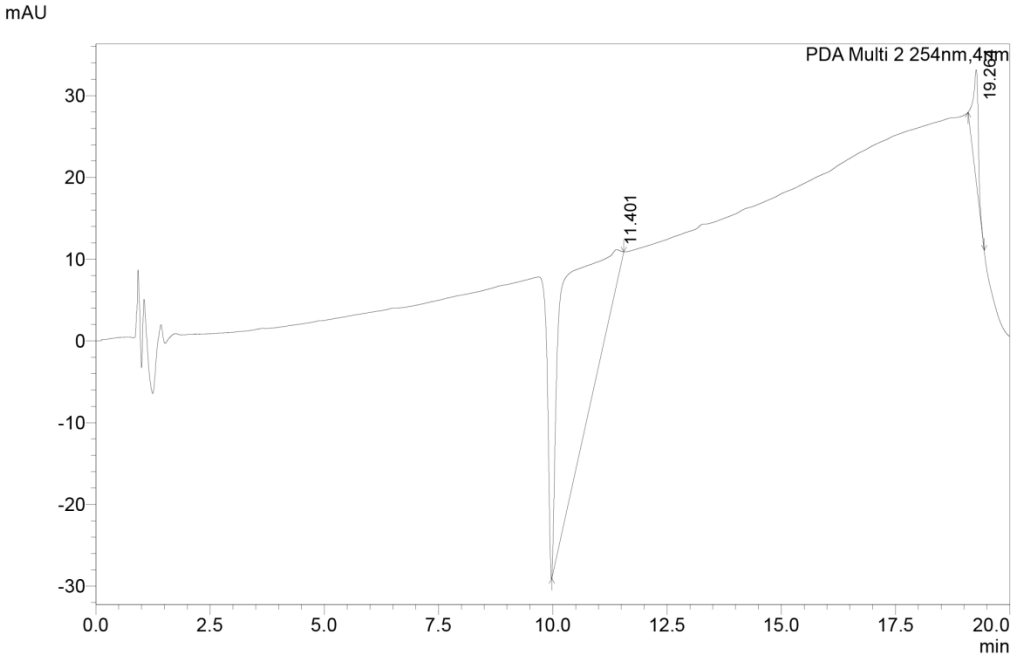
mAU
PDA Multi 2 254nm,4nm
11.401
19.267
30
20
10
0
-10
-20
-30
0.0
2.5
5.0
7.5
10.0
12.5
15.0
17.5
20.0
min

==== Shimadzu LabSolutions Data Report ====

<Spectrum>

Line#:1 R.Time:10.137(Scan#:5183)
MassPeaks:425
RawMode:Single 10.137(5183) BasePeak:375(8012982)
BG Mode:None Segment 1 - Event 1

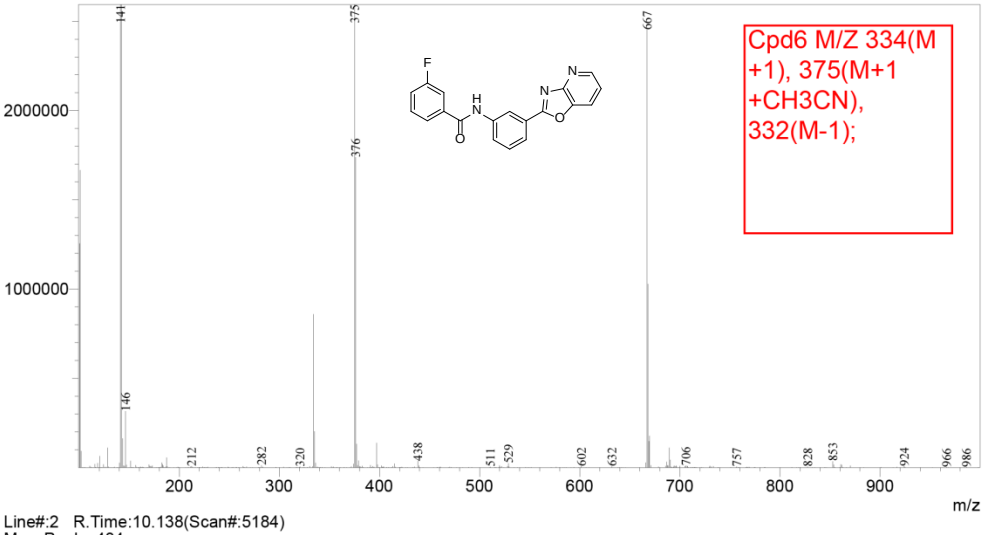

Line#:2 R.Time:10.138(Scan#:5184)
MassPeaks:434
RawMode:Single 10.138(5184) BasePeak:332(1092557)
BG Mode:None Segment 1 - Event 2

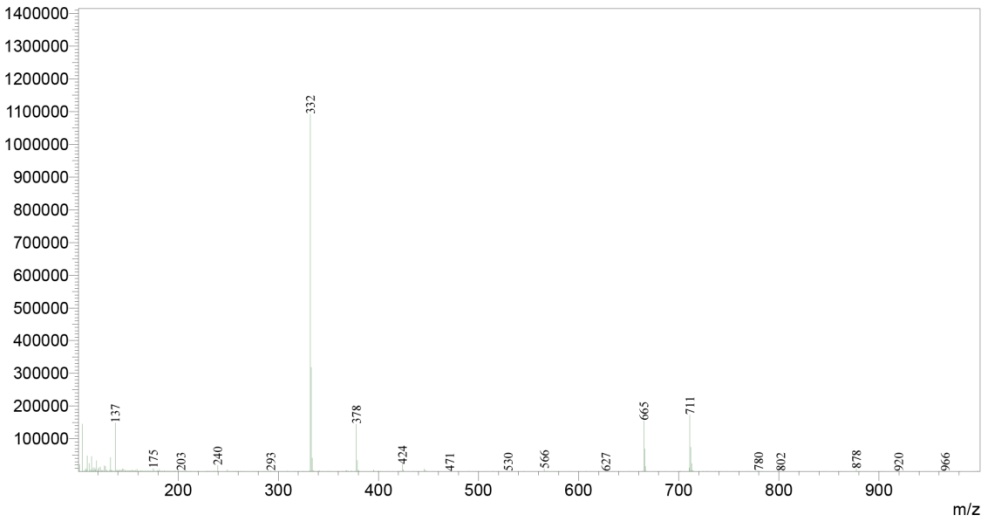

==== Shimadzu LabSolutions Multi-Chromatogram ====

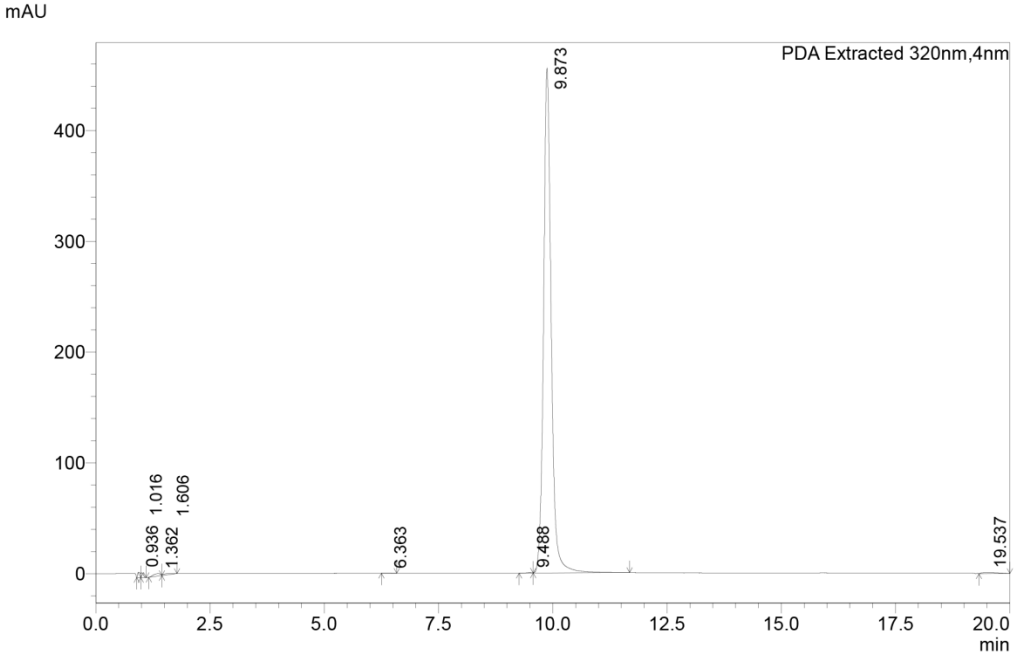

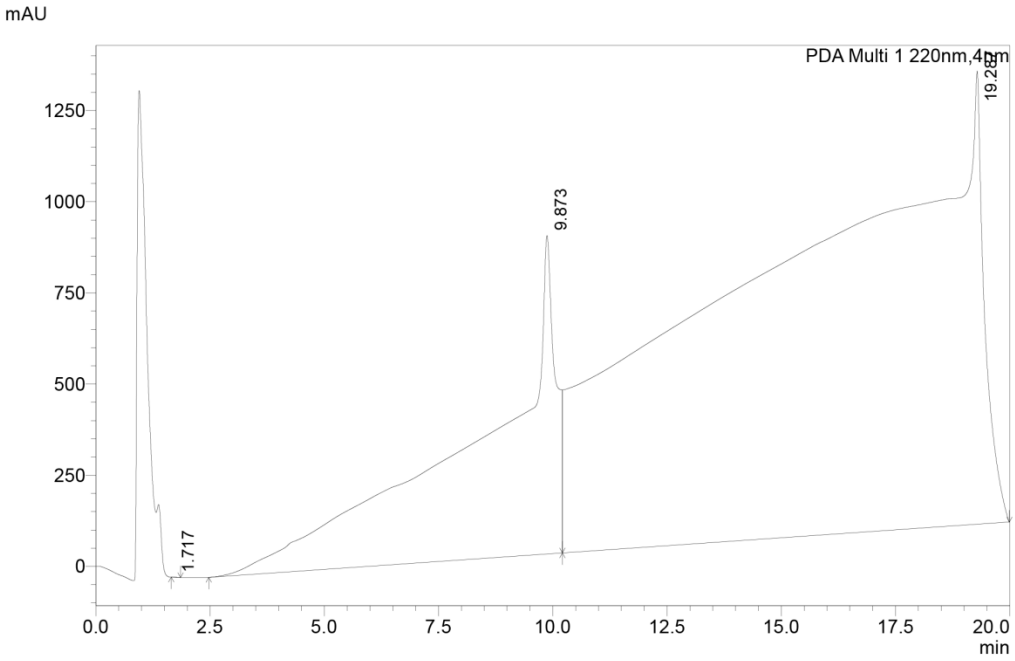

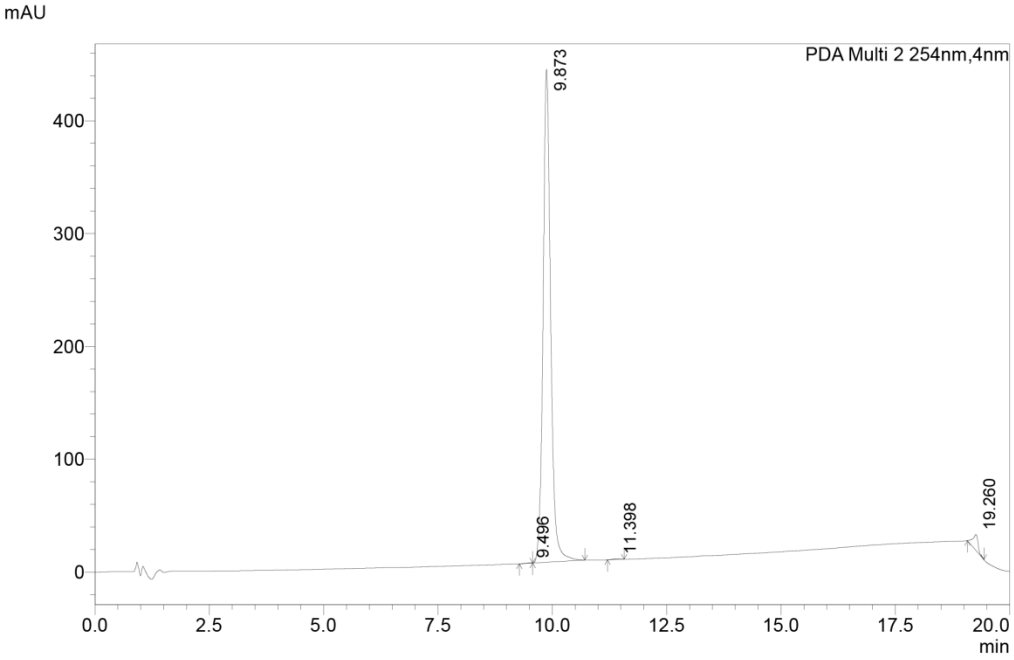
mAU
PDA Multi 2 254nm,4nm
9.873
9.496
11.398
19.260
400
300
200
100
0
0.0
2.5
5.0
7.5
10.0
12.5
15.0
17.5
20.0
min

==== Shimadzu LabSolutions Data Report ====

<Spectrum>

Line#:1 R.Time:10.387(Scan#:5333)
MassPeaks:459
RawMode:Single 10.387(5333) BasePeak:387(9237980)
BG Mode:None Segment 1 - Event 1

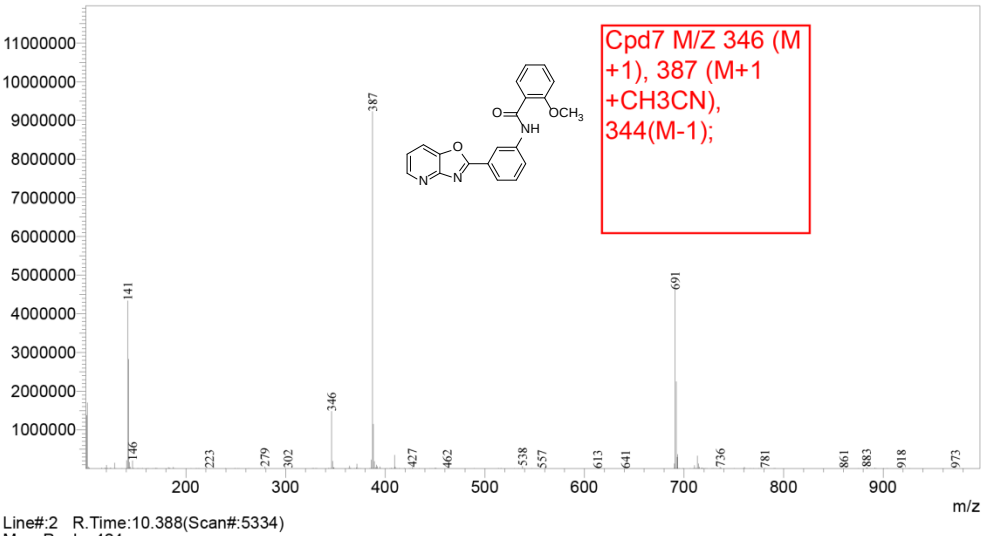

Line#:2 R.Time:10.388(Scan#:5334)
MassPeaks:424
RawMode:Single 10.388(5334) BasePeak:137(151769)
BG Mode:None Segment 1 - Event 2

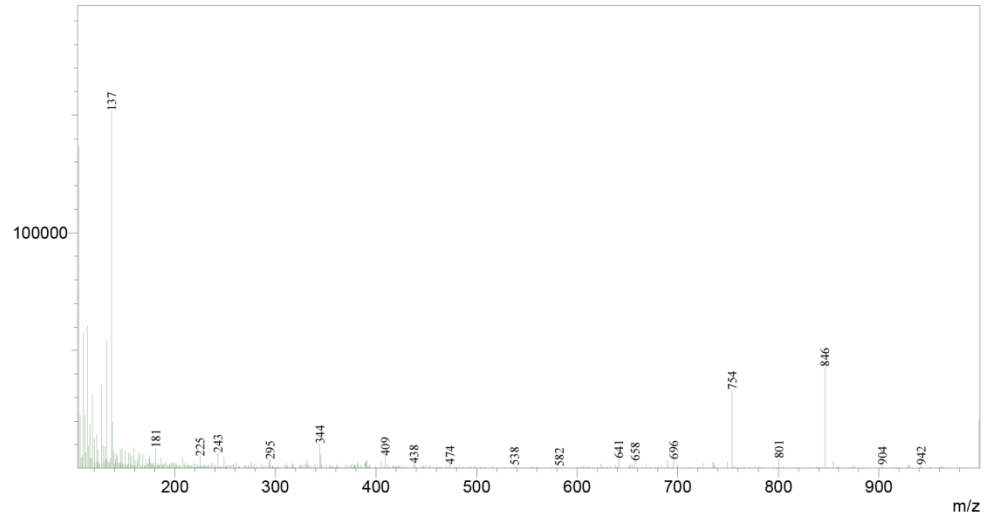

==== Shimadzu LabSolutions Multi-Chromatogram ====

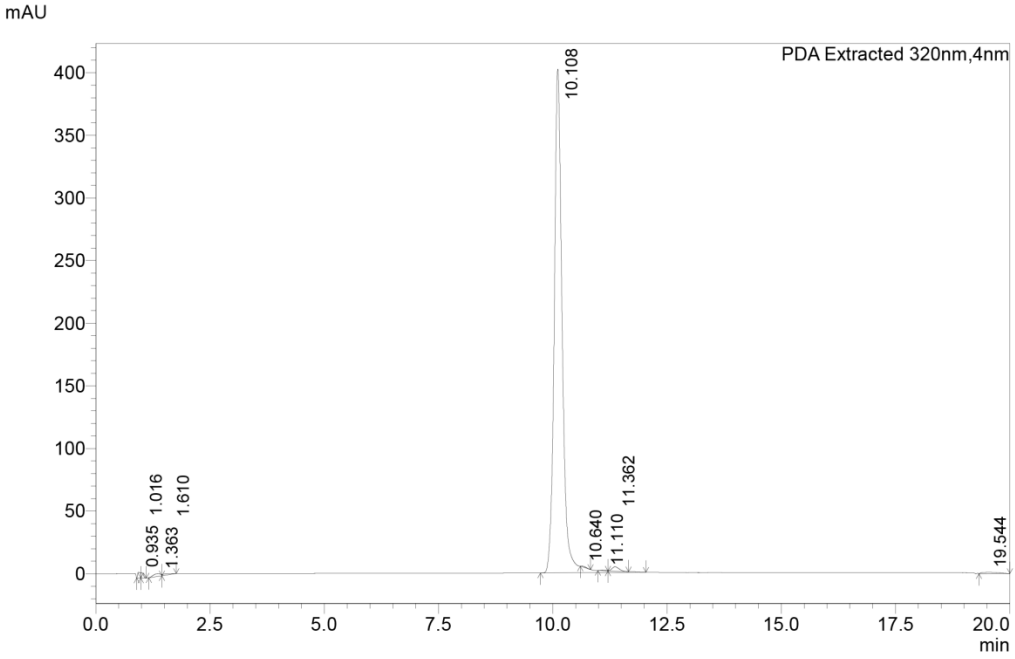

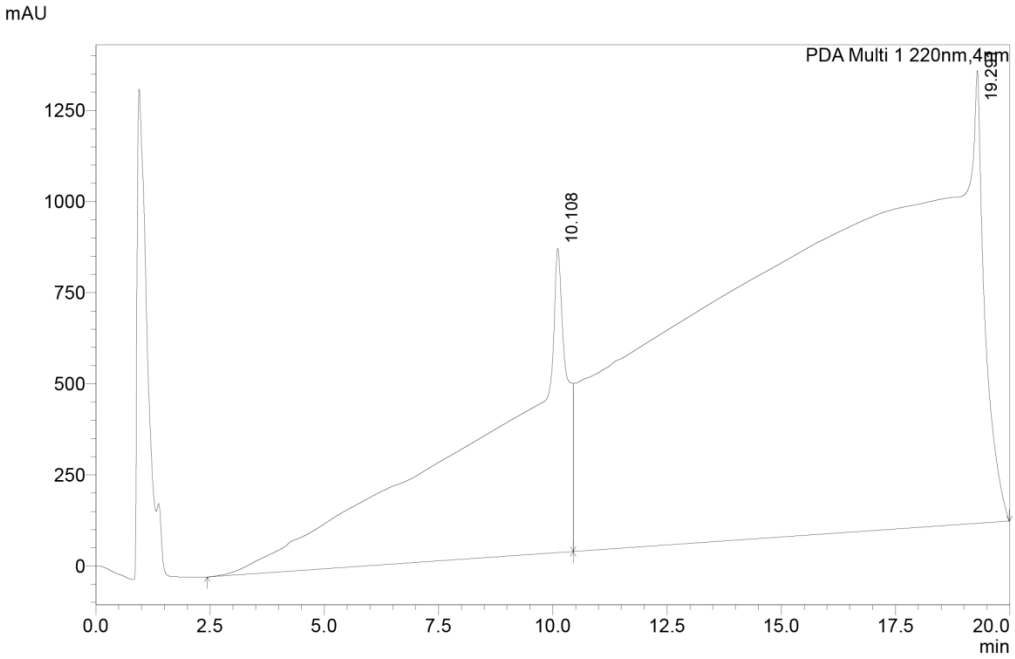

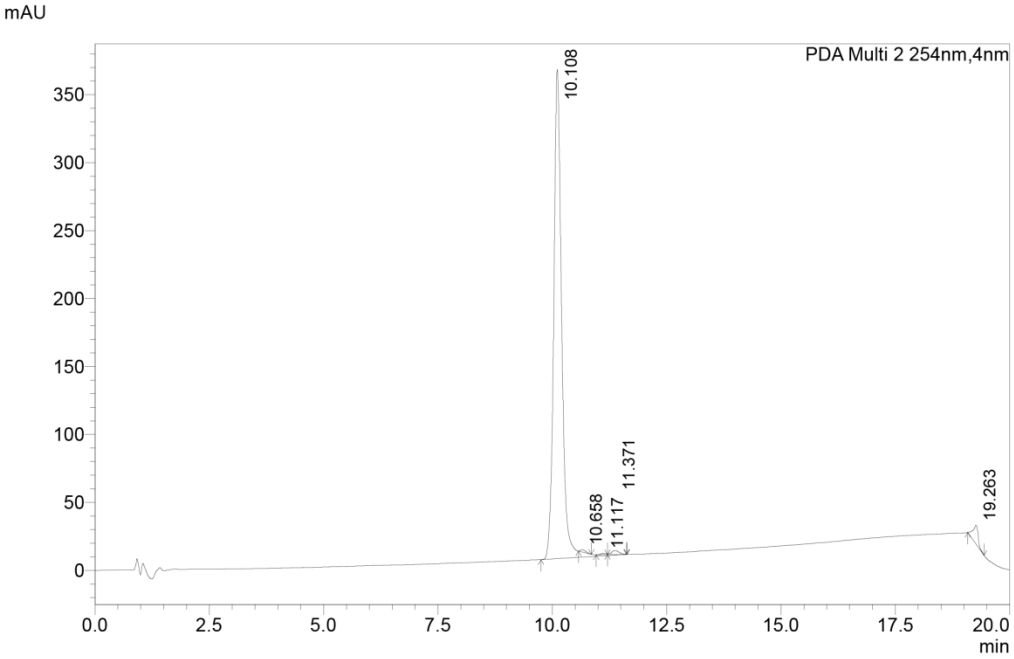
mAU
PDA Multi 2 254nm,4nm
10.108
10.658
11.117
11.371
19.263
350
300
250
200
150
100
50
0
0.0
2.5
5.0
7.5
10.0
12.5
15.0
17.5
20.0
min

==== Shimadzu LabSolutions Data Report ====

<Spectrum>

Line#:1 R.Time:10.267(Scan#:5261)
MassPeaks:460
RawMode:Single 10.267(5261) BasePeak:304(9583706)
BG Mode:None Segment 1 - Event 1

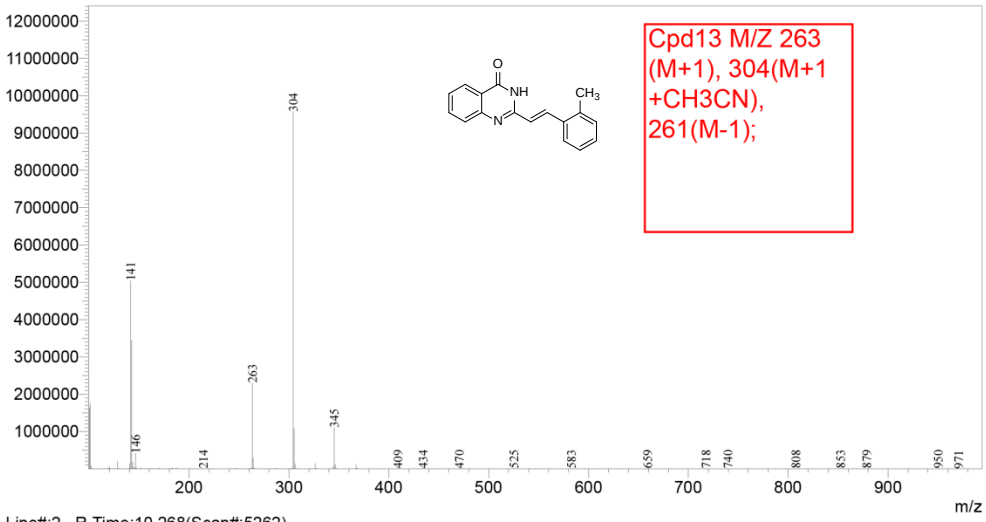

Line#:2 R.Time:10.268(Scan#:5262)
MassPeaks:485
RawMode:Single 10.268(5262) BasePeak:137(172534)
BG Mode:None Segment 1 - Event 2

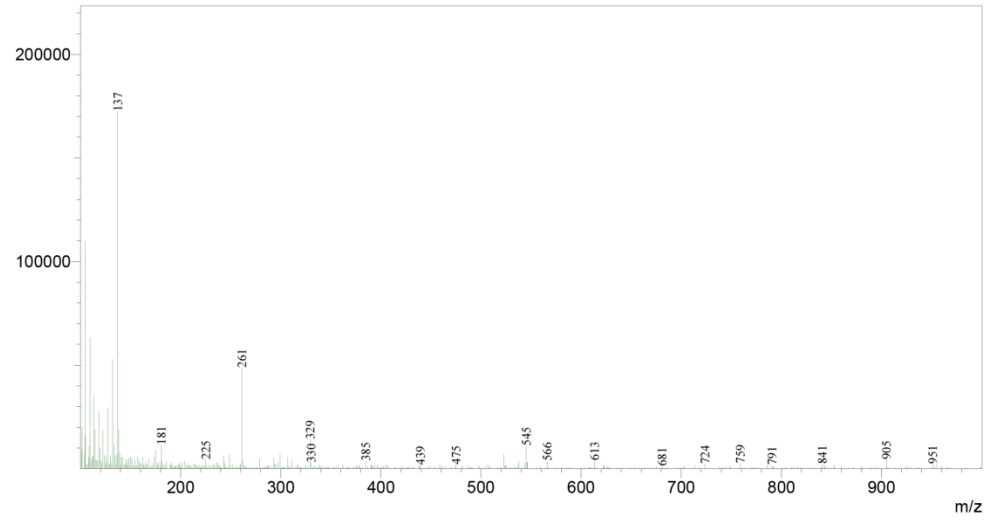

==== Shimadzu LabSolutions Multi-Chromatogram ====

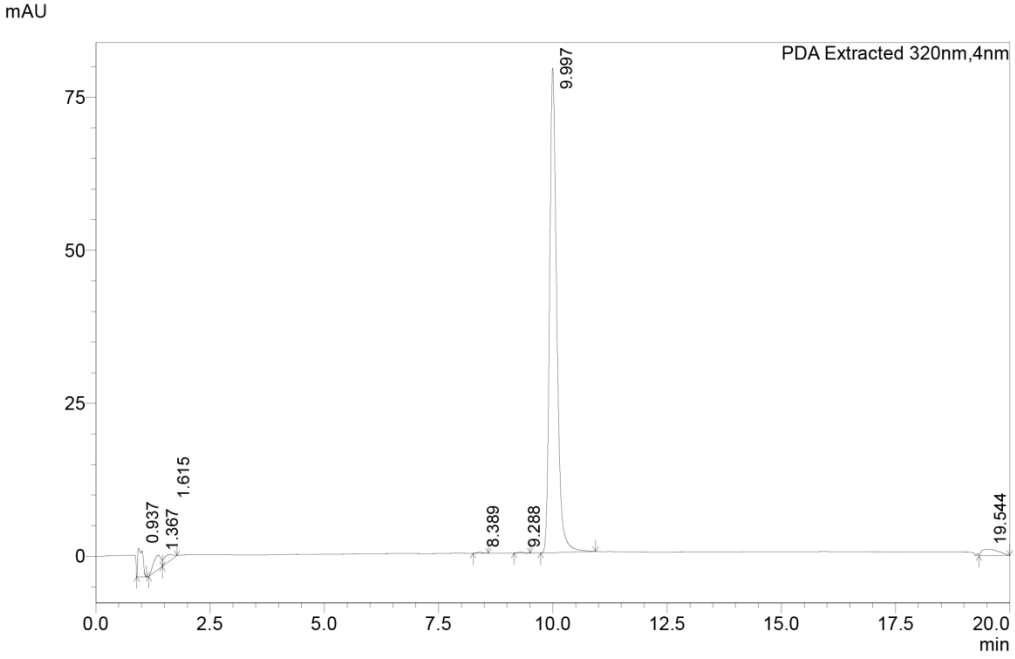

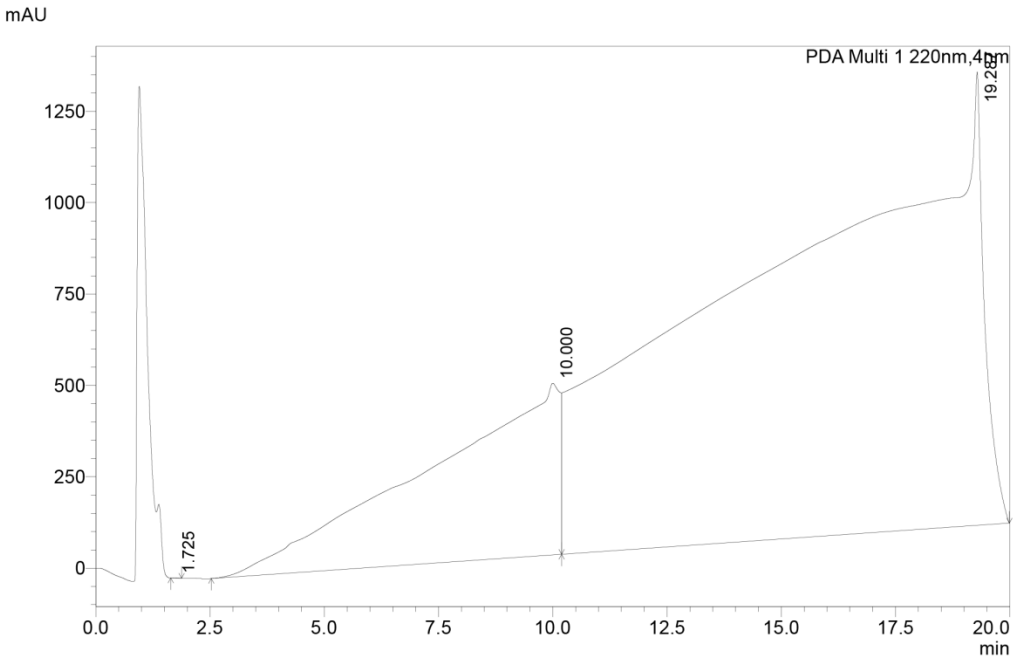

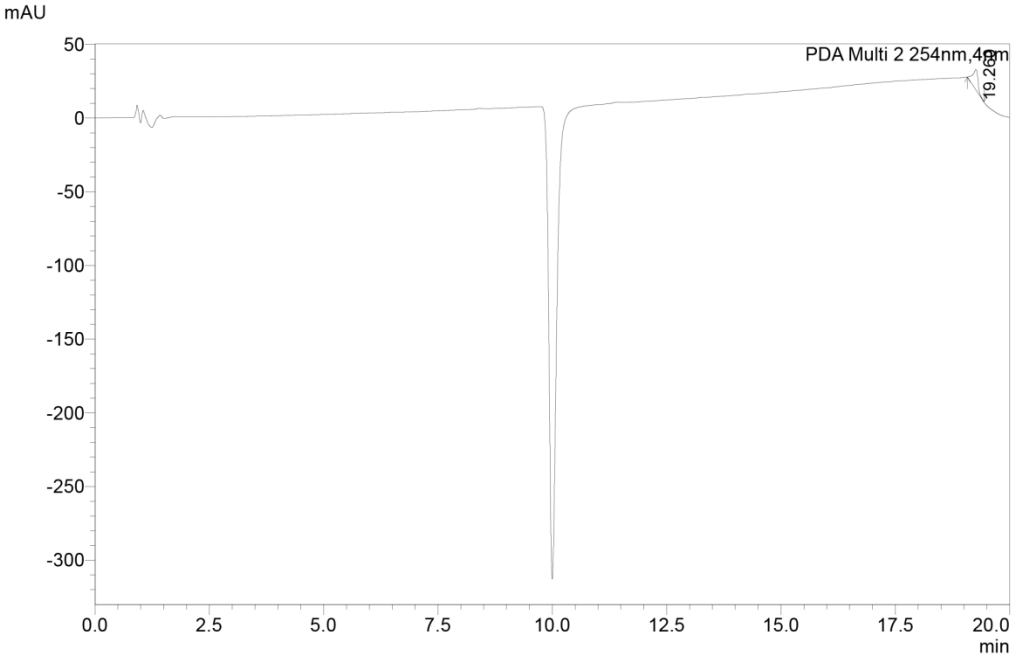
mAU
50
0
-50
-100
-150
-200
-250
-300
PDA Multi 2 254nm,4nm
19.28
0.0
2.5
5.0
7.5
10.0
12.5
15.0
17.5
20.0
min

==== Shimadzu LabSolutions Data Report ====

<Spectrum>

Line#:1 R.Time:10.347(Scan#:5309)
MassPeaks:478
RawMode:Single 10.347(5309) BasePeak:141(4571888)
BG Mode:None Segment 1 - Event 1

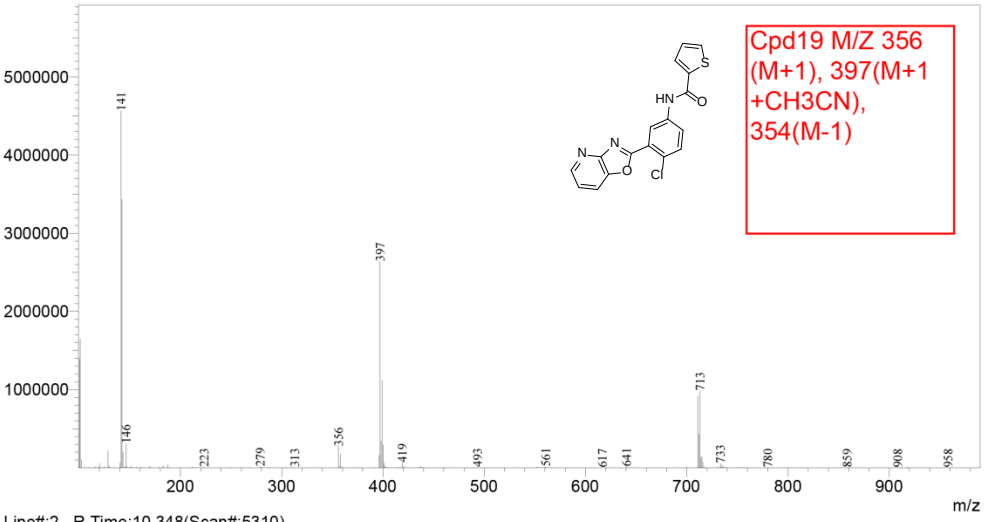

Line#:2 R.Time:10.348(Scan#:5310)
MassPeaks:409
RawMode:Single 10.348(5310) BasePeak:354(492225)
BG Mode:None Segment 1 - Event 2

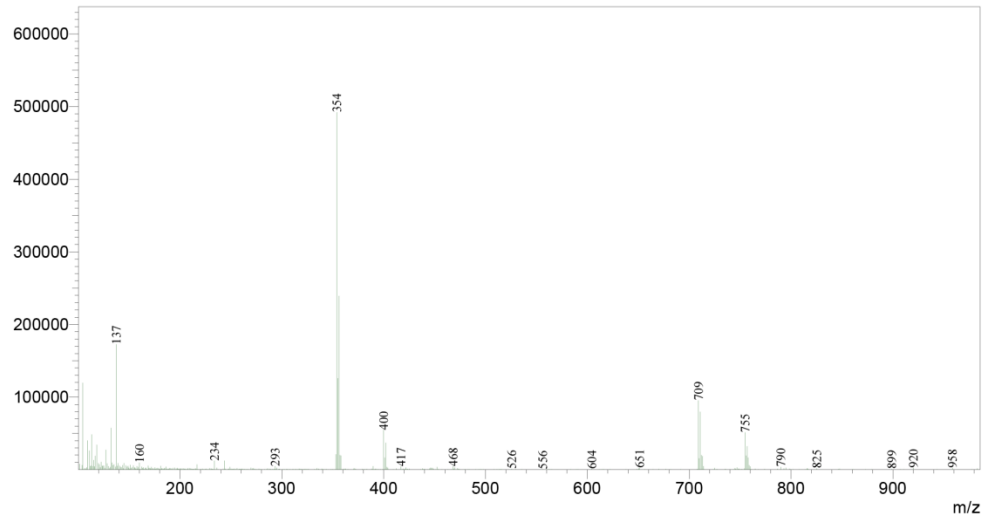

==== Shimadzu LabSolutions Multi-Chromatogram ====

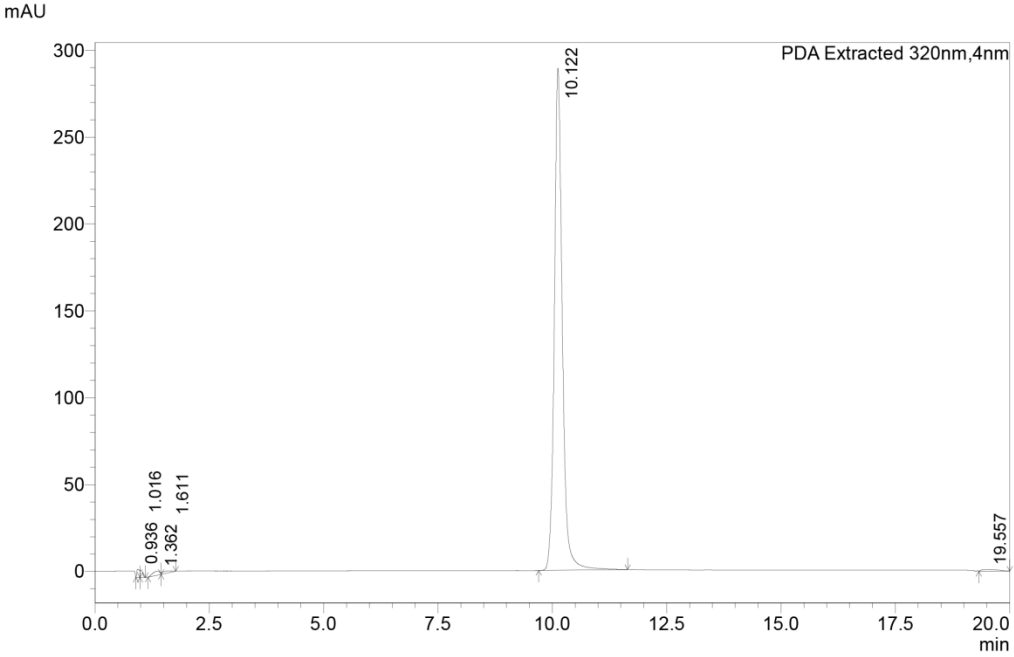

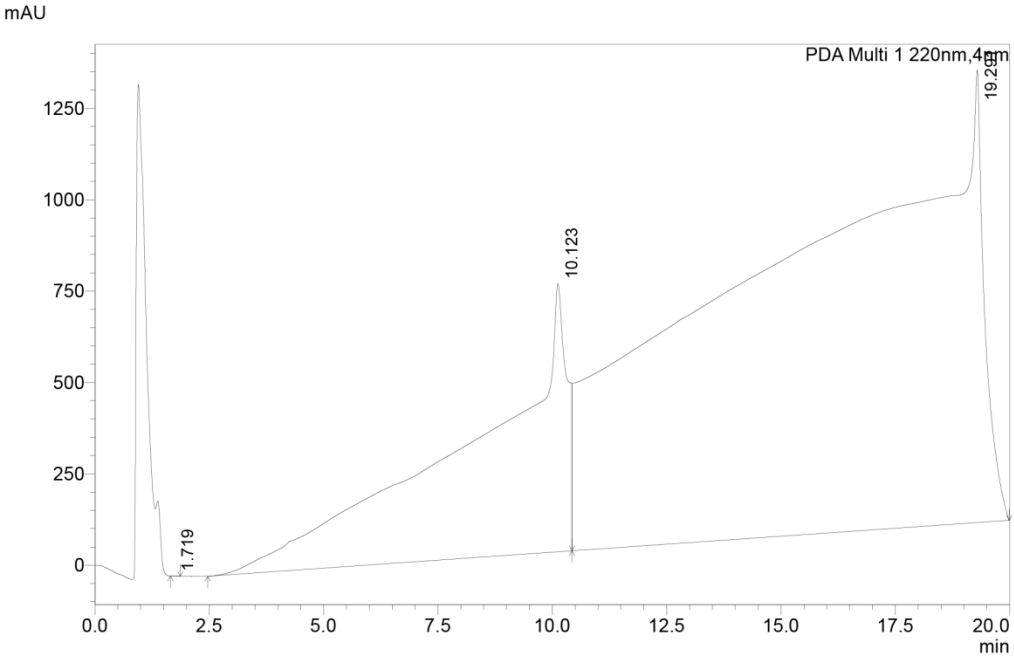

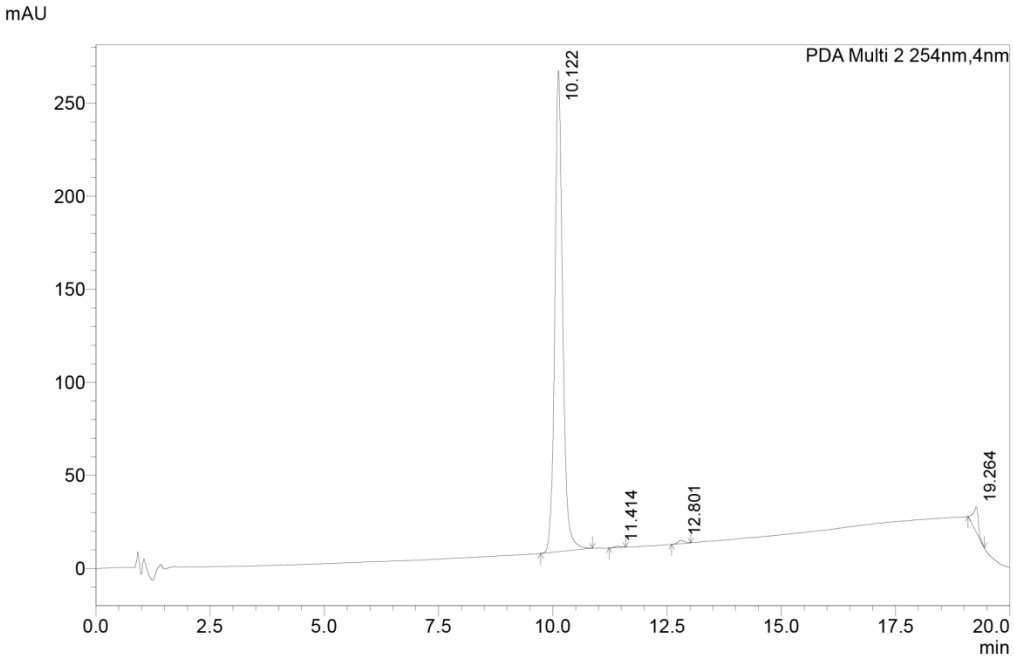
mAU
PDA Multi 2 254nm,4nm
10.122
11.414
12.801
19.264
250
200
150
100
50
0
0.0
2.5
5.0
7.5
10.0
12.5
15.0
17.5
20.0
min

Supporting Information - ONLINE METHODS.

Yeast and bacteria strains. The starting yeast strain in this work was "*fui1*Δ" in the BY4741 background (genotype *MAT*a, *his3*Δ1, *leu2*Δ0, *met15*Δ0, *ura3*Δ0, *fui1*Δ::kanMX4) from the knock-out collection.[5] Purine auxotrophic yeast used in the orthogonal assay and for the yeast [^{3}H]adenosine uptake experiments were constructed in the *fui1*Δ background by disrupting the *ADE2* gene using the hphNT1 marker from the pFA6a-hphNT1 plasmid (*ade2*Δ::hphNT1), which confers resistance to hygromycin B.[6] DH5α competent *E. coli* (Life Technologies) were used for plasmid propagation.

Plasmid construction and PfENT1 expression in yeast. Two plasmids were constructed to express PfENT1: pCM189m and pYMN11c. To generate the empty pCM189m plasmid, we removed the *Eco*RI restriction site upstream of the tetracycline transactivator module in the pCM189 shuttle vector by site-directed mutagenesis.[7] The *P. falciparum* native sequence *ENT1* gene (PlasmoDB ID: PF3D7_1347200) tagged with a C-terminal hemagglutinin epitope was subcloned from the pXOON plasmid.[8] For the subcloning, the pCM189m and pXOON/PfENT1-HA vectors were cut with *Bam*HI-HF and *Not*I-HF (all restriction enzymes were from New England Biolabs, NEB). The digests were run on a 1% agarose gel and fragments recovered using Qiaquick Gel Extraction kit (Qiagen). The PfENT1-HA insert was ligated with pCM189m using T4 DNA ligase (NEB). Plasmids were confirmed by sequencing (Genewiz). To generate a construct to integrate the PfENT1 gene plus the CYC1 promoter and CYC1 terminator into the *S. cerevisiae* genome by double homologous recombination we created a pYMN11c/PfENT1-HA plasmid. The plasmid was created by ligating three fragments with cohesive ends that would result in the proper orientation of all fragments. The pYMN11 plasmid [6] was cut with *Not*I-HF and *Bsp*QI; the pXOON/PfENT1-HA construct was cut with *Spe*I and *Not*I-HF; and the pCM189m construct was cut with *Bsp*QI and *Not*I-HF to obtain the CYC1 terminator. The

integrating PCR fragment was generated by performing 3 consecutive nested PCR reactions using *Pfu* Ultra II polymerase (Agilent Technologies). This added approximately 60 nucleotides homologous to regions flanking the 5' and 3' ends of the *FUI1* locus.

We purchased a synthetic yeast codon-optimized PfENT1-HA-CO (designated by "CO") gene in the pJ201 vector from DNA 2.0. The gene was flanked by *Spe*I and *Bam*HI sites on the 5'-end and *Eco*RI on the 3'-end. It was subcloned into the pCM189m and pYMN11c using the strategies described above. For the PfENT1-CO construct that lacked the HA epitope tag, the HA-tag was removed from the pJ201 vector by site directed mutagenesis before it was subcloned into the yeast expression vectors. The final plasmid used in this work was the yeast LEU2-selectable, mitochondrion-localized GFP vector (mtGFP) from Westermann and Neupert.[9] Yeast were transformed with 0.5–1.0 µg plasmid or PCR DNA using standard lithium-acetate/DMSO (8% v/v) method.[10]

Yeast culture media used. Three different yeast media were used in this work. The first, standard YPD, was used to propagate *fui1*Δ yeast. It consisted of 1% (w/v) yeast extract, 2% (w/v) peptone, and 2% (w/v) dextrose, all purchased from Fisher Scientific. The second, synthetic defined media (SDM) was used to grow the *ade2*Δ yeast. It contained 2% (w/v) dextrose, 0.5% (w/v) ammonium sulfate, 0.17% (w/v) yeast nitrogen base (US Biologicals, #Y2030), 0.02% (w/v) nutritional dropout mix (US Biologicals, #D9542; lacking uracil, adenine, histidine, and tryptophan), 40 mg L^{-1} tryptophan, and 40 mg L^{-1} histidine. Adenine (40 mg L^{-1}) or adenosine (267 mg L^{-1}) as the purine source were added as described in the text. The third, low fluorescence media (LFM), was used to grow the *fui1*Δ::PfENT1-HA-CO + mtGFP yeast. LFM was a modified version of low-fluorescence yeast nitrogen base described previously.[11] It contained 5 g L^{-1} $(NH_4)_2SO_4$, 0.5 g L^{-1} KH_2PO_4, 0.5 g L^{-1} $MgSO_4$, 0.1 g L^{-1} NaCl, 0.1 g L^{-1} $CaCl_2$, 0.5 mg L^{-1} H_3BO_4, 0.04 mg L^{-1} $CuSO_4$, 0.1 mg L^{-1} KI, 0.2 mg L^{-1} $FeCl_3$, 0.4 mg L^{-1} $MnSO_4$, 0.2 mg L^{-1} Na_2MoO_4, 0.4 mg L^{-1} $ZnSO_4$, 2 µg L^{-1} biotin, 0.4 mg L^{-1} calcium

pantothenate, 2 mg L^{-1} inositol, 0.4 mg L^{-1} niacin, 0.2 mg L^{-1} PABA, 0.4 mg L^{-1} pyridoxine HCl, 0.4 mg L^{-1} thiamine, 2% (w/v) glucose, 0.2% (w/v) nutritional dropout mix (US Biologicals, #D9544-20; lacking adenine, histidine, leucine, methionine, tryptophan, uracil), 40 mg L^{-1} tryptophan, 40 mg L^{-1} histidine, 40 mg L^{-1} adenine, 40 mg L^{-1} uracil. LFM also contained HEPES (1.13 g L^{-1}) and HEPES-Na (1.30 g L^{-1}) to increase the pH to 6.5 to bring the HTS assay conditions closer to physiological pH conditions. pH >6.5 resulted in extensive salt precipitation and therefore was not used. All reagents were purchased from Sigma Aldrich except where noted.

Western blot. Approximately 8 x 10^8 cells in mid-log phase growth were harvested by centrifugation at 4,000 x *g* for 2 min at room temperature (RT). Pellets were resuspended in 1 ml of 25 mM Tris/ 1 mM EDTA buffer (pH 7.5) with HALT™ Protease inhibitor diluted to 1x (Thermo Fisher). Cells were disrupted with 0.3 g of 0.5 mm glass beads for 3 min. Insoluble material was cleared by centrifugation at 2,000 x *g* for 2 min at 4 °C. The clear supernatants were transferred to a fresh tube and spun at 150,000 x *g* for 30 min 4 °C to pellet membranes. The pellets were dissolved in 30 µl denaturing sample buffer (62.5 mM Tris-Cl, pH 6.8, 10% glycerol [v/v], 2% SDS [w/v], 100 mM DTT, 0.005% bromophenol blue [w/v]), run on SDS-PAGE (10% acrylamide gel; Bio Rad, 456–1033) and blotted onto a PVDF membrane. Blots were blocked with 5% nonfat milk and probed with a 1:1000 dilution of mouse monoclonal anti-HA antibody (ascites fluid, Covance). The secondary antibody was a 1:1000 dilution of HRP-conjugated rabbit anti-mouse IgG antibody (Pierce). Blots were visualized by chemiluminescence using the Dura West Extended substrate (Pierce/ThermoFisher) and FluorChem FC3 Imaging System (Protein Simple).

Purine-auxotrophic yeast growth assay development. PfENT1-expressing *ade2*Δ yeast were grown overnight in SDM + adenosine shaking at 225 rpm, 30 °C to saturation. The

following day, saturated cultures were diluted to a final OD_{600} = 0.02 (96-well microplate, 96MP; BioRad Benchmark Plus) and were allowed to grow for two additional cycles in SDM + adenosine media. Cells were spun at 3,500 x *g* for 1 min, RT and the pellet was washed three times with 10 mL of SDM media lacking both adenine and adenosine. The final yeast pellet was resuspended in 2x SDM to a final OD_{600} = 0.08. 96-well microplates (TC-treated, clear flat-bottom, polystyrene; Corning Costar; #3596) were used for the growth assays. Wells were preloaded with 100 µL of serially-diluted purine- (adenine or adenosine; 2-fold serial dilution in sterile water). The maximum adenosine concentration was 9 mM; maximum adenine concentration was 500 µM. 100 µL of cells (in 2x SDM media) was added to the plates and resuspended three times; the starting OD_{600} (96MP) was 0.04. The plates were incubated at 30 °C for 15–17 h. OD_{600} was measured and values were plotted in Prism 6.02 (GraphPad). Biological replicates (n=3) were done on different days.

Yeast cell density determinations. Yeast cell density was determined spectrophotometrically using either a standard 1-cm cuvette spectrophotometer (OD_{600} = 0.1 correlated to ~2×10^6 cells mL^{-1}) or a 96-well microtiter plate spectrophotometer (OD_{600} or OD_{620} = 0.018 correlated to ~2×10^6 cells mL^{-1}). GFP fluorescence intensity measurements were determined by reading from the bottom of a plate using either a Molecular Probes™ SpectraMax M5 multimode reader (excitation = 475 nm, emission = 516 nm, cutoff filter = 515 nm) or a PerkinElmer™ Envision 2010 reader (FITC filter sets). 96-well plates were clear, flat-bottom (Corning, #3596). 384-well plates were tissue-culture treated black-walled, clear bottom plates (Corning, #3712).

High throughput screen. Each 384-well plate (black, clear/flat-bottom, tissue-culture treated polystyrene surface, Corning #3712) had 32 positive control wells, 32 negative control wells, and 320 test wells. For detailed media composition see Online Methods. The positive control wells contained low fluorescence media (LFM) with > 10 mM inosine (LFM+I). LFM+I was

prepared by adding 2x LFM to an equal volume of > 50 mM inosine in a 100 mM citrate buffer, pH 3, DMSO and 5-FUrd were added to final concentrations of 2% (v/v) and 250 μM, respectively. Negative control well media (LFM-neg) contained 1x LFM + 2% DMSO (v/v) + 250 μM 5-FUrd. Thus, after addition of an equal volume of yeast in LFM, as described below, the final concentrations in all wells would be 1% DMSO to control for potential DMSO solvent effects because the test compounds were in DMSO and 125 μM 5-FUrd.

The plates were set up as follows. First, 40 μL of media was aliquoted into each well, LFM into test wells, LFM+I into positive control wells and LFM-neg into negative control wells. Next 0.8 μL test compound was added from a 1 mM stock in DMSO, or nothing in the control wells. Finally, 40 μL of logarithmically-growing fui1Δ::PfENT1HA-CO yeast diluted to ~2 x 10^6 cells mL^{-1} in LFM was added to all wells. The final volume of each test well was 80.8 μL (10 μM test compound, 1% DMSO v/v, 125 μM 5-FUrd), and ~80,000 cells (positive control wells contained 12–15 mM inosine after dilution with cells). Plates were incubated at 30 °C in a humidified incubator for 18-20 h before the OD_{620} and GFP-fluorescence intensity was measured. Compounds were considered "hits" if both the OD_{620} and relative fluorescent units (RFU) values obtained for a well were > 4 SD above the mean of the negative control wells (i.e., significantly greater than wells with no growth) (Table S2).

Compound serial dilution for concentration-response assays. Several compounds identified in the primary screen were purchased from ChemBridge. All compounds were dissolved in DMSO at a stock concentration of 25 mM. For concentration-response assays, compounds were serially diluted in DMSO in 96-well polystyrene plates. Controls with no compound had an equal volume of DMSO added. Serial dilutions were either two, three- or four-fold. All compounds were tested in at least three separate biological replicates, except for compounds that were determined to have "no effect;" they were repeated only twice.

Concentration-response primary screen assay: Growth-rescue from 5-FUrd lethality. LFM + 250 µM 5-FUrd (40 µL) was added to each well in a 384 well microtiter plate. 0.8 µL of test compound that had previously been serially diluted in a 96-well plate was aliquoted into the 384-well plate so that each concentration of each compound was prepared in technical quadruplicate. Yeast, fui1Δ::PfENT1-HA-CO, (~80,000 cells in 40 µL LFM) growing in mid-log phase were added and incubated at 30 °C for 19 h. The final DMSO concentration was 1% (v/v). Relative Fluorescence Unit (RFU) values were normalized to be a percent of growth compared to an inosine positive control which gave maximal growth; minimum growth was determined in the absence of compound (DMSO solvent control) and this value is represented as the left-most value on the concentration-response graphs. The normalized data were fitted to a variable slope concentration-response model to determine the concentration that gave half-maximal rescue (EC_{50}) using Prism 6.02 software (GraphPad). Biological replicates ($n \geq 3$) were done on different days.

Secondary orthogonal compound validation assay: Viability of purine auxotrophic yeast grown with adenosine as the sole purine source. Eighty µl of logarithmically growing PfENT1-expressing *ade2*Δ yeast (~400,000 cells grown in synthetically-defined media + 1 mM adenosine) were added to each well of a 384-well microplate (black, clear/flat-bottom, polystyrene; Corning #3712). 0.8 µL of compound (serially diluted 3- or 4-fold in DMSO) was added to each well and resuspended three times. The final DMSO/compound added was 1% (v/v). The plates were incubated at 30 °C for 15–17 h. Growth was evaluated at OD_{600} and values were normalized to maximum growth (DMSO only) and minimum growth for each compound. The normalized data were fit to a variable slope concentration-response model to determine the concentration that gave half-maximal growth inhibition (IC_{50}) using Prism 6.02 software (GraphPad). Biological replicates ($n \geq 4$) were done on different days.

Yeast [^{3}H]adenosine uptake. Cells were grown to mid-log phase and harvested by centrifugation at 3,500 x *g* for 1 min, RT. Cells were washed three times in modified PBS (150 mM NaCl, 10 mM KH_2PO_4, 40 mM K_2HPO_4, 11 mM glucose, pH 7.2). The yeast pellets were resuspended in modified PBS to a final concentration of 2 x 10^8 cells mL^{-1}. 96-well microplate wells were preloaded with 100 µL of 100 nM [^{3}H]adenosine ([2,8-^{3}H]adenosine; 35 Ci $mmol^{-1}$ Moravek Biochemicals). 100 µL yeast aliquots were added to the [^{3}H]adenosine at the appropriate times to generate the time-course to give a final 50 nM [^{3}H]adenosine concentration. At the conclusion of the experiment, cells were harvested onto glass fiber filtermats (Filtermat A, GF/C; Perkin Elmer) using a TomTec 96-well cell harvester system (#96-3-469). Filtermats were dried for 1 h, sealed in plastic bags containing 5 mL of Optiphase Supermix scintillation fluid (Perkin Elmer) and placed into plastic adapters (#1450–104). Counts were measured using a microplate scintillation counter (1450 MicroBeta TriLux, Perkin Elmer). In some early experiments the glass fiber filtermats were cut up and individual wells loaded into individual liquid scintillation vials. The results were very similar to counting filtermats in bags so this practice was abandoned.

To measure the concentration dependence of compound inhibition of [^{3}H]adenosine uptake, 96-well plates were preloaded with 100 nM [^{3}H]adenosine in modified PBS, 0.5 µL of compound (serially diluted 3- or 4- fold in DMSO as described above) was added to each well and resuspended. 100 µL yeast (2 x 10^8 cells mL^{-1}) were added to each well to give a final 50 nM [^{3}H]adenosine concentration and incubated at RT for 15 min. At the end of each experiment, cells were harvested and counted as above.

***P. falciparum* parasite maintenance.** *P. falciparum* 3D7 and Dd2 WT parasites were grown in erythrocytes (RBCs) acquired from healthy human volunteers with consent (Albert Einstein College of Medicine IRB protocol #2013-2227). The parasites were maintained in continuous culture [12] at 4% hematocrit in complete malaria culture medium (MCM):[13] one liter contained:

10.4 g RPMI, 11 mM glucose, 27 mM $NaHCO_3$, 25 mM HEPES, 0.5% Albumax-II (w/v), 20 mg gentamicin, 10 µM hypoxanthine, pH 7.4. *pfent1*Δ parasites were grown in the same medium except supplemented with 75 µM hypoxanthine. Cultures were gassed with 90% N_2/5% CO_2/5% O_2 and grown under continuous shaking at 37 °C.[14]

One week prior to use in viability experiments, the cultures were enriched for trophozoite parasites by magnetic column purification followed by two rounds of sorbitol synchronization.[15, 16] Briefly, a MACS Separation Column (Miltenyi Biotec) attached to a magnetic stand was loaded with a 5 mL volume of parasite culture at >10% late-stage parasitemia at 37 °C. The column was washed three times with MCM to remove non-attached, uninfected RBCs and ring-stage parasites. The column was removed from the magnetic stand and washed with 5 mL MCM. The gravity-assisted flow-through containing trophozoite and schizont parasites was collected in a 15 mL conical tube. The parasite infected RBCs were pelleted at 600 × *g*, 2.5 min, RT, and added to media containing uninfected RBCs at 4% hematocrit. The following day, ring-stage parasites were synchronized by treatment with 5% sorbitol for 15 min to remove any trophozoite/schizont-stage parasites.[17] The culture was washed with MCM and pelleted, 600 × *g*, 2.5 min, RT. The parasites were treated with sorbitol again 4 h later to establish a more tightly synchronized culture. The final culture was allowed to recover for two growth cycles before being used for parasite viability assays.

Generation of *pfent1* knockout (*pfent1*Δ) parasites. 5' and 3' homologous regions of *pfent1* of 0.5 and 0.6kb, respectively, were amplified by PCR using primer pairs pENT1-5F/pNT1-5R and pENT1-3F/pENT1-3R. Sequences for these primers were as follows:

pENT1-5F: 5'CGCCTAGGCCGCGGAGTACCGGTAAAGAGTCATCTAAAGC

pENT1-5R: 5'GCGAATTCCGGGAGATACGAATTGATCAAG

pENT1-3F: 5'CTCACTAGTCAATGCCACATTATCTTATATGG

pENT1-3R: 5'GAGCCGCGGTTATTGTGTTACATCGATGGGTGG.

5’ and 3’ target fragments were inserted upstream and downstream of the hDHFR selectable marker cassette in the pCC1 vector [3] after digestion with *Sac*II / *Afl*II and *Avr*II / *Kas*I restriction enzymes, respectively.

Transfection of the resulting pCC1-ENT1 plasmid was performed using ring stage Dd2 parasites, at approximately 5% parasitemia. Cells were electroporated in a Gene Pulser II (BioRad) with 50 µg of plasmid DNA in 0.2 cm cuvettes using low voltage (0.31 kV) and high capacitance (950 µF) as previously described.[2] Parasites were continuously propagated in 2.5 nM WR99210 (Jacobus Pharmaceuticals), with fresh media added every 24 h for the first 6 days, and every 48 h thereafter. Drug-induced parasite clearance was confirmed on day 5-6 post-transfection by Giemsa thin smears and emergence of transformants was assessed from day 14.

After establishment of WR99210-resistant parasites, these were treated for 14 days with 1 µM of 5-fluorocytosine (5-FC) (Sigma) for negative selection, during which WR99210 pressure was maintained. WR/5-FC-resistant parasites were expected to correspond to parasites that possess the hDFR cassette and have lost CDUP.

ent1 disruption was confirmed by PCR amplification using primers p3 (5’ GTGCTGTTTACATATATATTAATAGG), p4 (5’ GAGGAGATATATACGAAATTTAC), both in the *ent1* locus and p5 (5’ CAGACAGTAAAAAAAATCGCTATC) located in hrp2 and p6 (5’ CTCTACAAATTTTATCTATTGGTTT) located in CAM coding sequence (Figure S8A and S8B), after extraction of parasite genomic DNA from saponin-lysed trophozoite cultures.

Validation of gene deletion. Trophozoite stage parasites were harvested and lysed in 0.15% saponin/Ringer solution. DNA from RBC-free parasite pellets was extracted using Qiagen DNeasy® Blood and Tissue Kit using manufacturer recommendations. The DNA was PCR amplified using the following primers that flanked the *pfent1* gene site: p3,

***pfent1*Δ parasite drug inhibition studies.** (also applies for the related 3D7 and Dd2 expts) *pfent1*Δ parasites were maintained in standard 4% hct culture supplemented with 75 µM hypoxanthine. RBCs were stored in RPMI media containing 1 µM hypoxanthine prior to use. Tightly synchronized ring stage parasites (described above) were used for the drug inhibition growth assays. Briefly, 350 µL cultures (1% hct) were added to each well of 96-well plates containing 1.7 µL of compound (serially diluted 1:2 in DMSO; final DMSO was 0.5%). Cultures were allowed to proliferate for 48-, 72-, and 96-hrs under static conditions at 37 °C. At each time point, 100 µL volume of culture was added to plates containing 100 µL of 2x-SYBRGreenI lysis solution. DNA content was evaluated using spectrofluorometric methods described above. Values represent biological triplicates (mean ± SD) done on different days.

Parasite viability assay. All viability (drug-susceptibility) assays started with ring-stage parasites. Culture synchrony and parasitemia was evaluated by microscopy using methanol-fixed, Giemsa-stained thin smear slides. 25 mL of tightly synchronized parasite culture was spun at 3,500 × *g*, 1 min (RT). The packed pellet was washed three times with 20 mL of culture media lacking hypoxanthine (MCM-HX). Uninfected RBCs (uRBCs) were washed with MCM-HX similar to the infected RBCs (iRBCs). Appropriate volumes of packed uRBC and iRBC were added to culture media containing 10 µM or 367 µM hypoxanthine (Low-HX and high-HX, respectively) or 225 µM xanthine to give a final starting culture of 1% hematocrit, 2% ring-stage parasitemia. 200 µL of culture was added to all wells in 96-well plates (tissue culture-treated, sterile white polystyrene, flat bottom; Corning Costar, #3917). Wells containing only uRBCs at 1% hematocrit were used for background subtraction (see below). 1 µL of compound (serially diluted 3- or 4-fold in DMSO) was added to each well and resuspended five times. Chloroquine (CQ) was used to establish a reference for maximal growth inhibition. The final DMSO concentration was 0.5% (v/v). The plates were placed into a sealed gas chamber and incubated at 37 °C for 72 h under 90% N_2/5% CO_2/5% O_2. Parasite viability was assessed using SYBR

Green I (10,000x, Invitrogen, S7567) DNA fluorometry.[18] Briefly, after 72 h growth, 100 µL of lysis buffer (20 mM Tris-HCl, pH 7.5; 5 mM EDTA, pH 8; 0.08% Triton X–100; 0.008% saponin) containing SYBR Green I (0.2 µL mL^{-1} of total volume; Invitrogen) was added to each well. Samples were resuspended three times and stored at RT for 1 h in the dark. DNA quantification was performed using a Spectramax M5 (Molecular Devices) microplate detection system (Ex. 488/DC 495/Em. 515; top read; 6 reads/well). Fluorescence values were background subtracted (uRBC only), normalized to maximum and minimum growth (100 and 0%, respectively), and plotted using Prism 6.02 (GraphPad). Since not all compounds achieved maximum kill at the concentrations tested due to compound solubility issues at higher concentrations, maximum growth inhibition (0% growth) was normalized to the SYBR Green I fluorescence detected at the maximum CQ concentration. IC_{50} values were obtained from a normalized, non-linear regression model (Y=100/(1+10^((LogIC_{50}-X)*HillSlope))). Biological replicates (n=4) were done on different days.

Giemsa-stained parasites were visualized using a Zeiss Axio Observer Z1 microscope with a 100x/1.4 NA oil objective and a Zeiss Axiocam HRc Camera (color; CCD, 14 bit). Images were processed with Axiovision software.

Purine-dependent growth assays. 3D7 and Dd2 WT and *pfent1*Δ parasite cultures were grown and synchronized as described above. RBCs were stored in RPMI media containing 1 µM hypoxanthine prior to use. Ring stage parasites were harvested and washed three times in purine-free malaria media. 175 µL of culture at 2% hct, 2% parasitemia was added to plates containing 175 µL media supplemented with either serially-diluted hypoxanthine (HX) or xanthine (Xan) (max concentration 500- and 450-µM, respectively). The final starting culture conditions were 1% hct, 2% parasitemia. Cultures were allowed to grow for 48-, 72-, and 96-h under static conditions at 37 °C. At each time point, 100 µL volume of culture was added to plates containing 100 µL of 2x-SYBRGreenI lysis solution. DNA content was evaluated using

spectrofluorometric methods described above. Values represent biological triplicates (mean ± SD) done on different days.

Isolated parasite [^{3}H]adenosine uptake assay. Parasites were sorbitol synchronized (see above) one day before the start of the experiments. On the experimental day, trophozoite-stage 3D7 parasites (25 mL, 4% hematocrit, <10% parasitemia) were centrifuged at 600 × g, 2.5 min (RT) to remove old media. The pellet was washed once in Ringer's solution (1x Ringer solution: 122.5 mM NaCl, 5.4 mM KCl, 1.2 mM $CaCl_2$, 0.8 mM $MgCl_2$, 11 mM D-glucose, 25 mM HEPES, 1 mM Na_2HPO_4, pH 7.4). To release functionally isolated parasites from infected RBCs, we performed saponin permeabilization of the RBC membrane and the parasitophorous vacuolar membrane as described elsewhere.[19, 20] Mild saponin treatment releases *Plasmodium* parasites from their RBC hosts while preserving parasite plasma membrane integrity. Briefly, the infected RBC pellet was resuspended with 25 mL of freshly prepared 0.15% saponin in iso-osmotic Ringer's solution, incubated at RT for 2.5 min, spun at 1,800 × *g*, 5 min and washed two times in Ringer's solution to remove RBC debris and hemoglobin. The final RBC-free parasite pellet was resuspended in Ringer's solution (0.2% parasite vol/Ringer's vol). 96-well microplate wells were preloaded with 100 µL of 100 nM [^{3}H]adenosine ([2,8-^{3}H]adenosine; 35 Ci mmol^{-1} Moravek Biochemicals) and serially diluted compound. 100 µL of parasite suspension in Ringer's solution was added to the [^{3}H]adenosine/compound mix (final 0.083% DMSO, final 50 nM [^{3}H]adenosine concentration) and incubated at RT for 15 min. At the end of all experiments, cells were harvested onto glass fiber filtermats (Filtermat A, GF/C; Perkin Elmer) using TomTec 96-well cell harvester system (#96-3-469). Filtermats were allowed to dry for 1 h, sealed in plastic membrane bags containing 5 mL of Betaplate Scint scintillation fluid (Perkin Elmer) and placed into plastic adapters (#1450–104). Counts were measured using a 1450 MicroBeta TriLux microplate scintillation counter (Perkin Elmer; counts/30sec/well). Counts were normalized to maximum and minimum inhibition of [^{3}H]adenosine uptake. The normalized data

were fit to a variable slope concentration-response model to determine the concentration that gave half-maximal adenosine uptake inhibition (IC_{50}) using Prism 6.02 software (GraphPad).

[^{14}C]2'-deoxyadenosine uptake assay into PfENT4 expressing *Xenopus laevis* oocytes. *In vitro* transcription of PfENT4 mRNA, PfENT4 expression in *Xenopus laevis* oocytes, and radiolabeled substrate uptake assays into PfENT4-expressing oocytes was performed as described previously.[21] Stage V to Stage VI oocytes were harvested from *X. laevis* female toads (Nasco), approved for use by the Albert Einstein College of Medicine Institutional Animal Care and Use Committee (Protocol #20110905). A PfENT4 cDNA optimized for *X. laevis* expression was used as a template for *in vitro* capped mRNA synthesis using the mMESSAGE mMACHINE RNA synthesis kit. The mRNA was purified using the MegaClear kit (Life Technologies) and further precipitated and resuspended to a final concentration of 1 μg μL^{-1}. 23 nL of mRNA was injected into oocytes. Oocytes were incubated at 16 °C for three or four days prior to the uptake experiment to allow for protein expression. On the day of the experiment, oocytes were washed in ENT4 transport buffer (96 mM NaCl, 1 mM $MgCl_2$, 2 mM KCl, 1 mM $CaCl_2$, 10 mM HEPES/10 mM MES, pH adjusted to 7.4 with NaOH) then incubated in the presence of 1.5 μM 2'-[8–1^4C]deoxyadenosine (48.8 mCi $mmol^{-1}$, Moravek Biochemicals) and in the presence or absence of 50 μM compound **AKR–122**. The DMSO concentration was 0.5% (v/v). Oocytes were then washed 5 times in ice-cold buffer and individual oocytes were counted using liquid scintillation spectrometry.

Supporting Information - REFERENCES

(1) Iversen, P. W., Beck, B., Chen, Y.-F., Dere, W., Devanarayan, V., Eastwood, B. J., Farmen, M. W., Iturria, S. J., Montrose, C., Moore, R. A., Weidner, J. R., and Sittampalam, G. S. (2004) HTS Assay Validation, In *Assay Guidance Manual* (Sittampalam, G. S., Gal-Edd, N., Arkin, M., Auld, D., Austin, C., Bejcek, B., Glicksman, M., Inglese, J., Lemmon, V., Li, Z., McGee, J., McManus, O., Minor, L., Napper, A., Riss, T., Trask, O. J., and Weidner, J., Eds.), Bethesda MD.

(2) Fidock, D. A., and Wellems, T. E. (1997) Transformation with human dihydrofolate reductase renders malaria parasites insensitive to WR99210 but does not affect the intrinsic activity of proguanil, *Proc Natl Acad Sci U S A 94*, 10931–10936.

(3) Maier, A. G., Braks, J. A., Waters, A. P., and Cowman, A. F. (2006) Negative selection using yeast cytosine deaminase/uracil phosphoribosyl transferase in Plasmodium falciparum for targeted gene deletion by double crossover recombination, *Mol Biochem Parasitol 150*, 118–121.

(4) Lévai, A., and Jekö, J. (2005) An efficient procedure for the preparation of 4-methyl-2-thiocoumarins by the reaction of 4-methylcoumarins with Lawesson's reagent., *J. Heterocyclic Chem. 42*, 739-742.

(5) Winzeler, E. A., Shoemaker, D. D., Astromoff, A., Liang, H., Anderson, K., Andre, B., Bangham, R., Benito, R., Boeke, J. D., Bussey, H., Chu, A. M., Connelly, C., Davis, K., Dietrich, F., Dow, S. W., El Bakkoury, M., Foury, F., Friend, S. H., Gentalen, E., Giaever, G., Hegemann, J. H., Jones, T., Laub, M., Liao, H., Liebundguth, N., Lockhart, D. J., Lucau-Danila, A., Lussier, M., M'Rabet, N., Menard, P., Mittmann, M., Pai, C., Rebischung, C., Revuelta, J. L., Riles, L., Roberts, C. J., Ross-MacDonald, P., Scherens, B., Snyder, M., Sookhai-Mahadeo, S., Storms, R. K., Veronneau, S., Voet, M., Volckaert, G., Ward, T. R., Wysocki, R., Yen, G. S., Yu, K., Zimmermann, K., Philippsen, P., Johnston, M., and Davis, R. W. (1999) Functional characterization of the S. cerevisiae genome by gene deletion and parallel analysis, *Science 285*, 901-906.

(6) Janke, C., Magiera, M. M., Rathfelder, N., Taxis, C., Reber, S., Maekawa, H., Moreno-Borchart, A., Doenges, G., Schwob, E., Schiebel, E., and Knop, M. (2004) A versatile toolbox for PCR-based tagging of yeast genes: new fluorescent proteins, more markers and promoter substitution cassettes, *Yeast 21*, 947-962.

(7) Gari, E., Piedrafita, L., Aldea, M., and Herrero, E. (1997) A set of vectors with a tetracycline-regulatable promoter system for modulated gene expression in Saccharomyces cerevisiae, *Yeast 13*, 837-848.

(8) Riegelhaupt, P. M., Cassera, M. B., Frohlich, R. F., Hazleton, K. Z., Hefter, J. J., Schramm, V. L., and Akabas, M. H. (2010) Transport of purines and purine salvage pathway inhibitors by the Plasmodium falciparum equilibrative nucleoside transporter PfENT1, *Mol Biochem Parasitol 169*, 40-49.

(9) Westermann, B., and Neupert, W. (2000) Mitochondria-targeted green fluorescent proteins: convenient tools for the study of organelle biogenesis in Saccharomyces cerevisiae, *Yeast 16*, 1421–1427.

(10) Hill, J., Donald, K. A., and Griffiths, D. E. (1991) DMSO-enhanced whole cell yeast transformation, *Nucleic Acids Res 19*, 5791.

(11) Sheff, M. A., and Thorn, K. S. (2004) Optimized cassettes for fluorescent protein tagging in Saccharomyces cerevisiae, *Yeast 21*, 661-670.

(12) Trager, W., and Jensen, J. B. (1976) Human malaria parasites in continuous culture, *Science. 193*, 673-675.

(13) Cranmer, S. L., Magowan, C., Liang, J., Coppel, R. L., and Cooke, B. M. (1997) An alternative to serum for cultivation of Plasmodium falciparum in vitro, *Trans R Soc Trop Med Hyg 91*, 363-365.

(14) Allen, R. J., and Kirk, K. (2010) Plasmodium falciparum culture: the benefits of shaking, *Mol Biochem Parasitol 169*, 63-65.
(15) Bates, A. H., Mu, J., Jiang, H., Fairhurst, R. M., and Su, X. Z. (2010) Use of magnetically purified Plasmodium falciparum parasites improves the accuracy of erythrocyte invasion assays, *Exp Parasitol 126*, 278-280.
(16) Kim, C. C., Wilson, E. B., and DeRisi, J. L. (2010) Improved methods for magnetic purification of malaria parasites and haemozoin, *Malar J 9*, 17.
(17) Lambros, C., and Vanderberg, J. P. (1979) Synchronization of Plasmodium falciparum erythrocytic stages in culture, *J Parasitol 65*, 418-420.
(18) Smilkstein, M., Sriwilaijaroen, N., Kelly, J. X., Wilairat, P., and Riscoe, M. (2004) Simple and inexpensive fluorescence-based technique for high-throughput antimalarial drug screening, *Antimicrob Agents Chemother 48*, 1803–1806.
(19) Hsiao, L. L., Howard, R. J., Aikawa, M., and Taraschi, T. F. (1991) Modification of host cell membrane lipid composition by the intra-erythrocytic human malaria parasite Plasmodium falciparum, *Biochem J 274 (Pt 1)*, 121–132.
(20) Saliba, K. J., Horner, H. A., and Kirk, K. (1998) Transport and metabolism of the essential vitamin pantothenic acid in human erythrocytes infected with the malaria parasite Plasmodium falciparum, *J Biol Chem 273*, 10190–10195.